Electronic Supplementary Material (ESI) for Organic & Biomolecular Chemistry.

PEG-modified aziridines for stereoselective synthesis of water-soluble pyrrolofullerenes

Angelina V. Kazakova, Alexander S. Konev,* Ivan M. Zorin, Igor S. Poshekhonov, Victor A. Korzhikov-Vlakh and Alexander F. Khlebnikov

Supplementary information

Table of contents

Figure S1. ^{1}H NMR spectrum of compound 2 ($CDCl_3$, 400 MHz), full range.

To enhance resolution, FID was subjected to apodization procedure with exponential (-0.3) and gauss (1.9) functions.

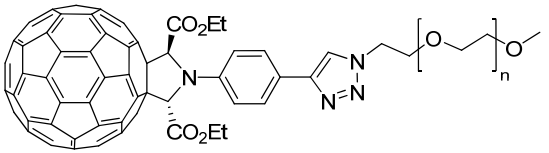

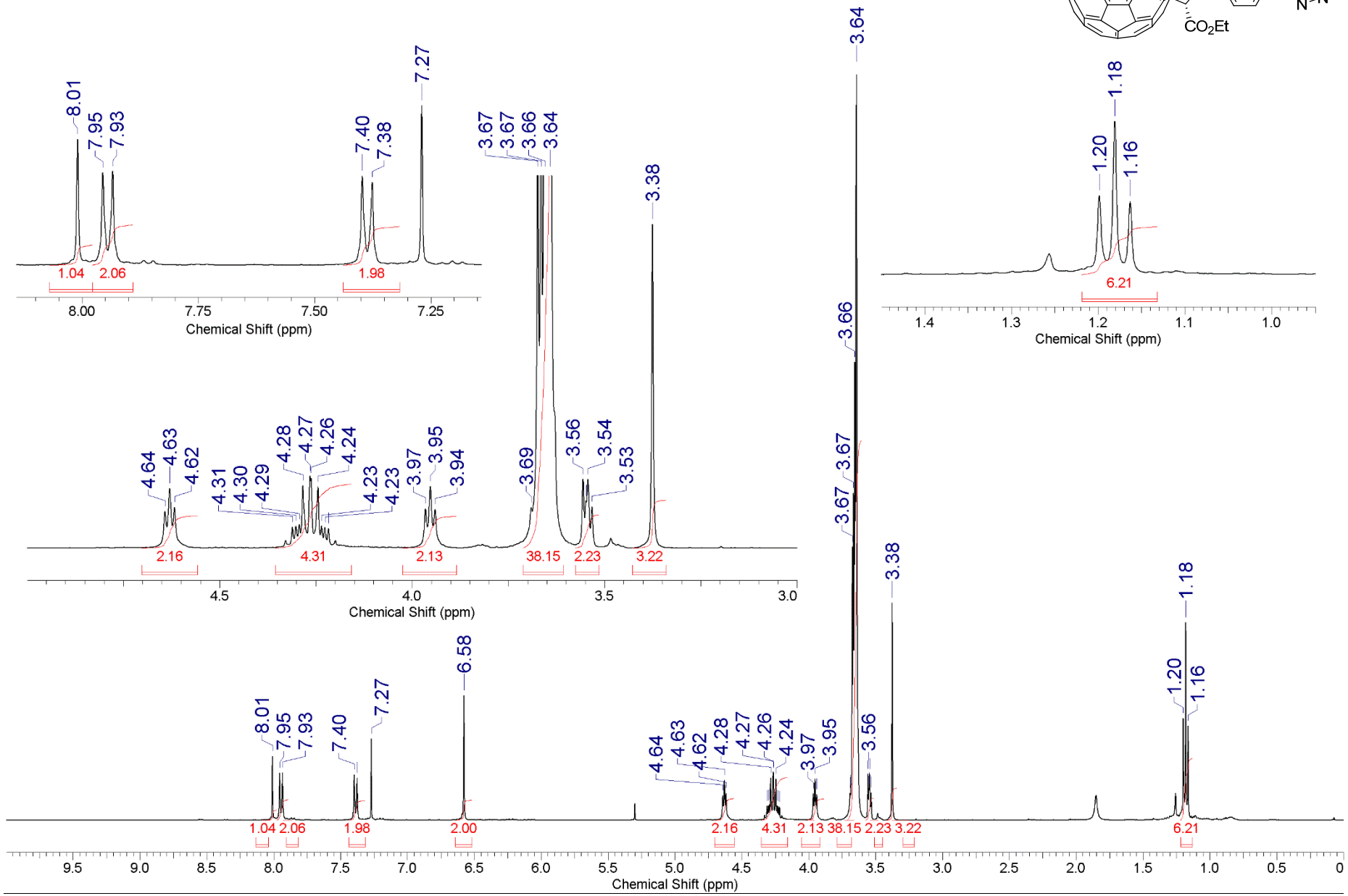

Figure S2. ^{13}C NMR spectrum of compound 2 ($CDCl_3$, 100 MHz), full range.

To enhance resolution, FID was subjected to apodization procedure with exponential (-0.5) and gauss (1.5) functions.

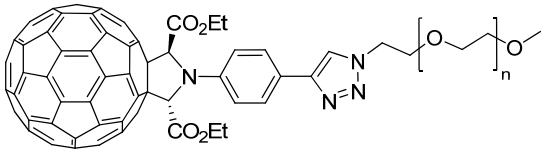

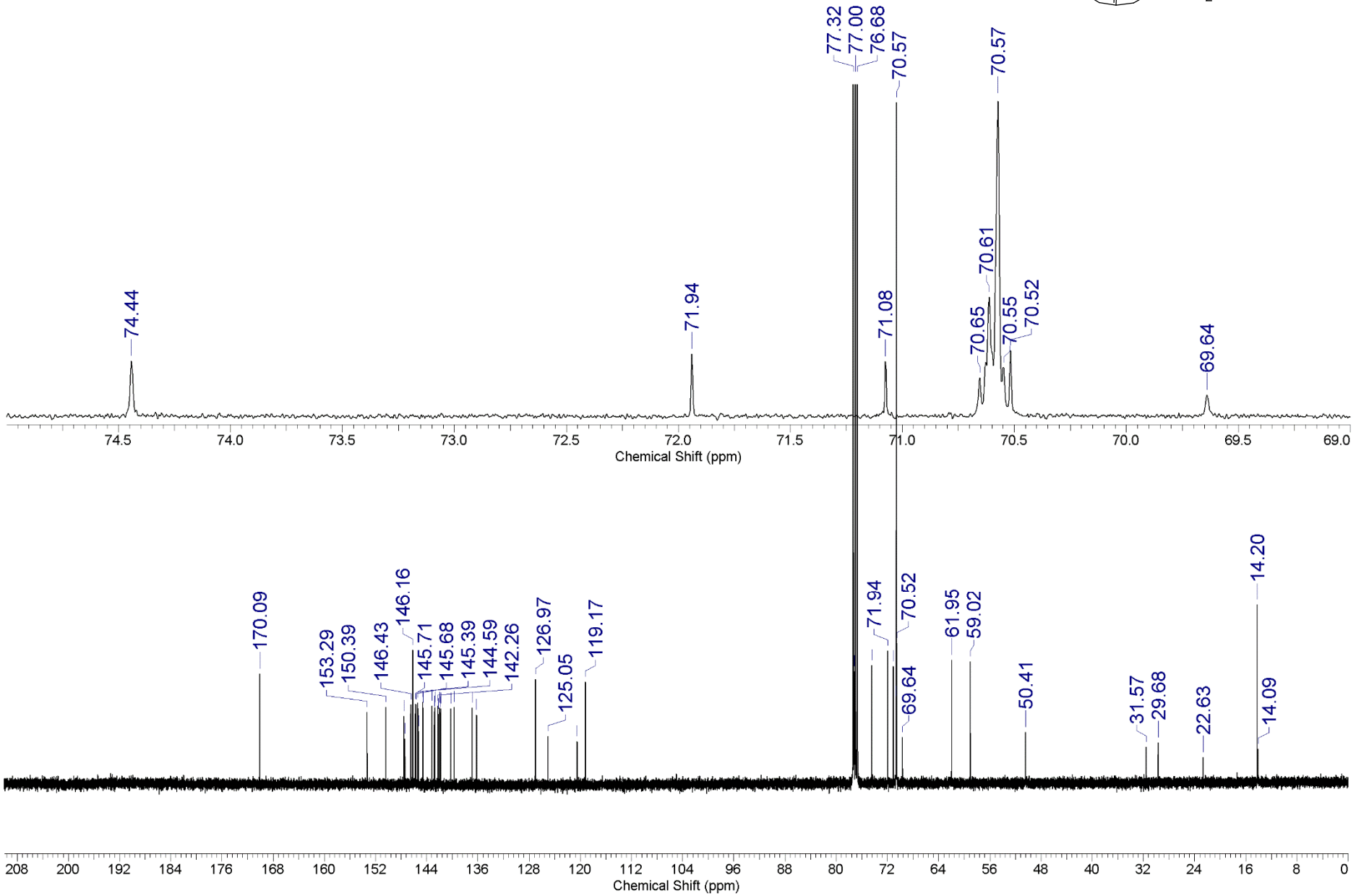

Figure S3. ^{13}C NMR spectrum of compound 2 ($CDCl_3$, 100 MHz), extension for 118 – 149 ppm range.

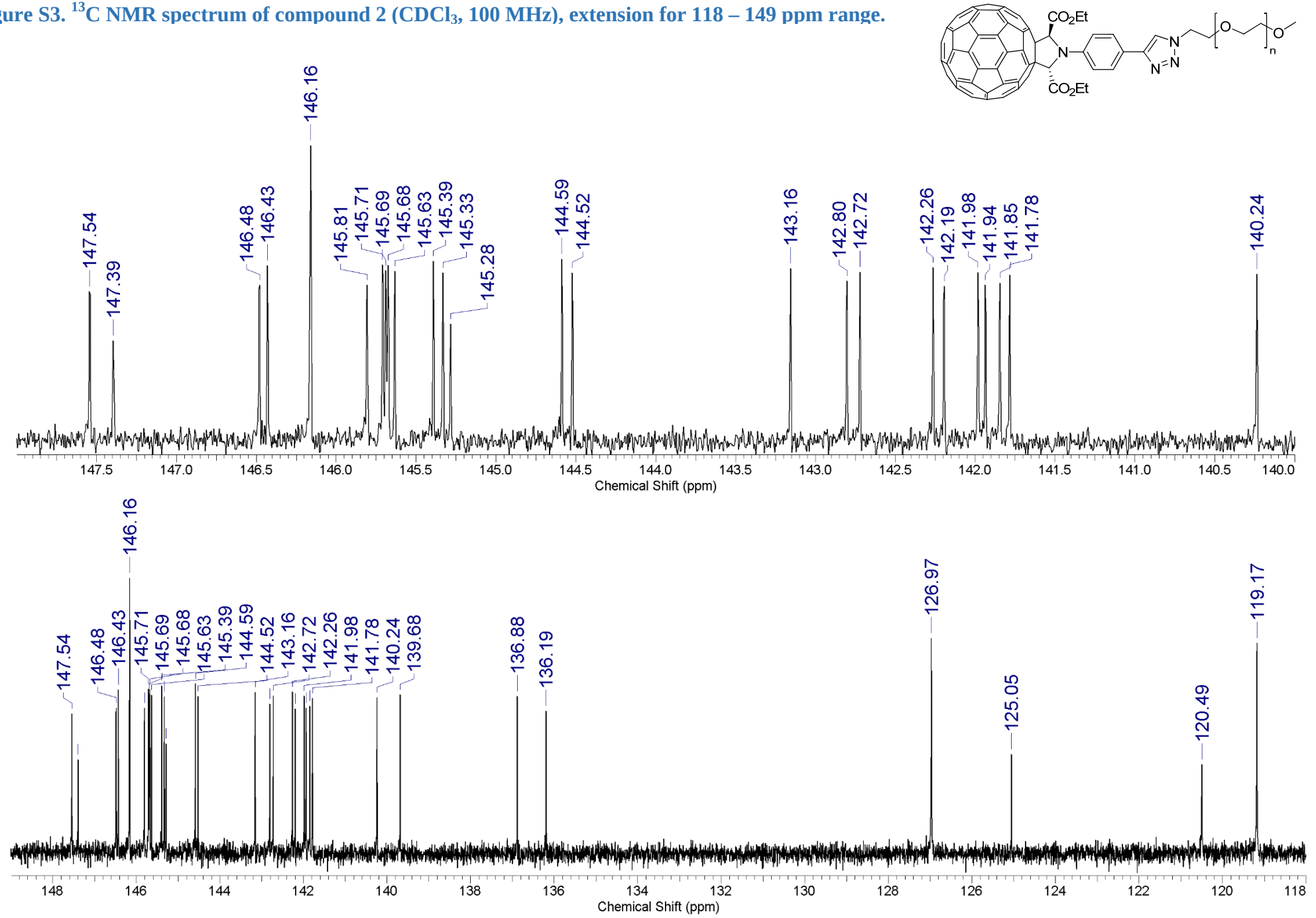

Figure S4. ^{1}H NMR spectrum of compound 3 ($CDCl_3$, 400 MHz), full range.

To enhance resolution, FID was subjected to apodization procedure with exponential (-0.3) and gauss (1.7) functions.

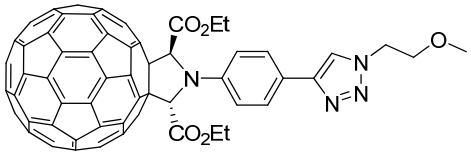

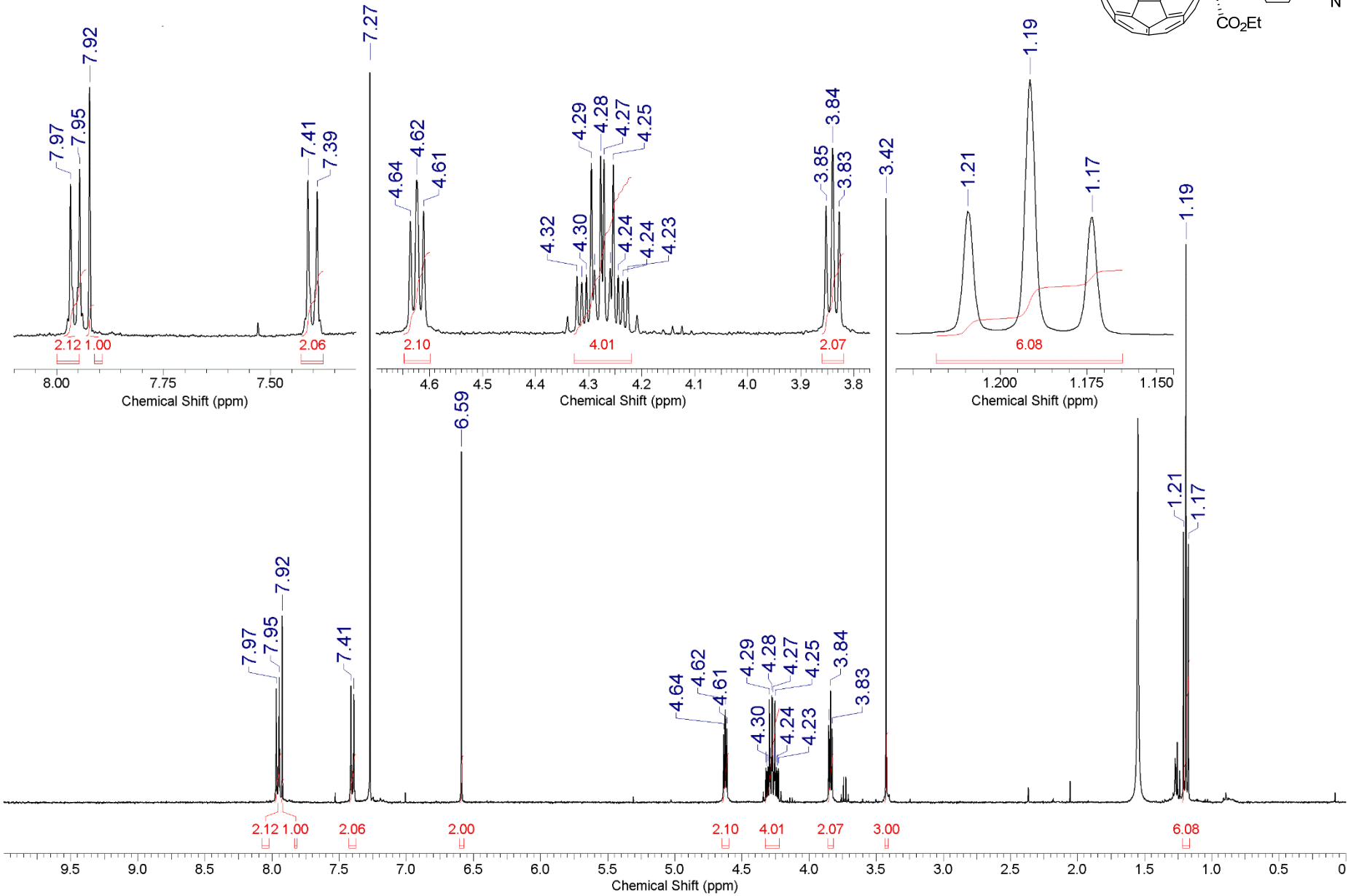

Figure S5. ^{13}C NMR spectrum of compound 3 ($CDCl_3$, 100 MHz), full range.

To enhance resolution, FID was subjected to apodization procedure with exponential function (1.0).

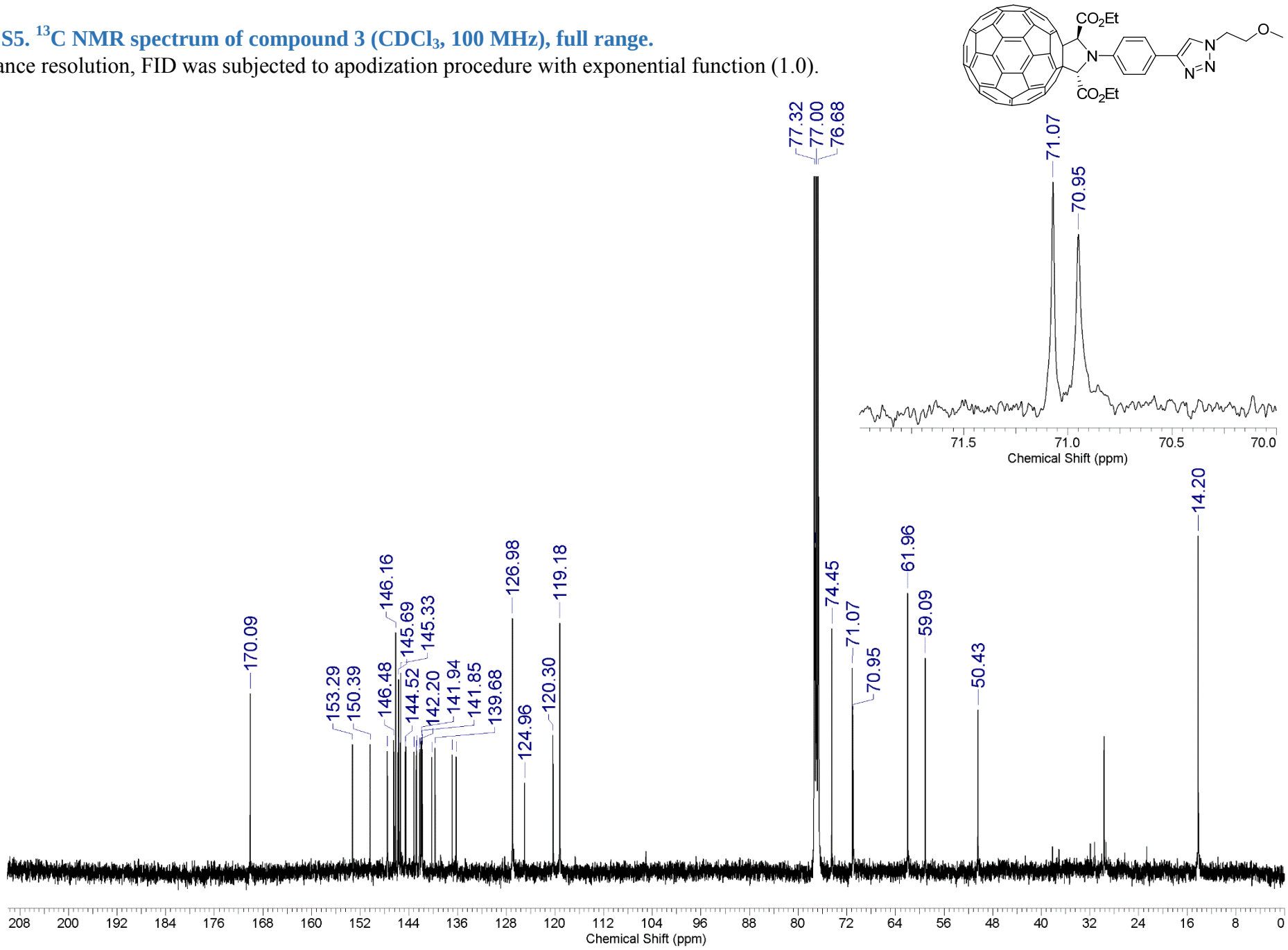

Figure S6. ^{13}C NMR spectrum of compound 3 ($CDCl_3$, 100 MHz), extension for 135 – 148 ppm range.

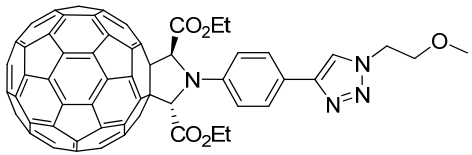

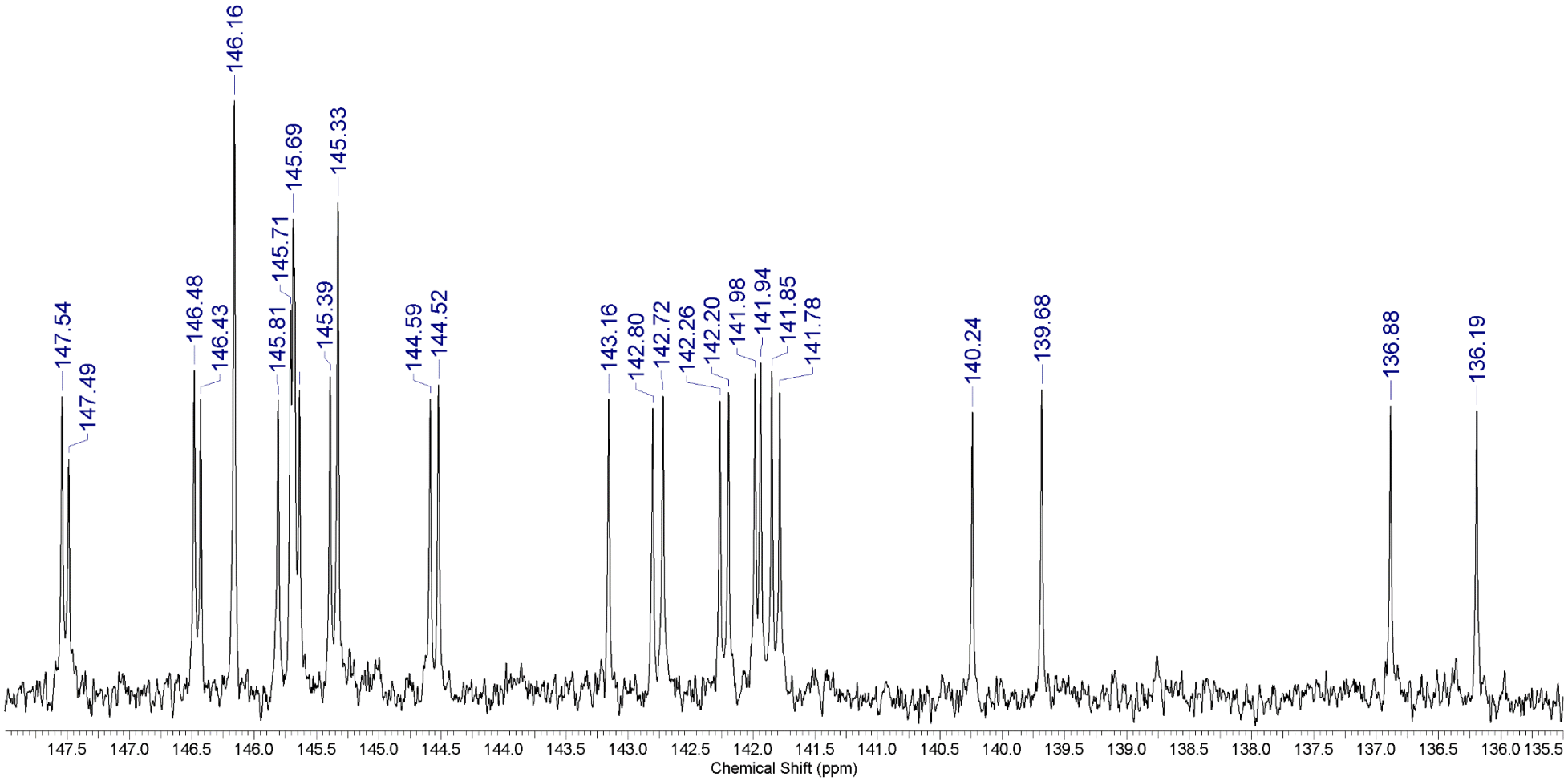

Figure S7. ^{1}H NMR spectrum of compound 4 ($CDCl_3$, 400 MHz), extension for 3.2 – 3.6 ppm range.

The spectrum is recorded in a DMF solution (0.6 *wt%*) due to the explosion hazard of compound **4**. To enhance resolution, FID was subjected to apodization procedure with exponential (-0.3) and gauss (1.1) functions.

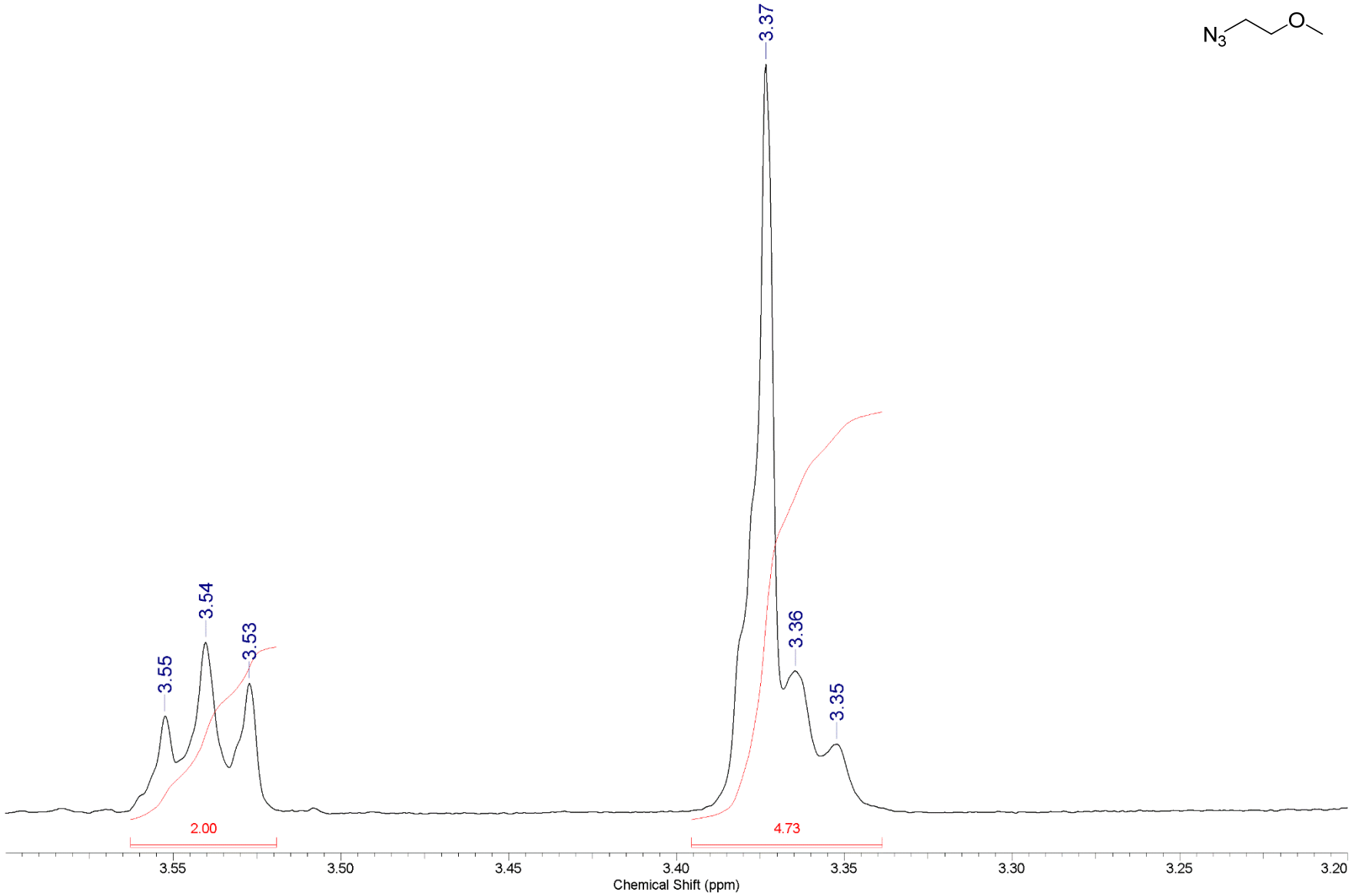

Figure S8. ^{1}H NMR spectrum of compound 5 ($CDCl_3$, 400 MHz), full range.

To enhance resolution, FID was subjected to apodization procedure with exponential (-0.3) and gauss (2.0) functions.

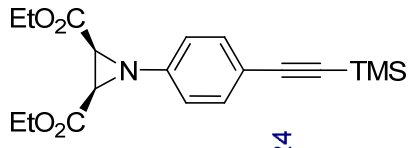

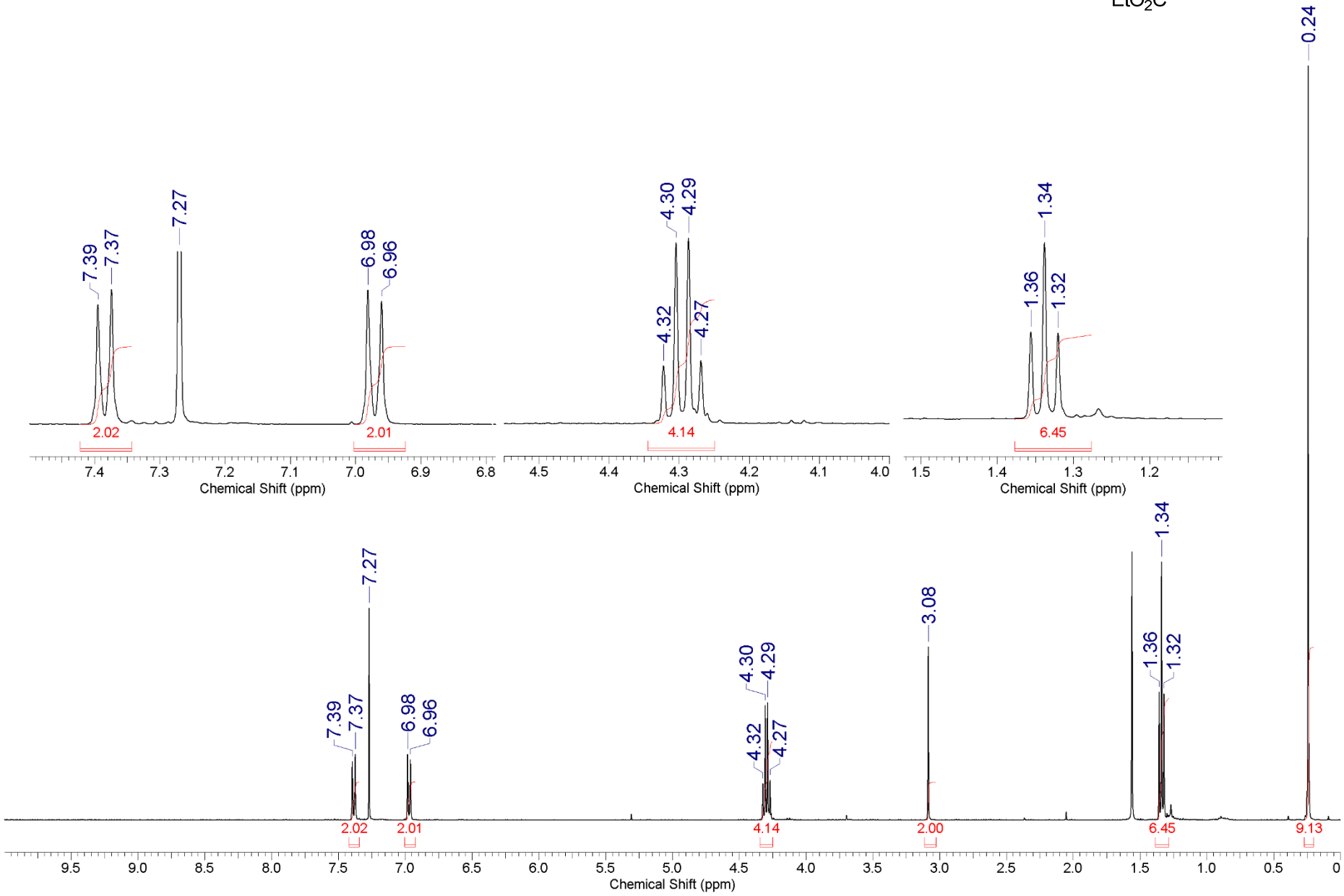

Figure S9. ^{13}C NMR spectrum of compound 5 ($CDCl_3$, 100 MHz), full range.

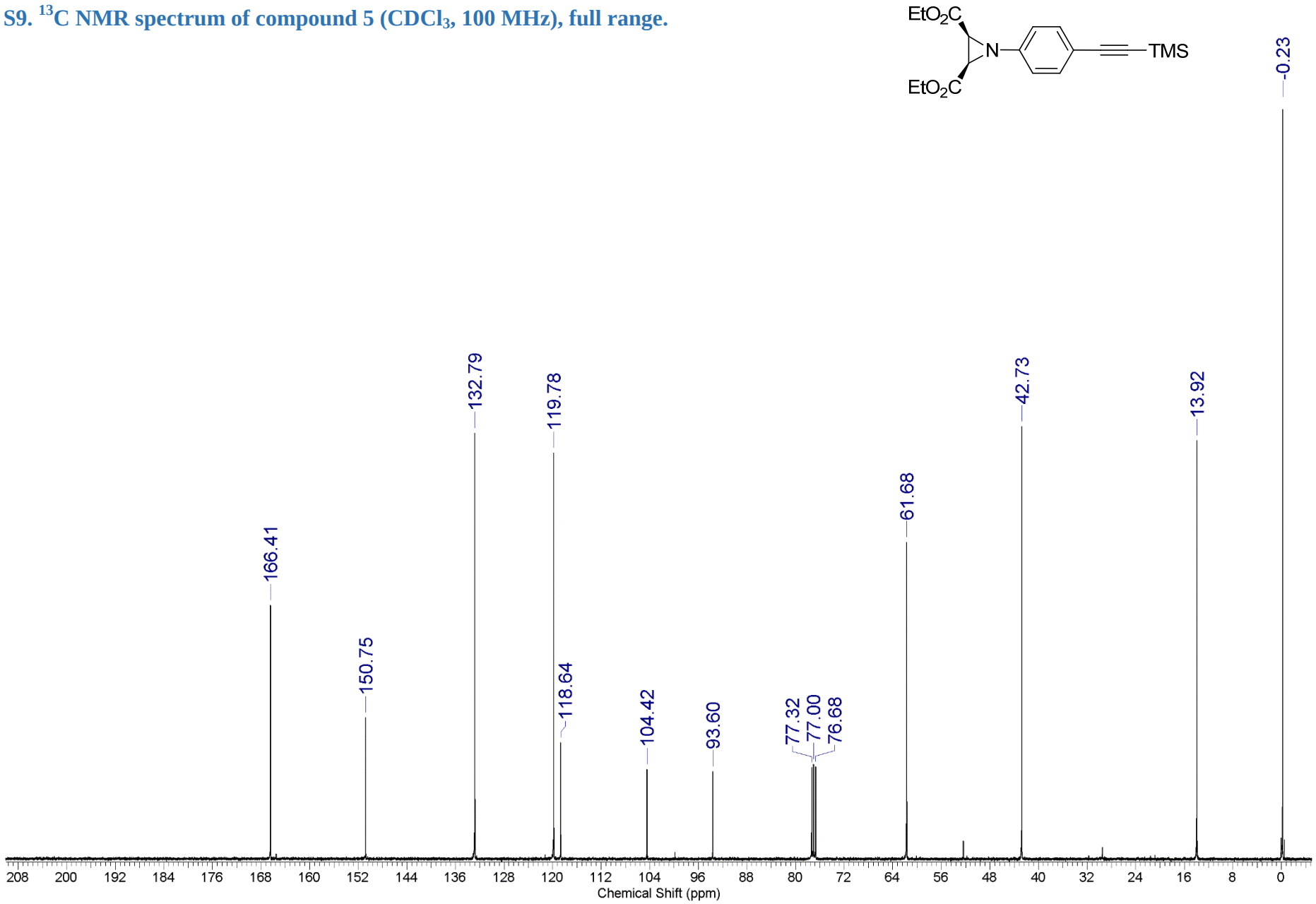

Figure S10. ^{1}H NMR spectrum of compound 7 ($CDCl_3$, 400 MHz), full range.

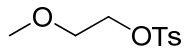

To enhance resolution, FID was subjected to apodization procedure with exponential (-0.3) and gauss (1.3) functions.

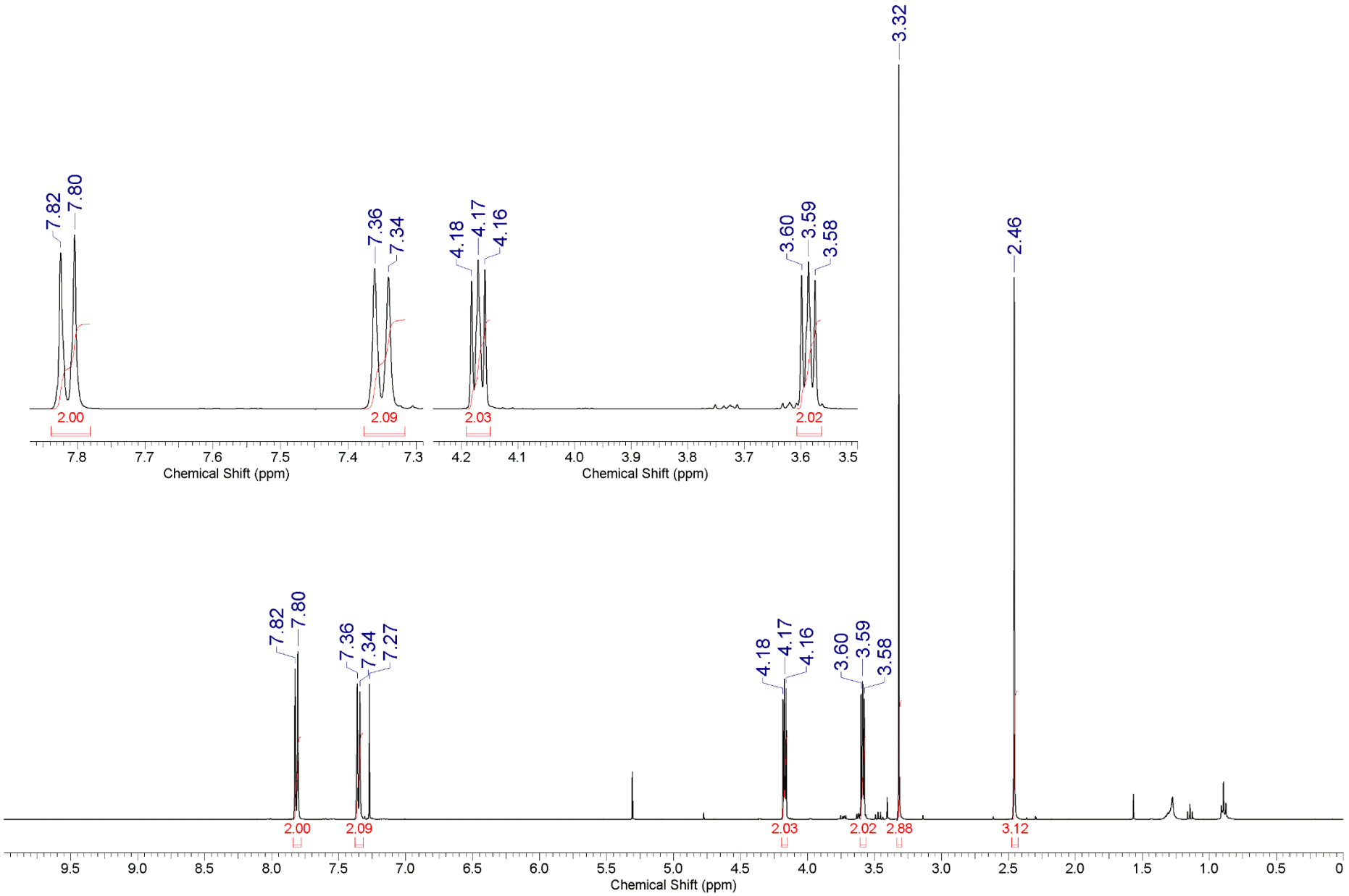

Figure S11. ^{1}H NMR spectrum of compound 8 ($CDCl_3$, 400 MHz), full range.

To enhance resolution, FID was subjected to apodization procedure with exponential (-0.3) and gauss (1.7) functions.

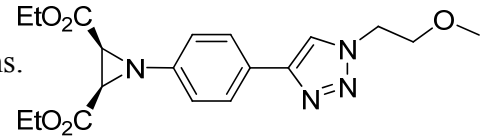

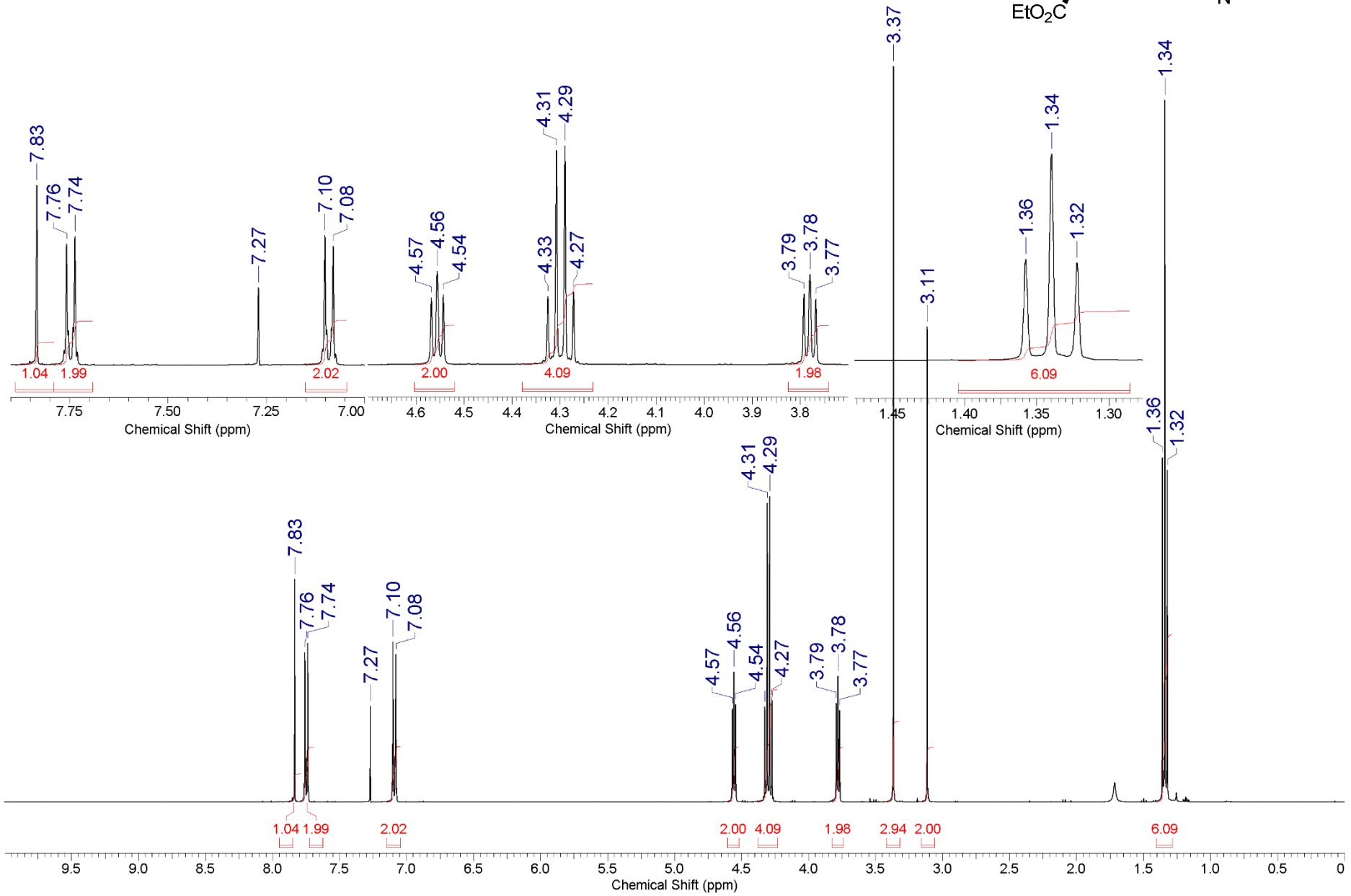

Figure S12. ^{13}C NMR spectrum of compound 8 ($CDCl_3$, 100 MHz), full range.

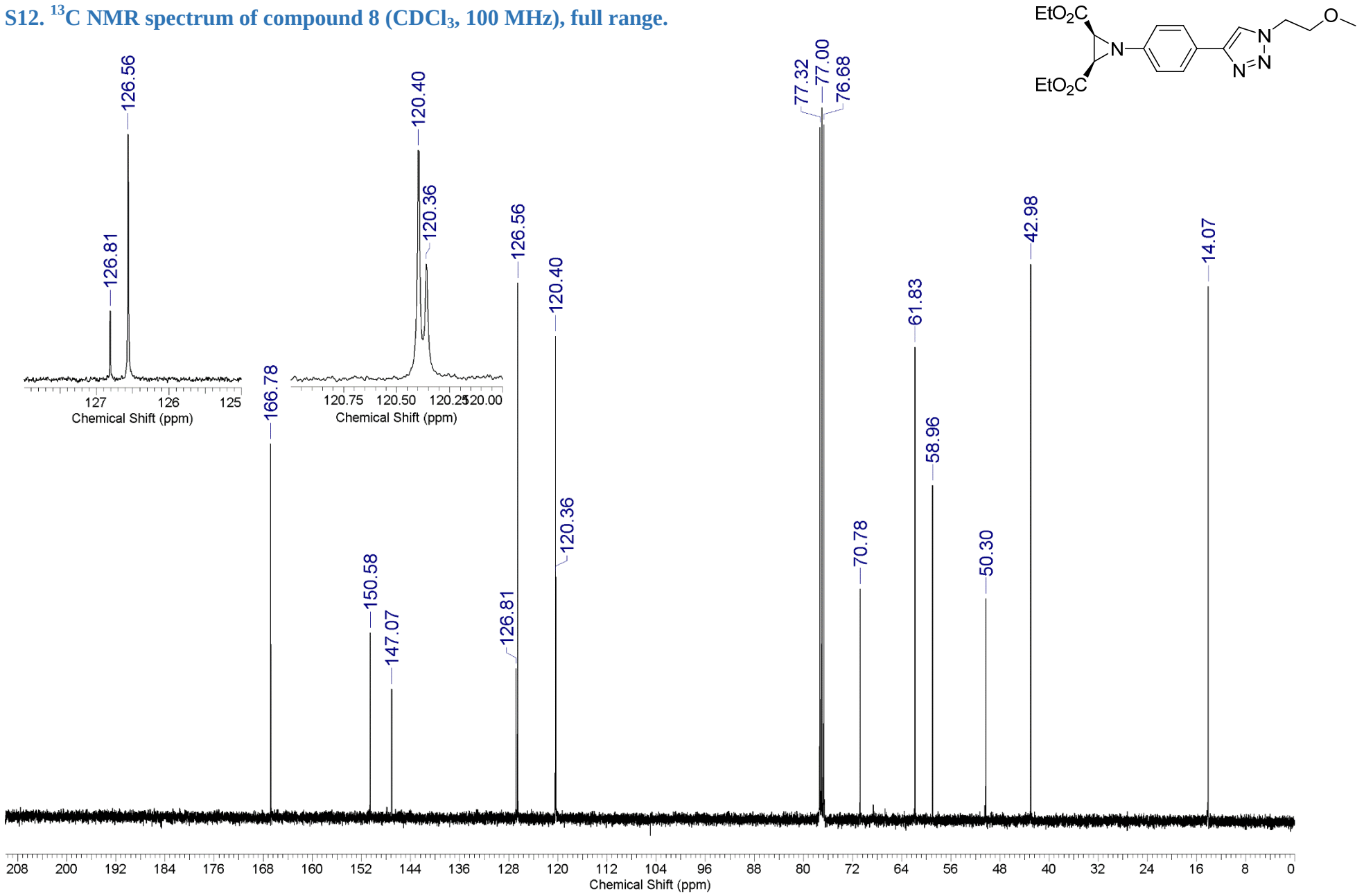

Figure S13. ^{1}H NMR spectrum of compound 9 ($CDCl_3$, 400 MHz), full range.

To enhance resolution, FID was subjected to apodization procedure with exponential (-0.3) and gauss (1.2) functions.

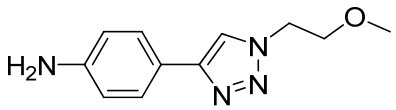

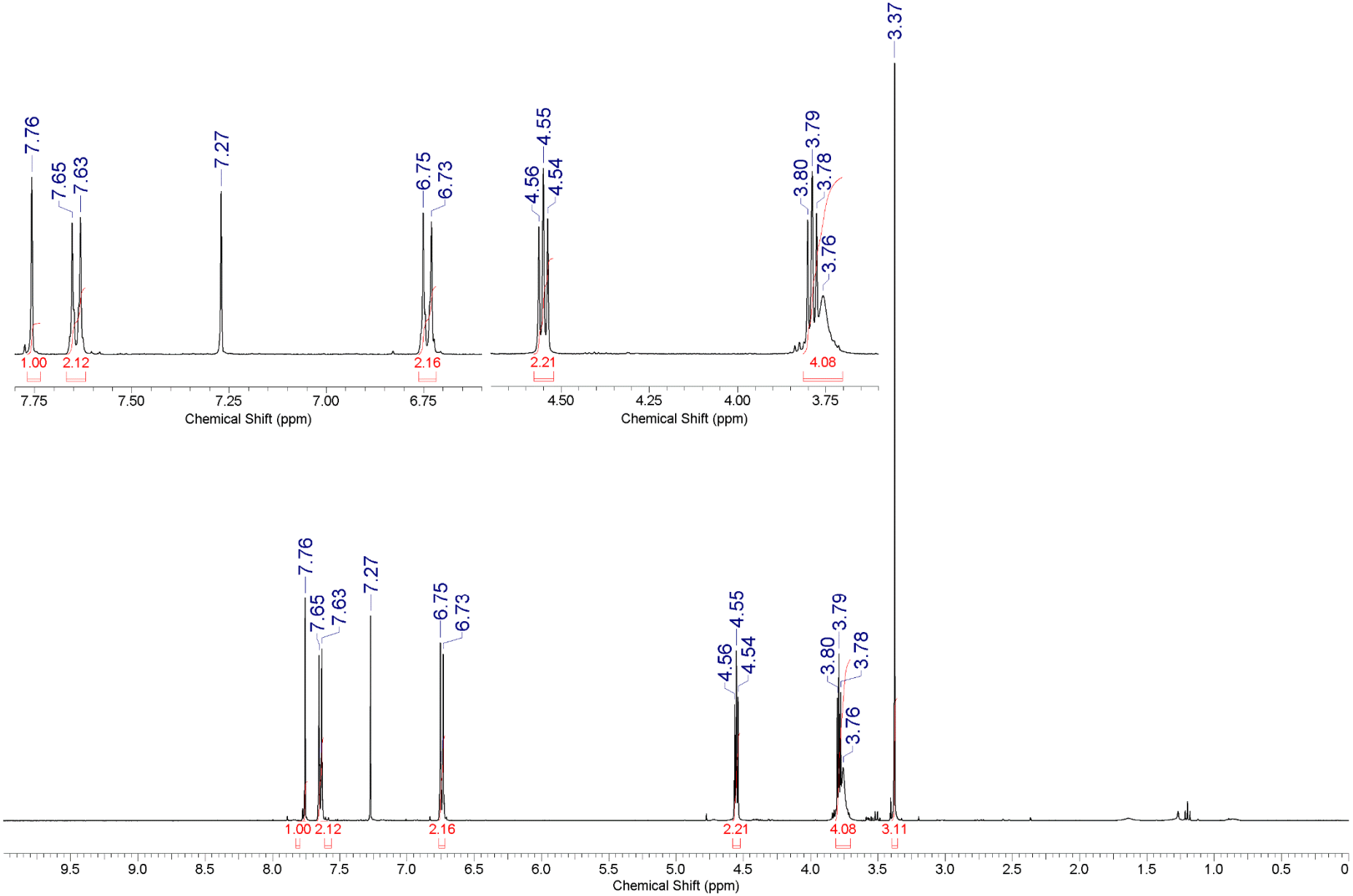

Figure S14. ^{13}C NMR spectrum of compound 9 ($CDCl_3$, 100 MHz), full range.

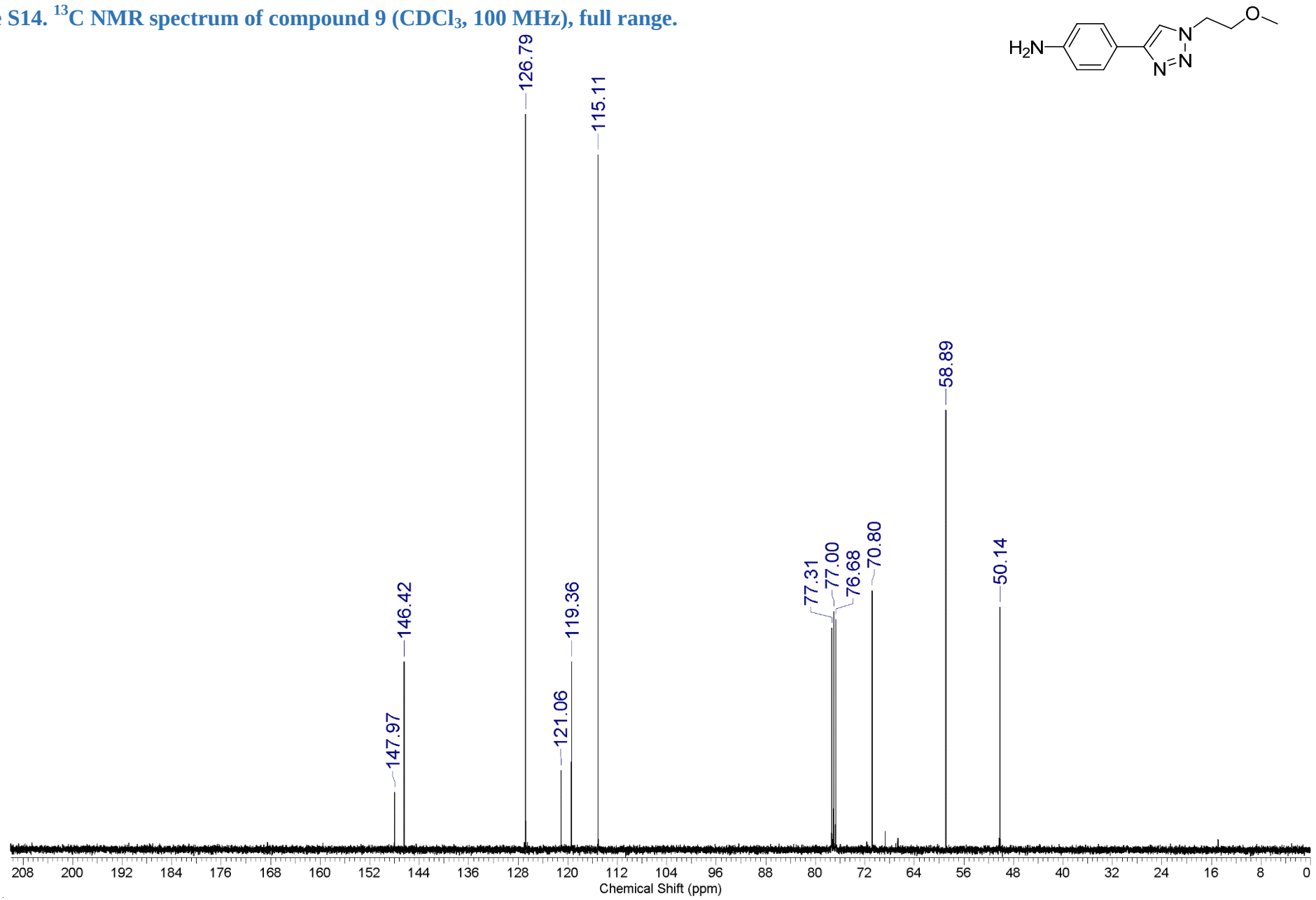

Figure S15. ^{1}H NMR spectrum of compound 10 ($CDCl_3$, 400 MHz), full range.

To enhance resolution, FID was subjected to apodization procedure with exponential (-0.3) and gauss (1.7) functions.

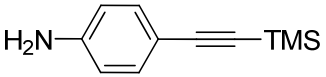

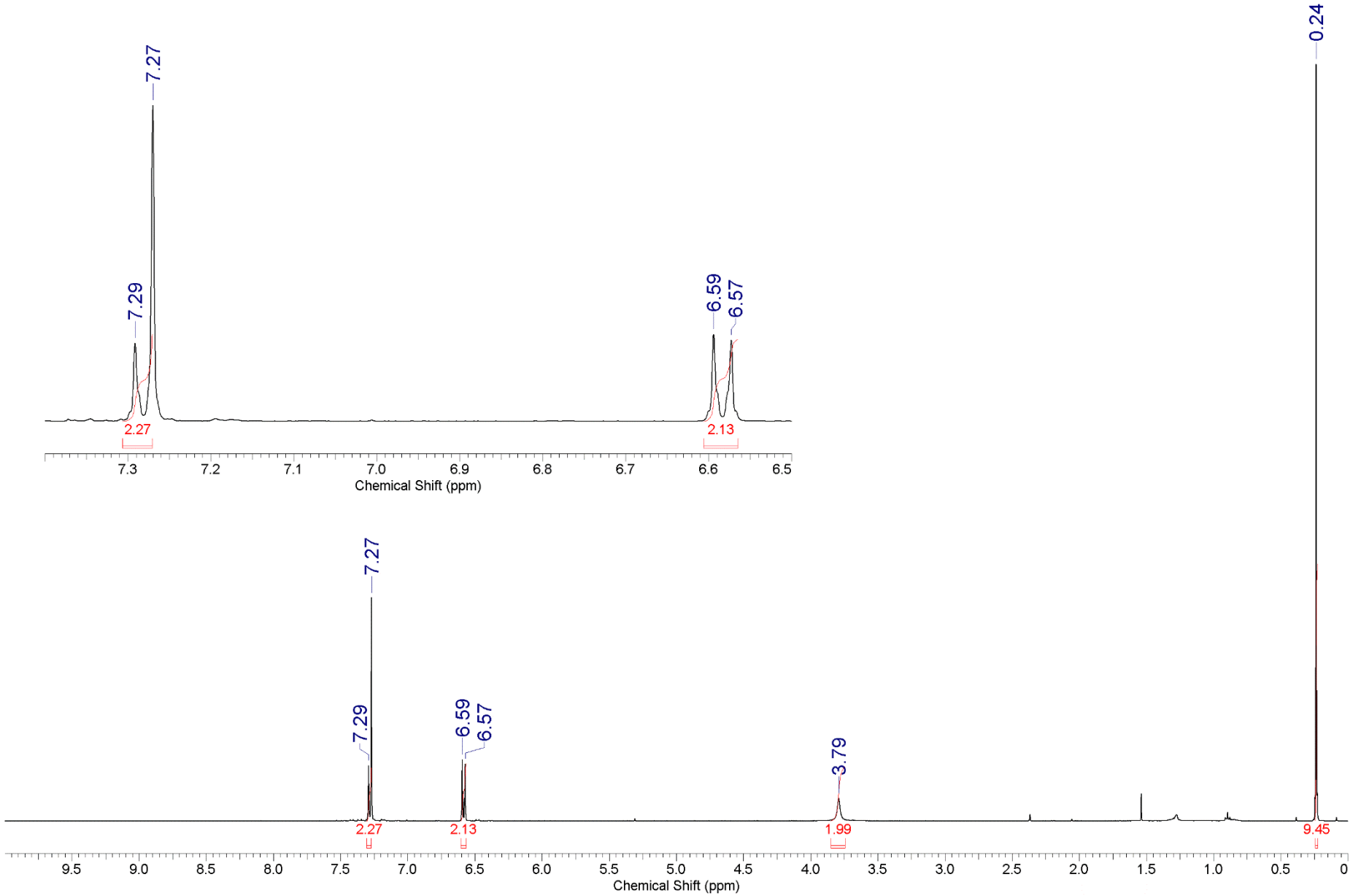

Figure S16. ^{1}H NMR spectrum of compound 11 ($CDCl_3$, 400 MHz), full range.

To enhance resolution, FID was subjected to apodization procedure with exponential (-0.3) and gauss (1.7) functions.

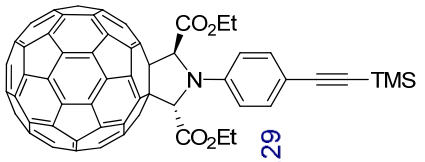

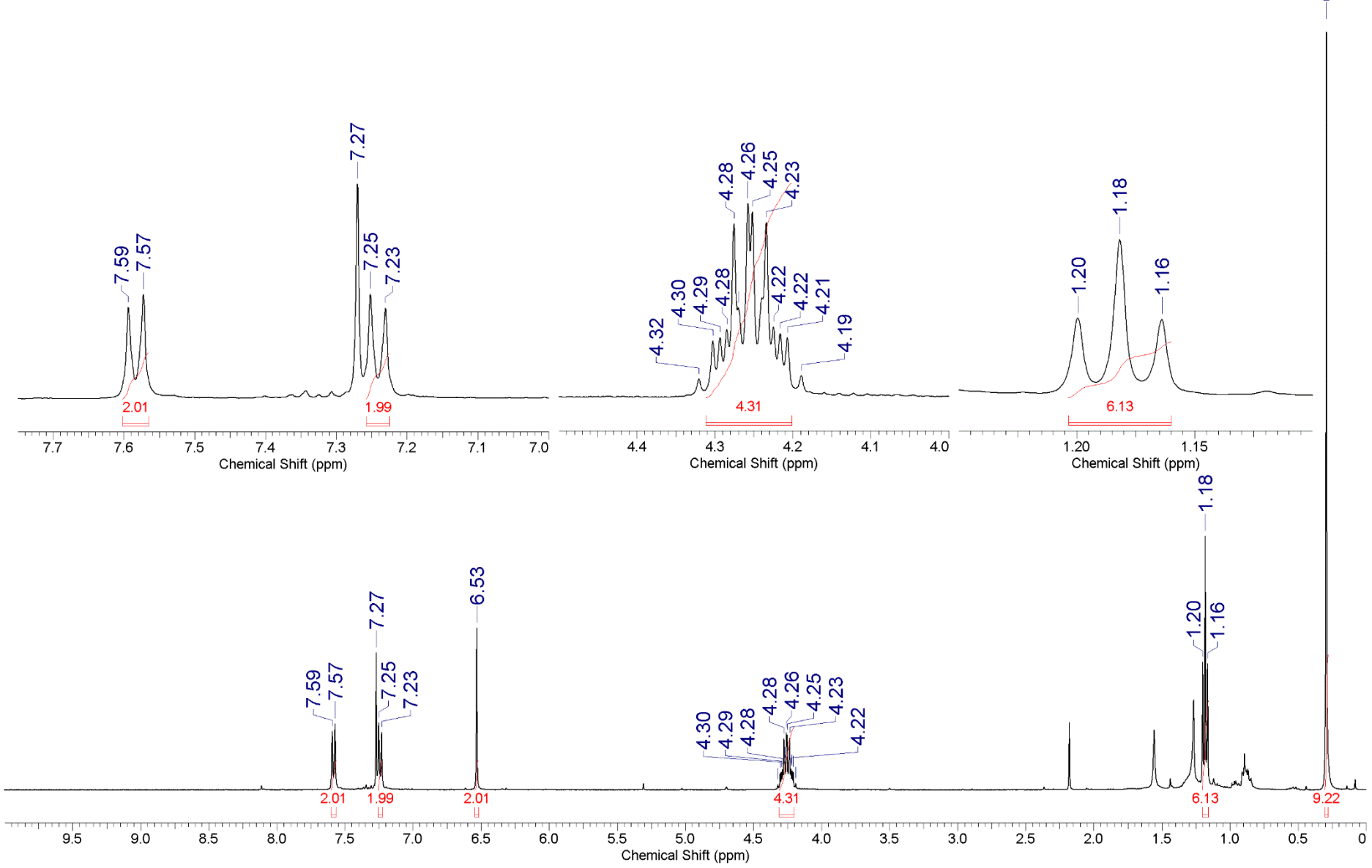

Figure S17. ^{13}C NMR spectrum of compound 11 ($CDCl_3$, 100 MHz), full range.

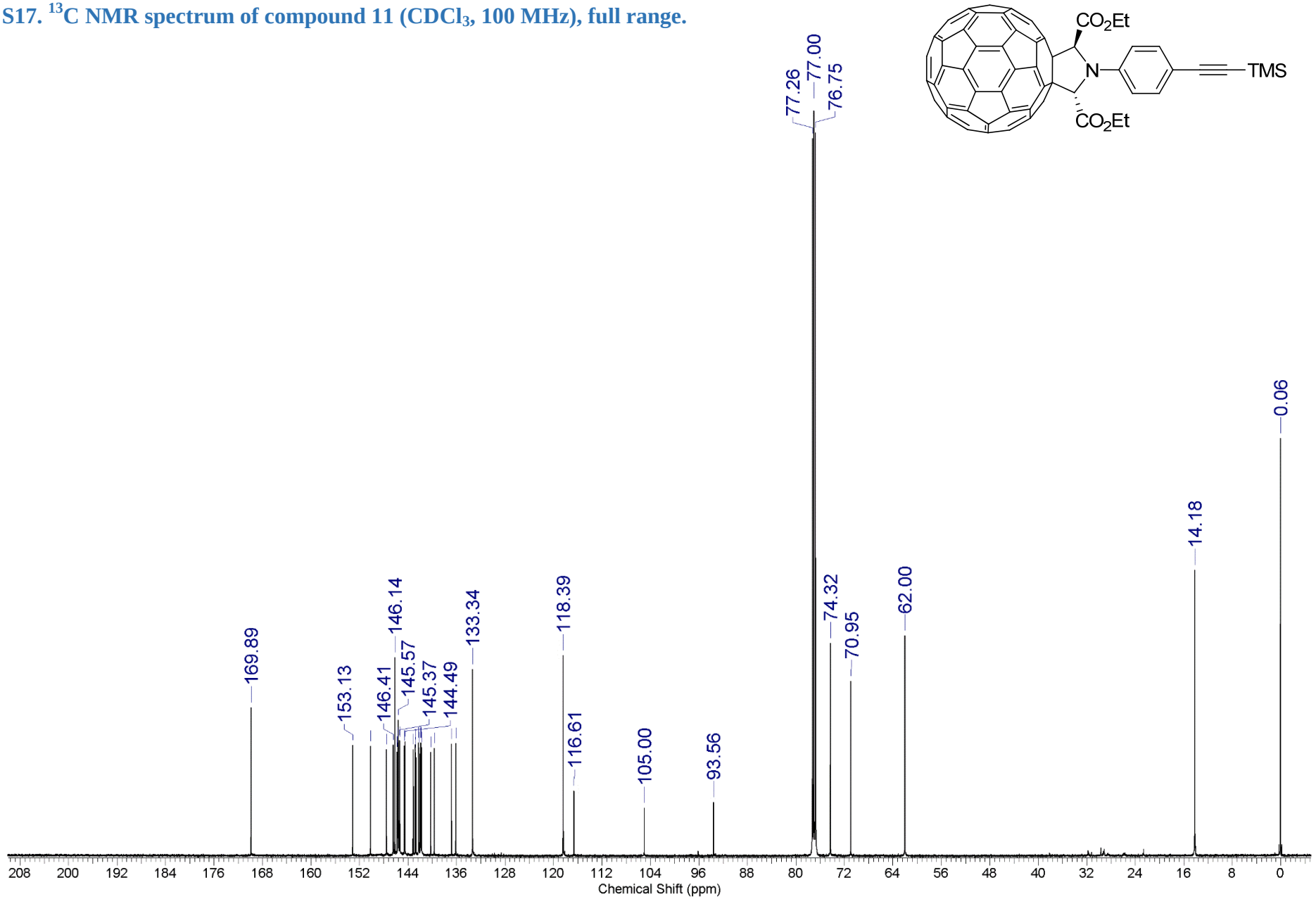

Figure S18. ^{13}C NMR spectrum of compound 11 ($CDCl_3$, 100 MHz), extension for 135 – 151 ppm range.

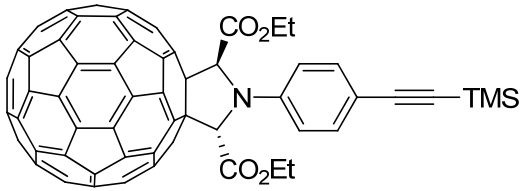

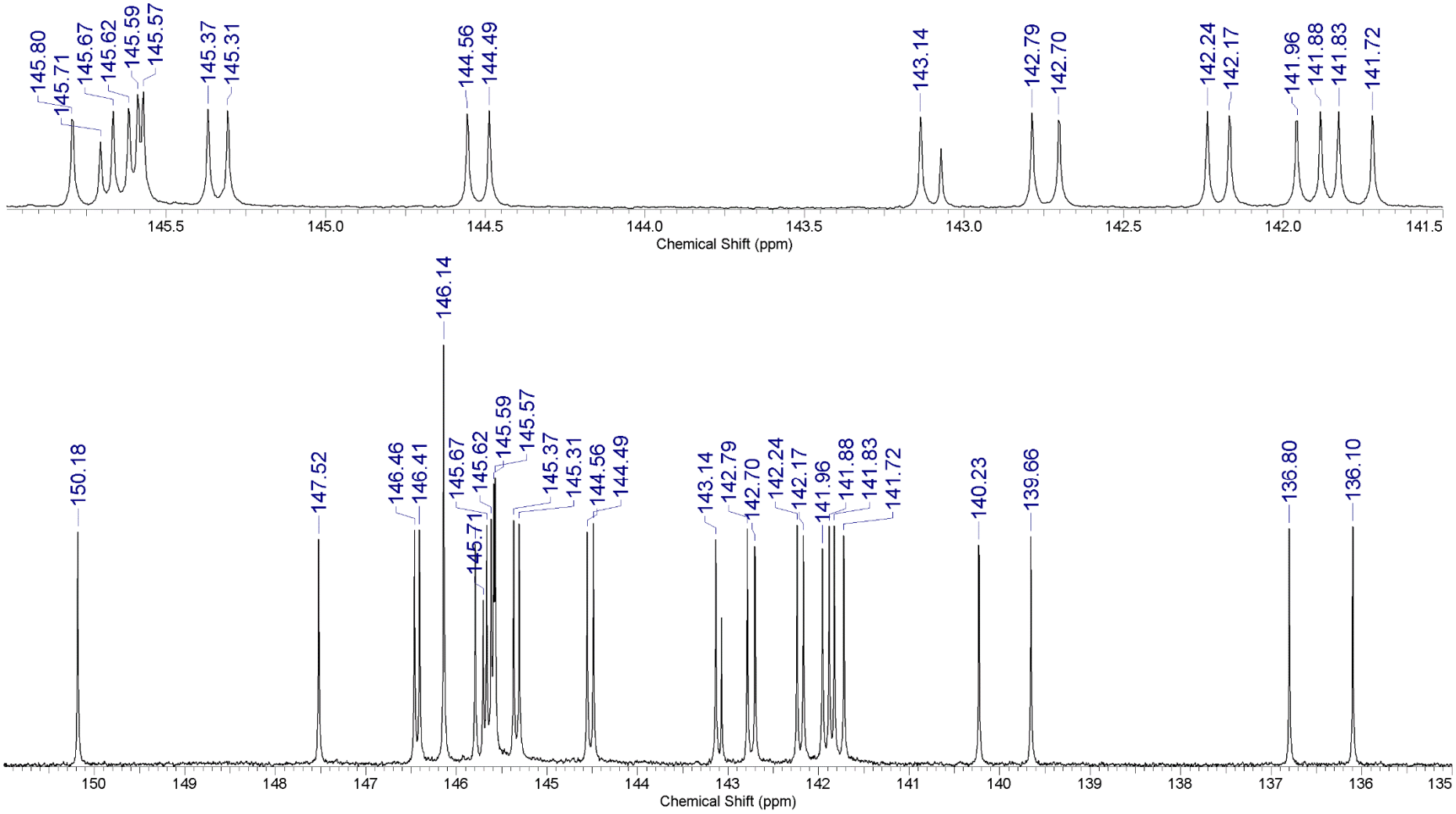

Figure S19. ^{1}H NMR spectrum of compound 12 (CS_2, 300 MHz), full range.

To enhance resolution, FID was subjected to apodization procedure with exponential (-0.3) and gauss (1.7) functions.

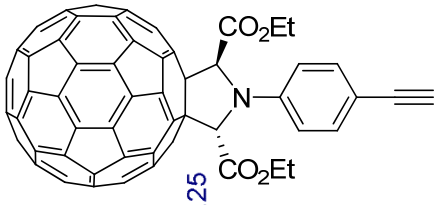

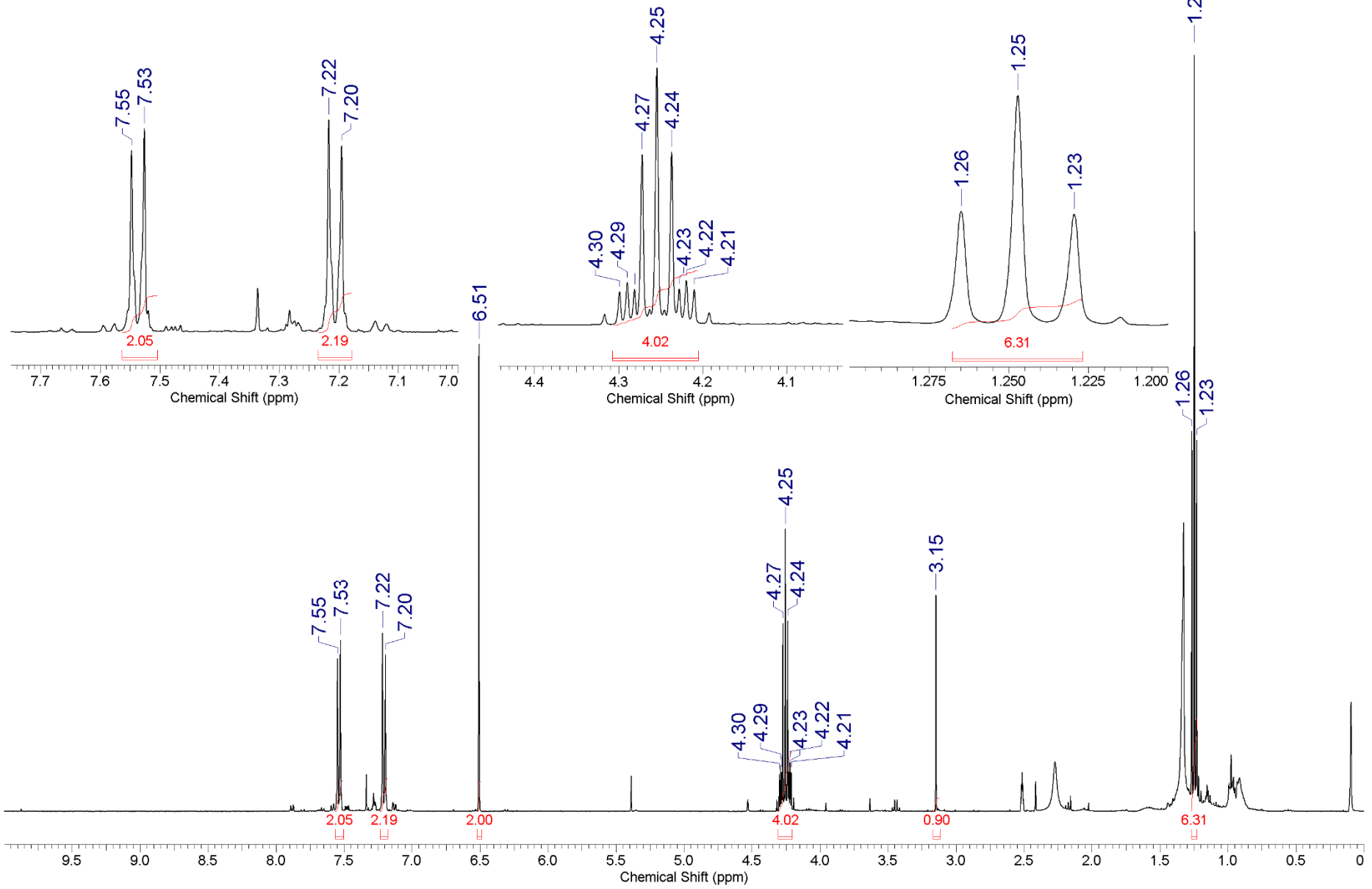

Figure S20. ^{13}C NMR spectrum of compound 12 (CS_2, 100 MHz), extension for 0 – 180 ppm range.

To enhance resolution, FID was subjected to apodization procedure with exponential (-0.5) and gauss (1.5) functions. Asterisk (*) marks C_{60} signal.

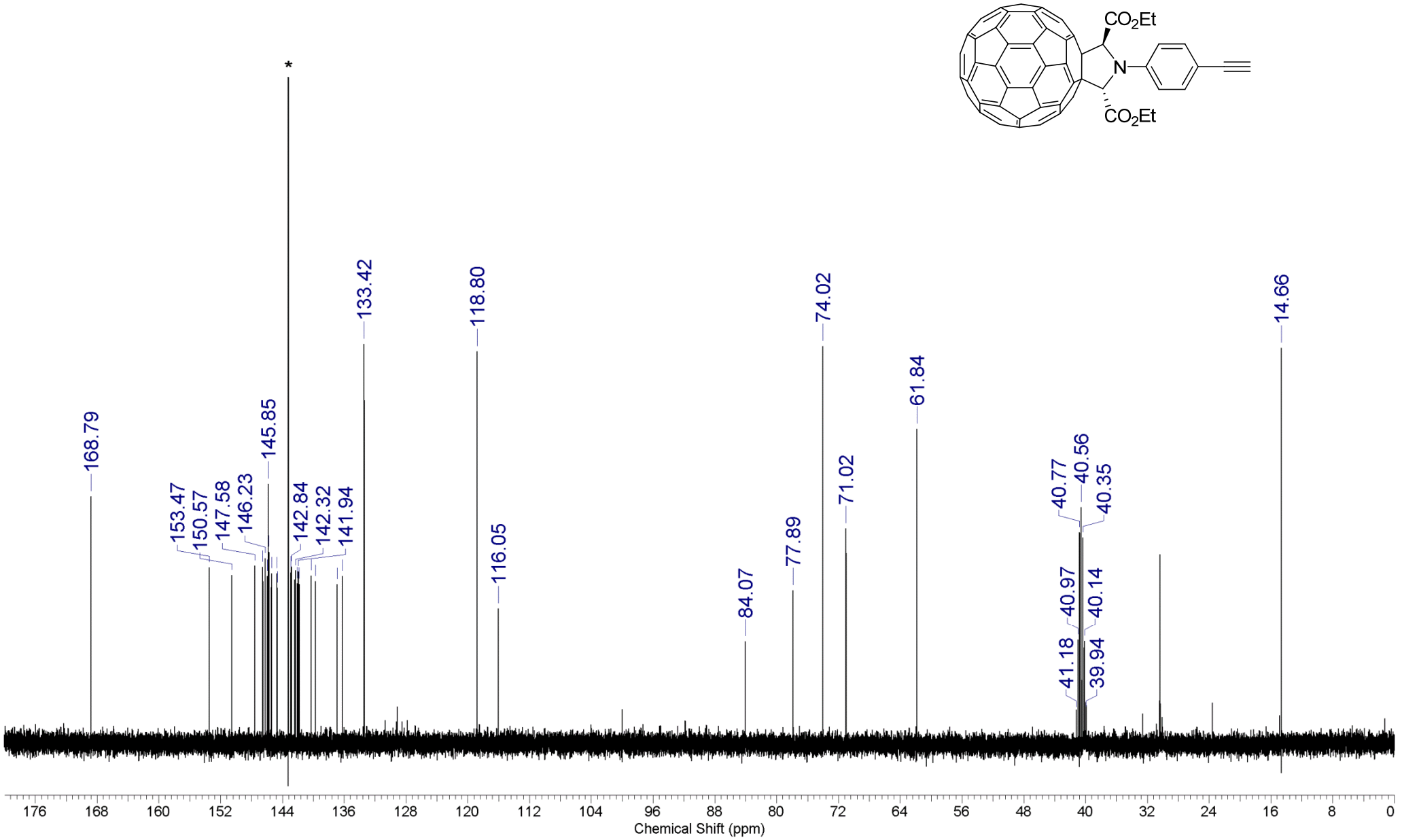

Figure S21. ^{13}C NMR spectrum of compound 12 (CS_2, 100 MHz), extension for 141 – 148 ppm range.

To enhance resolution, FID was subjected to apodization procedure with exponential (-0.5) and gauss (1.5) functions. Asterisk (*) marks C_{60} signal.

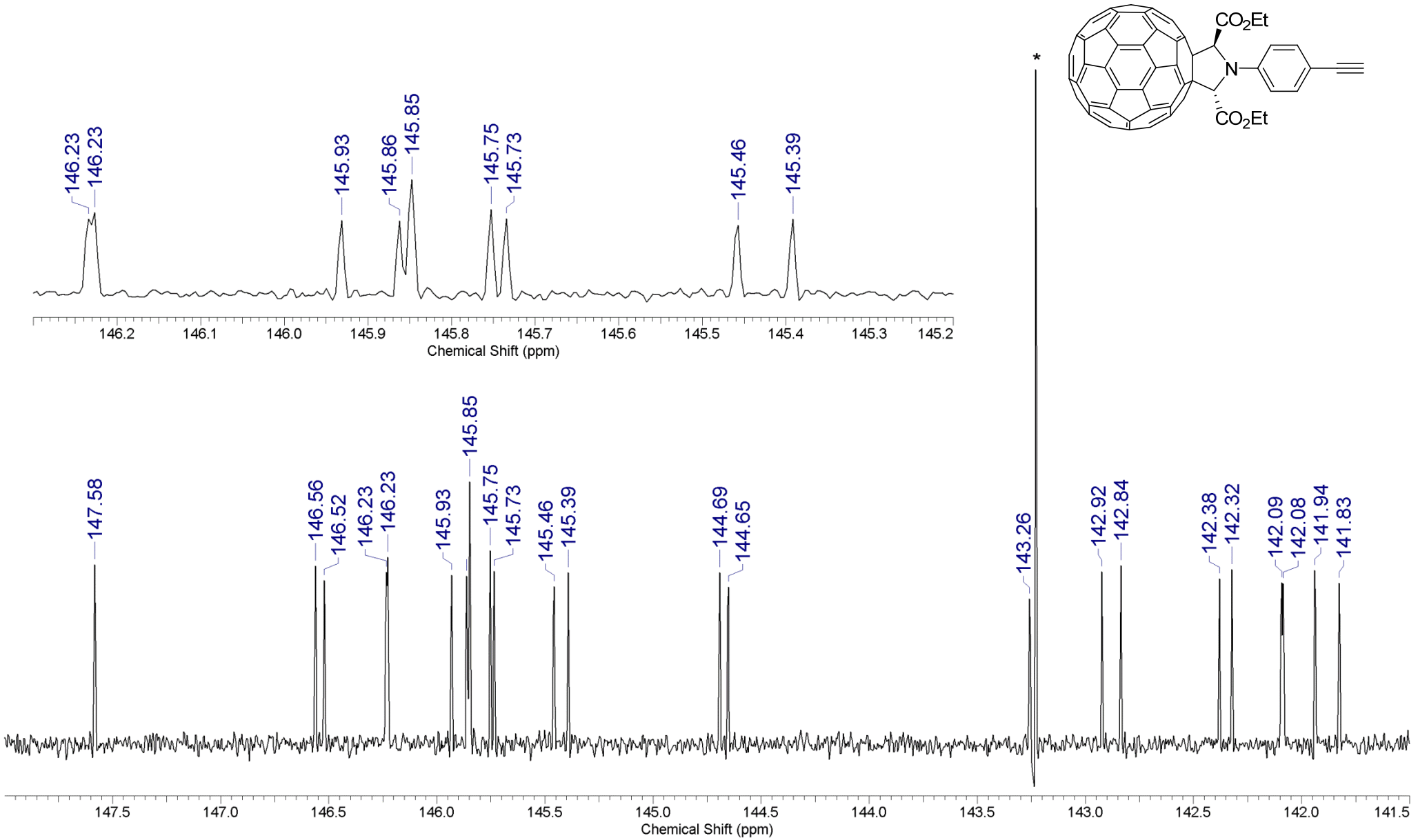

Figure S22. ^{1}H NMR spectrum of compound 14 ($CDCl_3$, 400 MHz), full range.

To enhance resolution, FID was subjected to apodization procedure with exponential (-0.3) and gauss (1.8) functions.

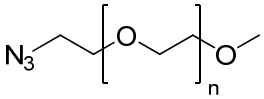

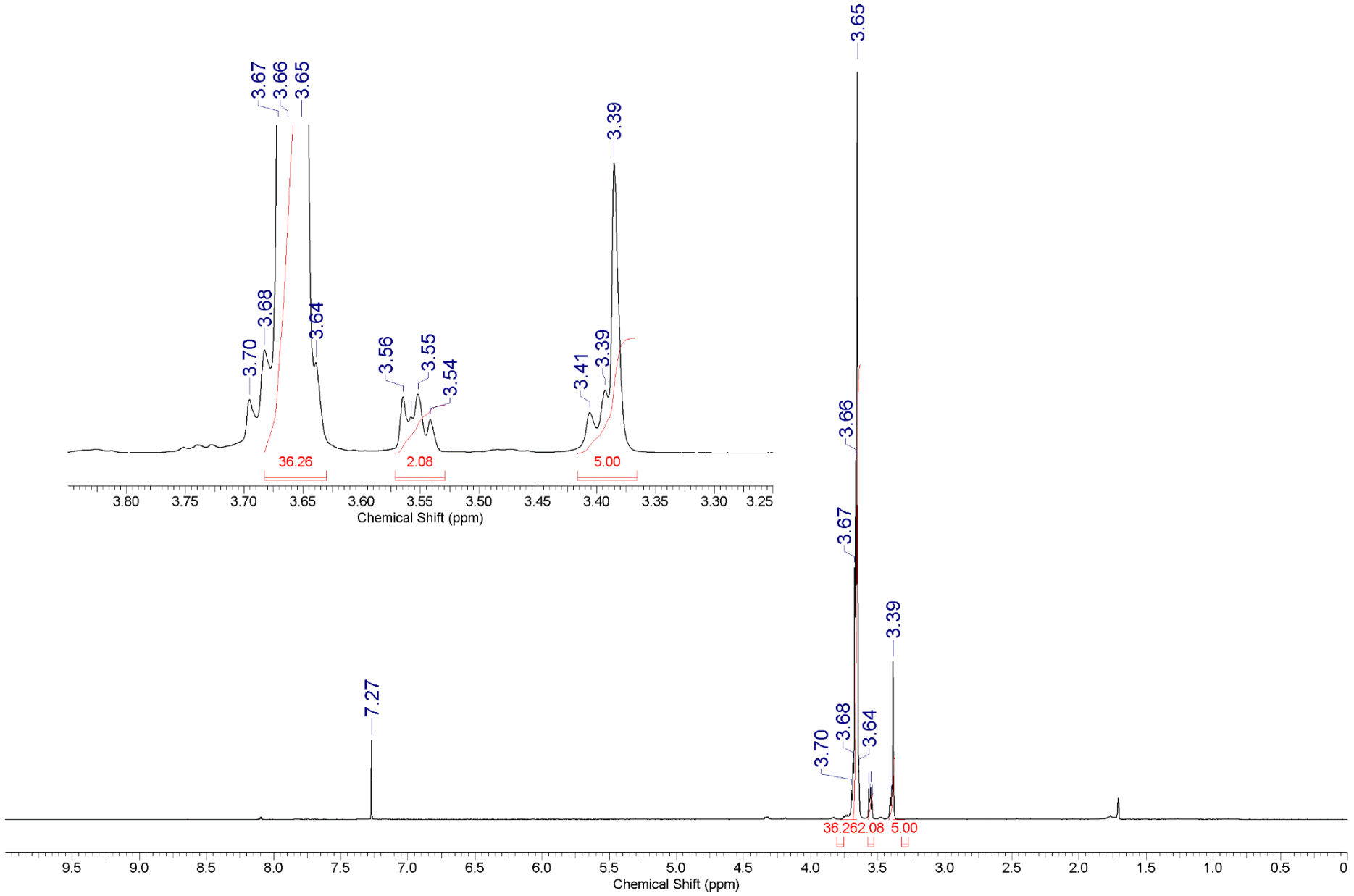

Figure S23. ^{1}H NMR spectrum of compound 15 ($CDCl_3$, 400 MHz), full range.

To enhance resolution, FID was subjected to apodization procedure with exponential (-0.3) and gauss (1.7) functions.

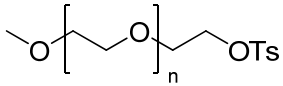

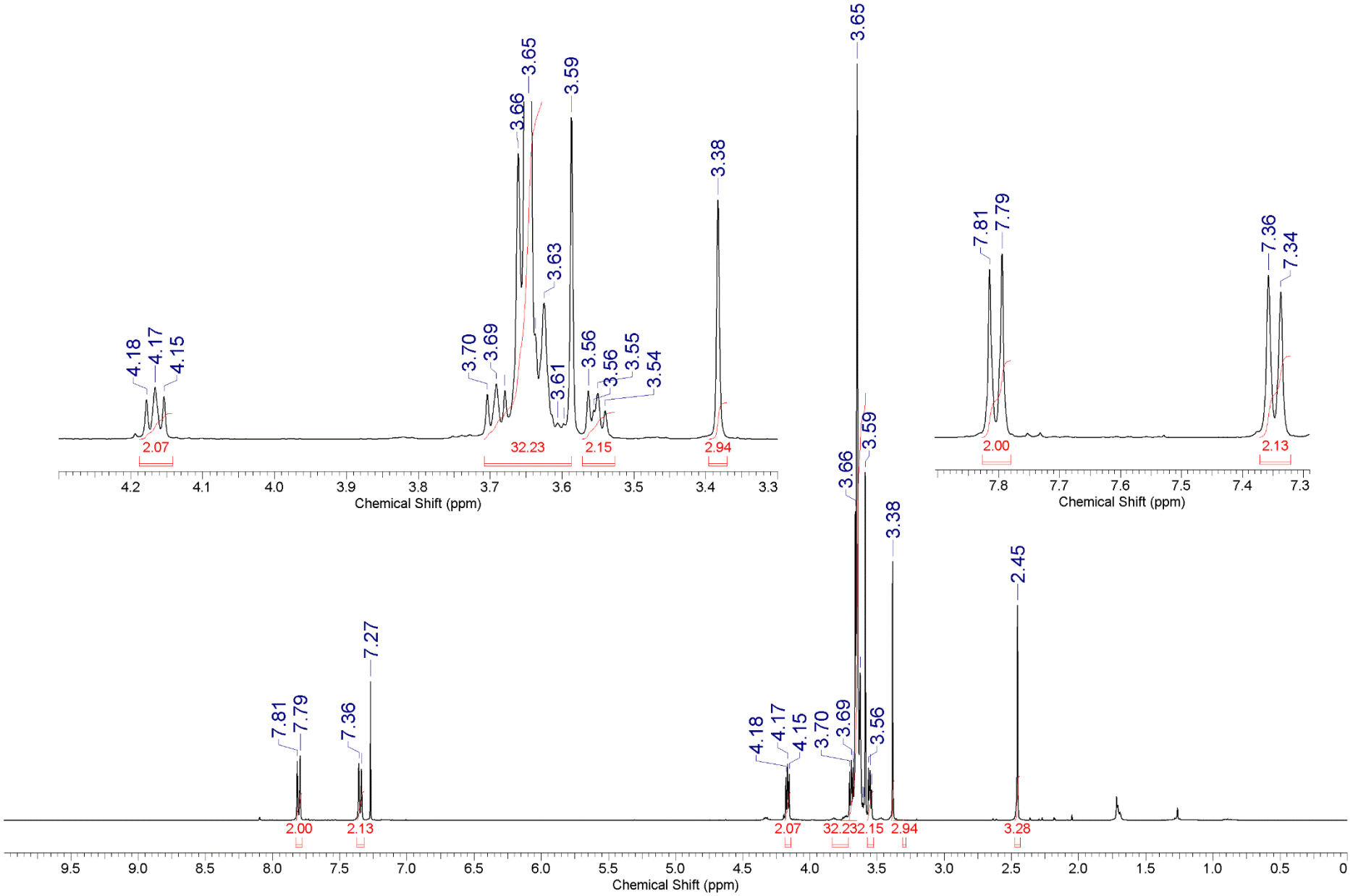

Figure S24. ^{1}H NMR spectrum of compound 16 ($CDCl_3$, 400 MHz), full range.

To enhance resolution, FID was subjected to apodization procedure with exponential (-0.3) and gauss (1.7) functions.

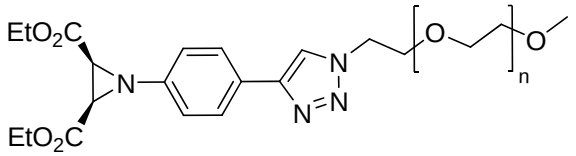

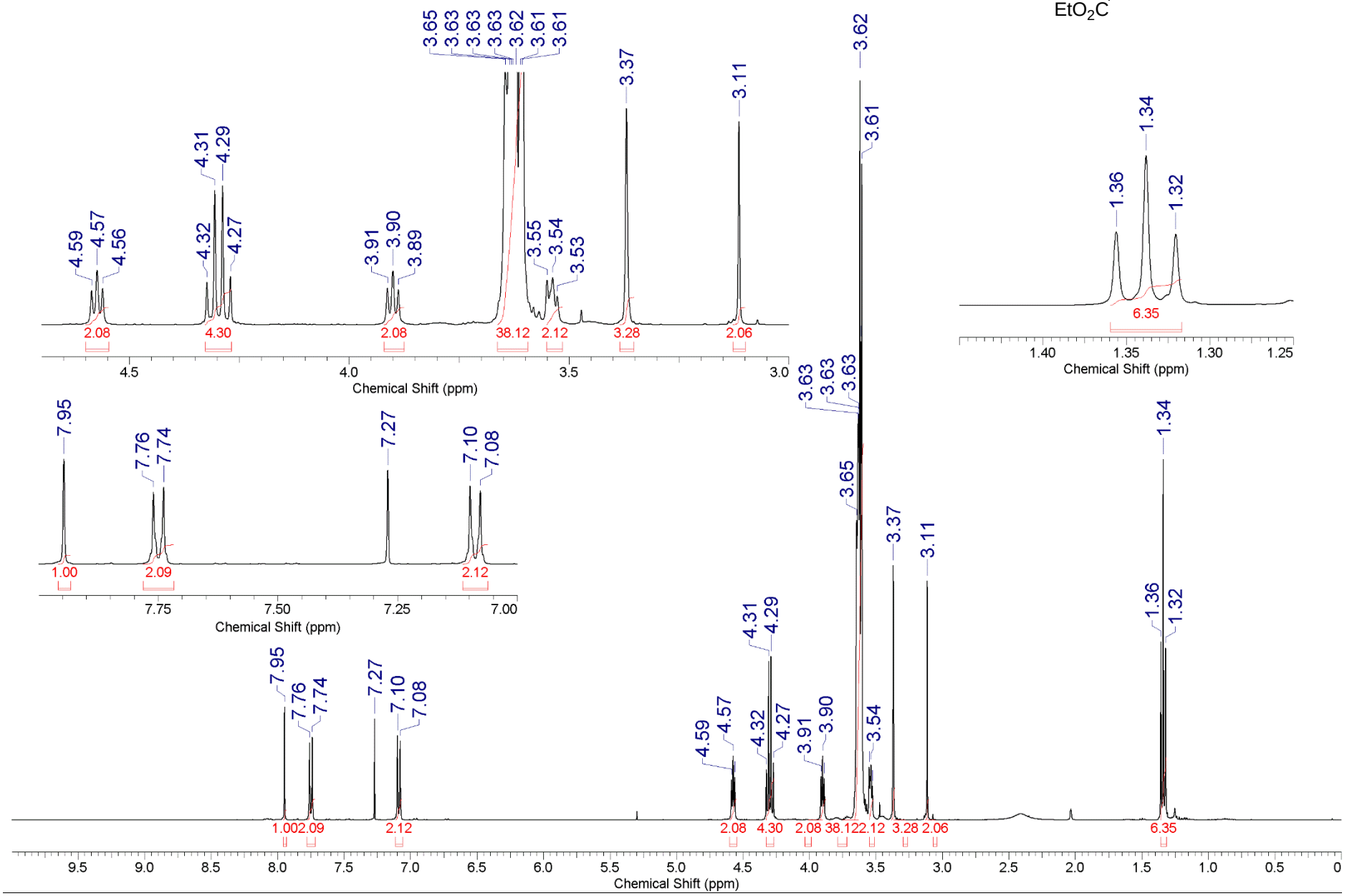

Figure S25. ^{13}C NMR spectrum of compound 16 ($CDCl_3$, 100 MHz), full range.

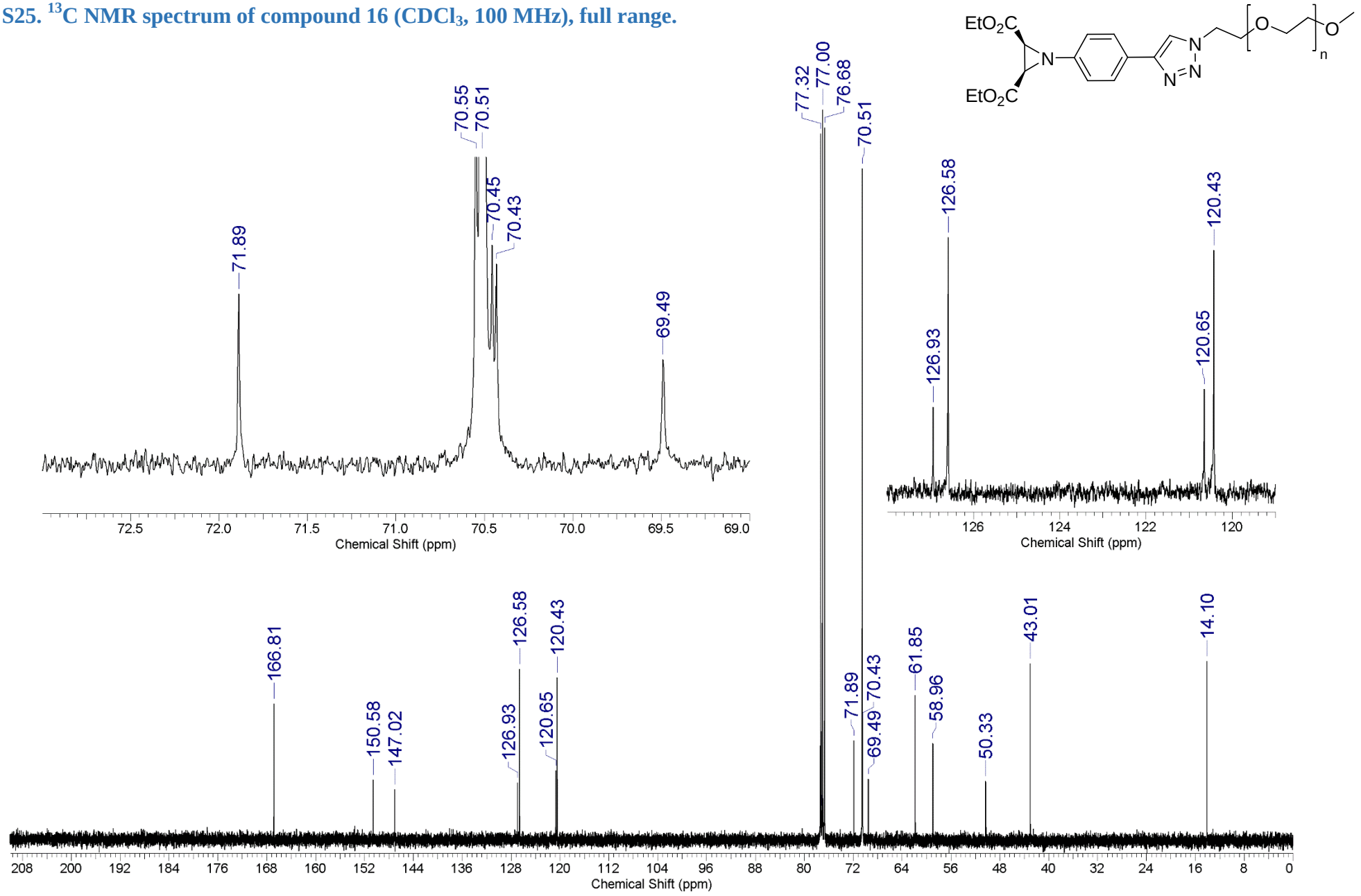

Table S1. AFM data for samples of compound 2 deposited on mica from aqueous solutions.

Sample number	Concentration, mg/L	Deposition	Delay, min	Image number	Max height, nm	Average height, nm	Median height, nm	Max equivalent disc radius, nm	Average equivalent disc radius, nm	Median equivalent disc radius, nm	Number of grains, pc	Density, pc/μm	Image area, μm^2
1	0.5	spin-coating	0.5	1	1.7	1.0	0.9	15.8	11.4	11.0	23	2.6	9
				2	2.3	1.1	1.0	17.2	11.9	11.0	64	2.6	25
2	0.05	spin-coating	0.5	1	4.8	1.1	0.9	36.0	13.7	13.0	270	30.0	9
				2	2.9	1.0	0.8	31.0	10.8	9.6	185	46.3	4
				3	11.4	0.9	0.7	54.5	10.5	7.8	1050	42.0	25
3	0.05	spin-coating	0.5	1	4.1	1.6	0.8	15.6	10.2	9.4	6	0.2	25
4	0.05	spin-coating	1	1	5.0	1.1	0.8	16.2	8.1	7.8	94	3.8	25
				2	4.8	1.3	0.9	13.2	7.5	7.4	43	4.8	9
				3	4.5	1.1	0.6	13.1	5.6	4.9	20	5.0	4
				4	5.5	1.1	0.9	12.3	5.7	4.9	24	6.0	4
5	0.5	spin-coating	0.5	1	1.7	0.9	0.8	30.5	13.4	11.7	23	5.8	4
				2	2.8	0.8	0.7	37.3	11.7	10.5	91	10.1	9
				3	1.4	0.8	0.7	19.8	8.9	9.4	95	23.8	4
6	0.5	spin-coating	1	1	2.5	0.9	0.8	54.0	10.0	9.1	353	88.3	4
				2	4.4	0.8	0.7	67.0	10.7	9.5	3134	125.4	25
				3	2.0	1.1	1.0	34.0	18.0	16.7	122	30.5	4
				4	2.6	1.0	0.9	39.5	14.6	13.8	700	77.8	9
7	5	spin-coating	0.5	1	1.2	0.7	0.6	29.0	7.6	5.8	24	2.7	9
8	0.5	spin-coating	-	1	1.2	0.8	0.7	11.2	7.5	7.0	40	10.0	4
9	0.00005	dropcasting	-	1	7.0	1.6	1.4	124.0	23.2	22.0	2419	24.2	100
				2	7.6	1.7	1.5	106.0	26.2	24.6	2293	22.9	100
				3	5.6	1.8	1.6	86.0	29.0	27.7	493	19.7	25
				4	4.6	1.6	1.5	74.0	24.3	24.2	219	24.3	9
				5	4.1	1.5	1.4	56.0	26.0	26.3	156	17.3	9
				6	3.9	1.7	1.6	39.3	25.6	25.4	70	17.5	4
				7	3.6	1.9	1.9	38.0	24.9	24.6	80	20.0	4
				8	5.3	1.8	1.7	104.0	26.2	25.3	617	24.7	25
				9	7.5	1.5	1.3	118.0	29.4	22.0	6627	16.6	400
10	0.00005	dropcasting	-	1	2.7	1.1	1.0	37.3	20.4	20.1	249	27.7	9
				2	3.4	1.1	1.1	47.0	24.4	23.7	442	17.7	25
				3	2.7	1.2	1.2	40.0	25.1	24.8	85	21.3	4

Figure S26. AFM image 1.1 of compound 2 (top), height (middle) and equivalent radius (bottom) distribution of grains (red mask, top picture).

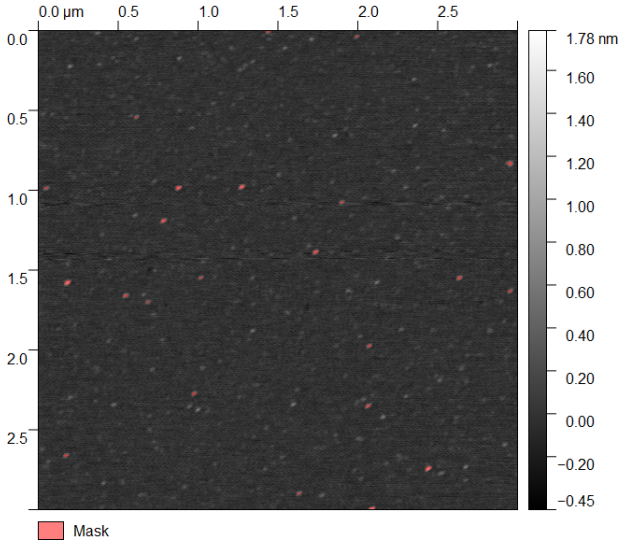

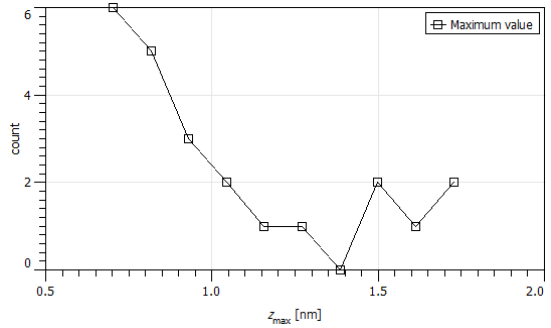

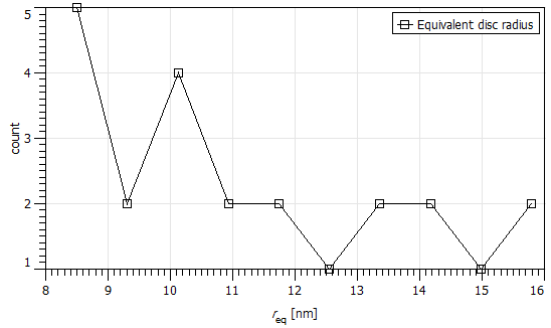

Figure S27. AFM image 1.2 of compound 2 (top), height (middle) and equivalent radius (bottom) distribution of grains (red mask, top picture).

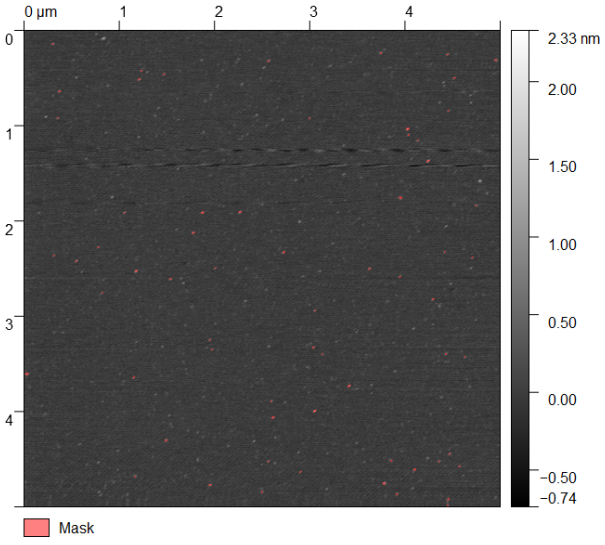

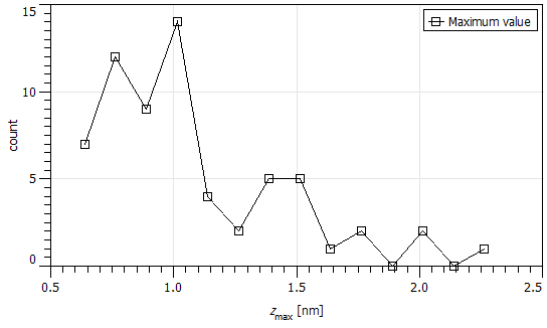

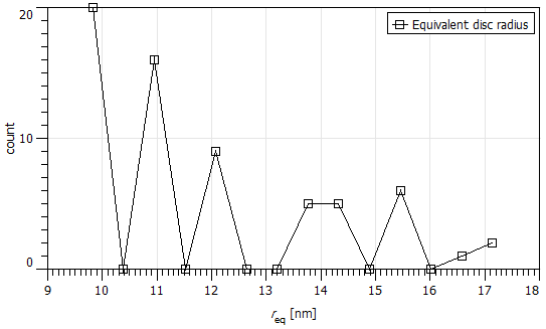

Figure S28. AFM image 2.1 of compound 2 (top), height (middle) and equivalent radius (bottom) distribution of grains (red mask, top picture).

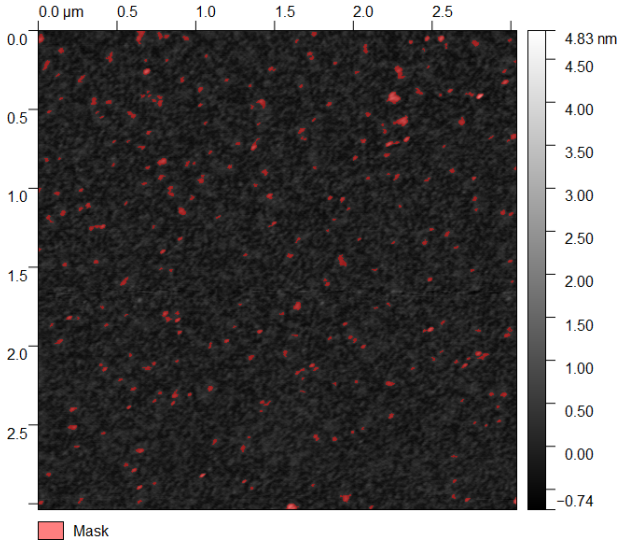

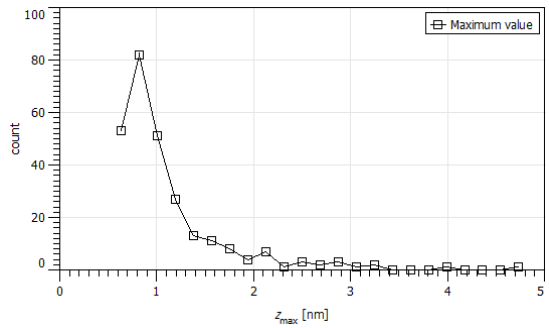

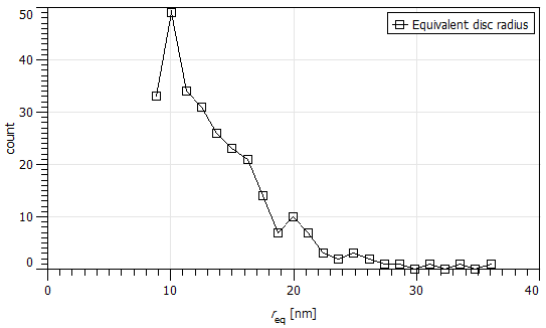

Figure S29. AFM image 2.2 of compound 2 (top), height (middle) and equivalent radius (bottom) distribution of grains (red mask, top picture).

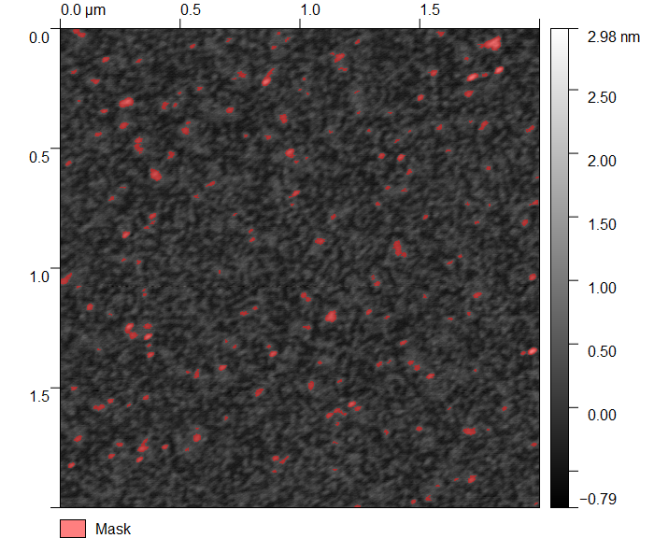

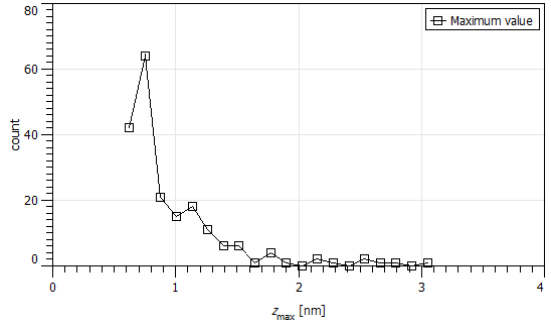

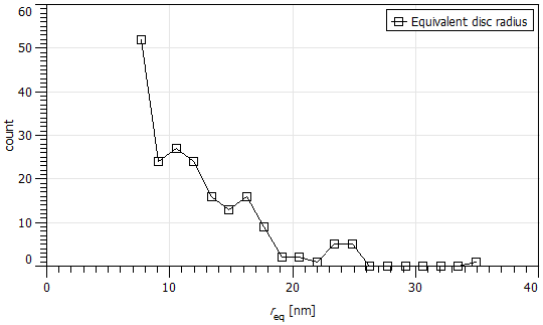

Figure S30. AFM image 2.3 of compound 2 (top), height (middle) and equivalent radius (bottom) distribution of grains (red mask, top picture).

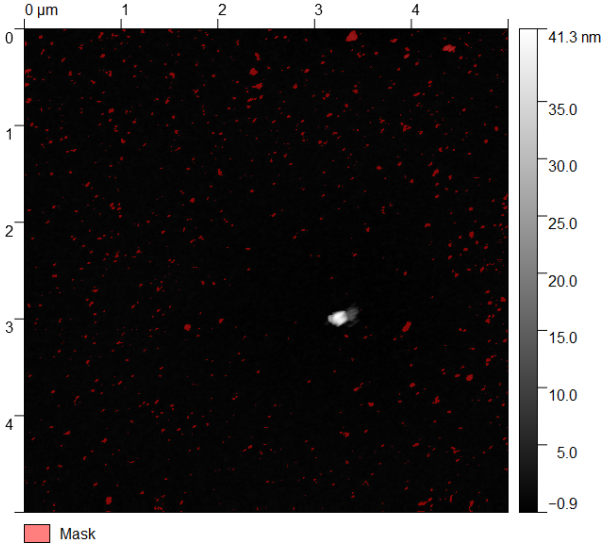

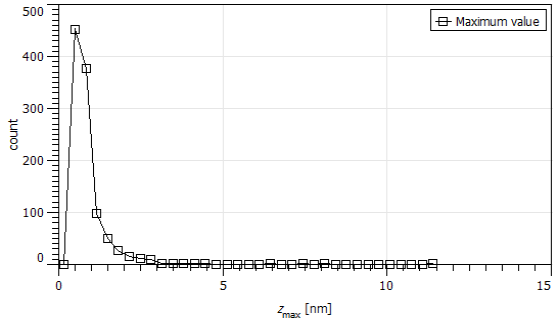

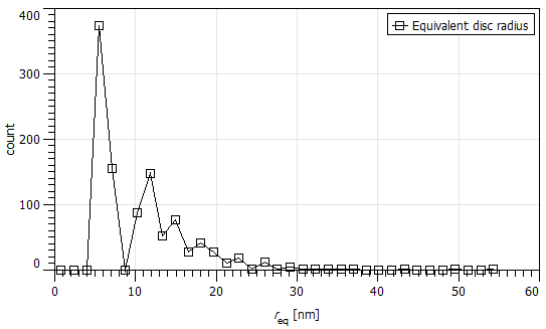

Figure S31. AFM image 3.1 of compound 2 (top), height (middle) and equivalent radius (bottom) distribution of grains (red mask, top picture).

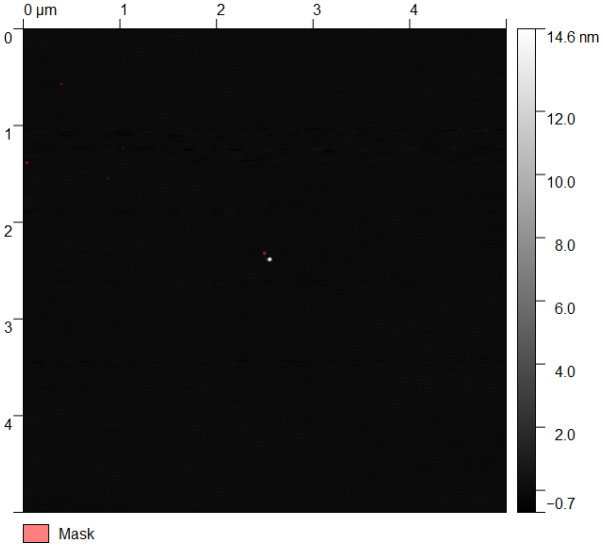

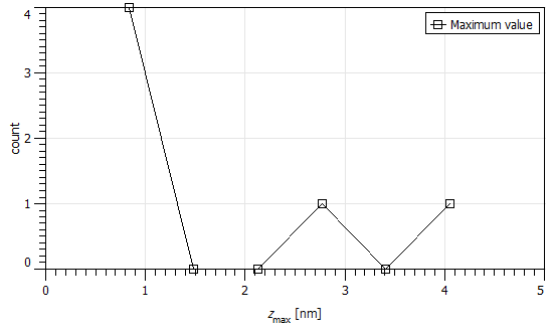

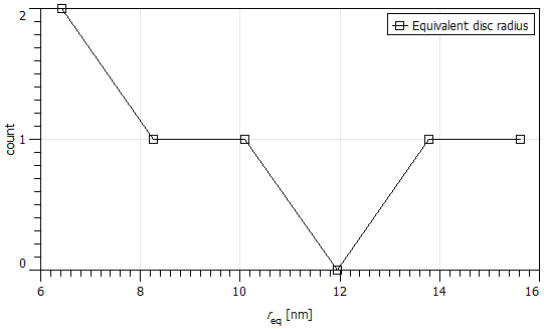

Figure S32. AFM image 4.1 of compound 2 (top), height (middle) and equivalent radius (bottom) distribution of grains (red mask, top picture).

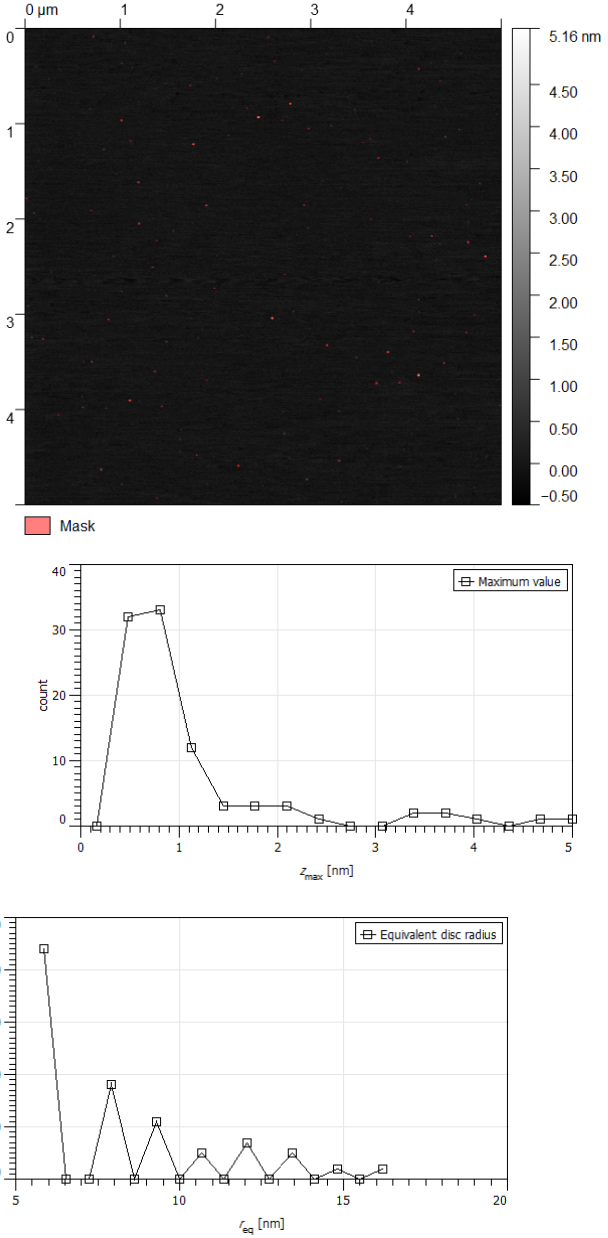

Figure S33. AFM image 4.2 of compound 2 (top), height (middle) and equivalent radius (bottom) distribution of grains (red mask, top picture).

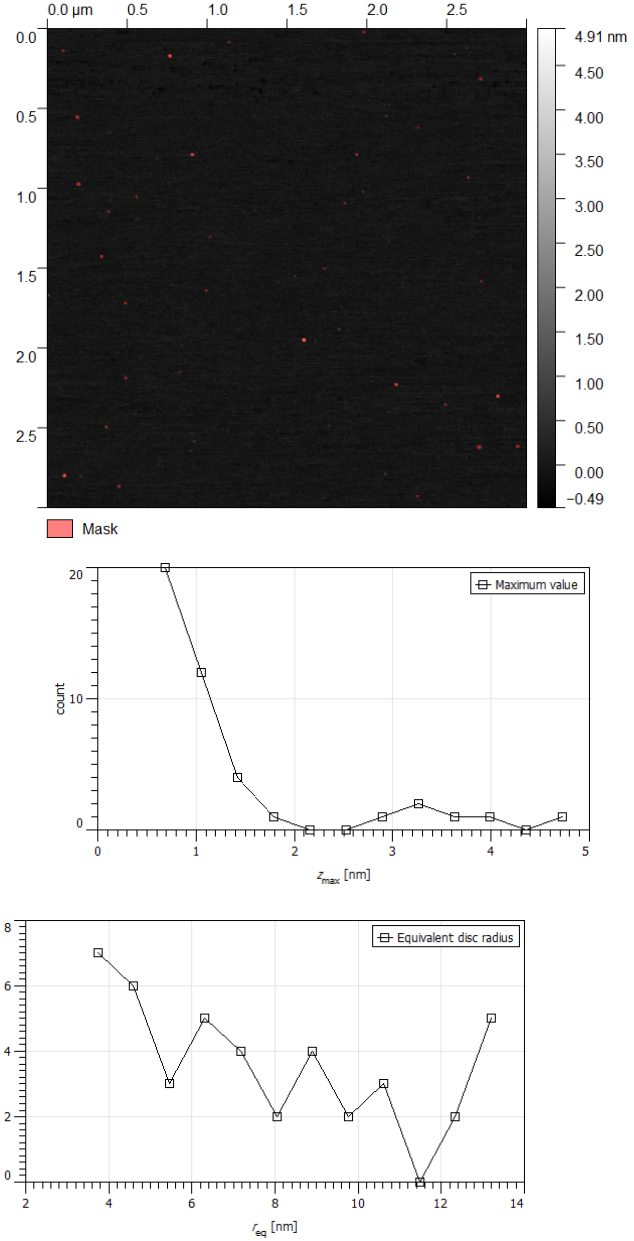

Figure S34. AFM image 4.3 of compound 2 (top), height (middle) and equivalent radius (bottom) distribution of grains (red mask, top picture).

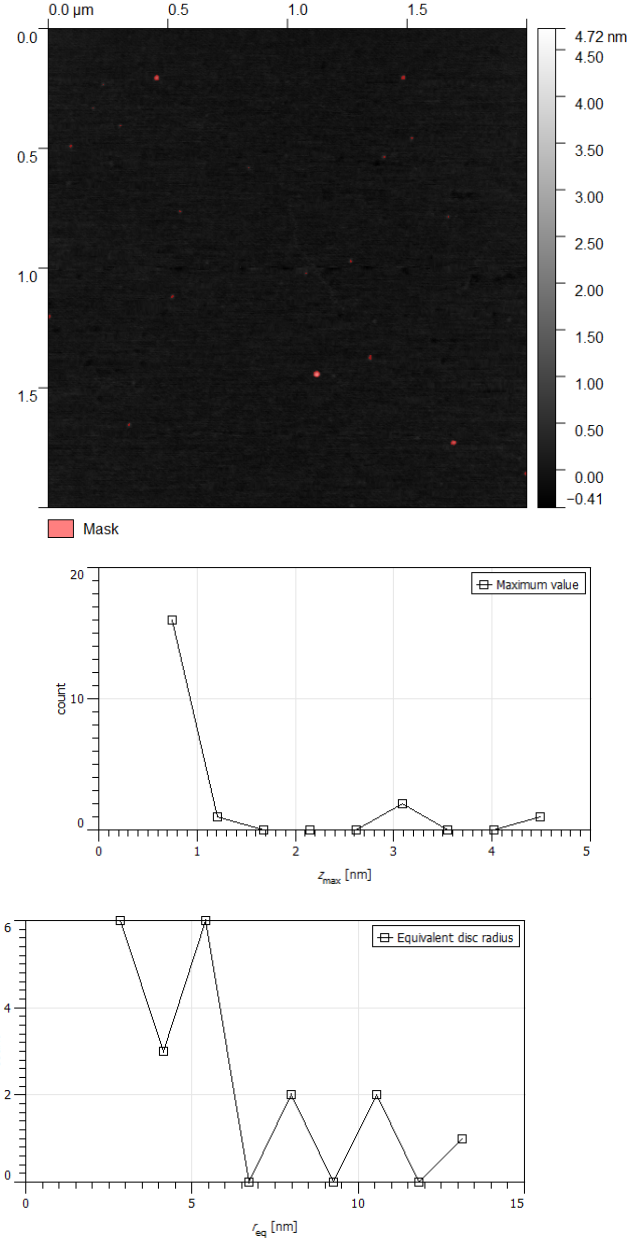

Figure S35. AFM image 4.4 of compound 2 (top), height (middle) and equivalent radius (bottom) distribution of grains (red mask, top picture).

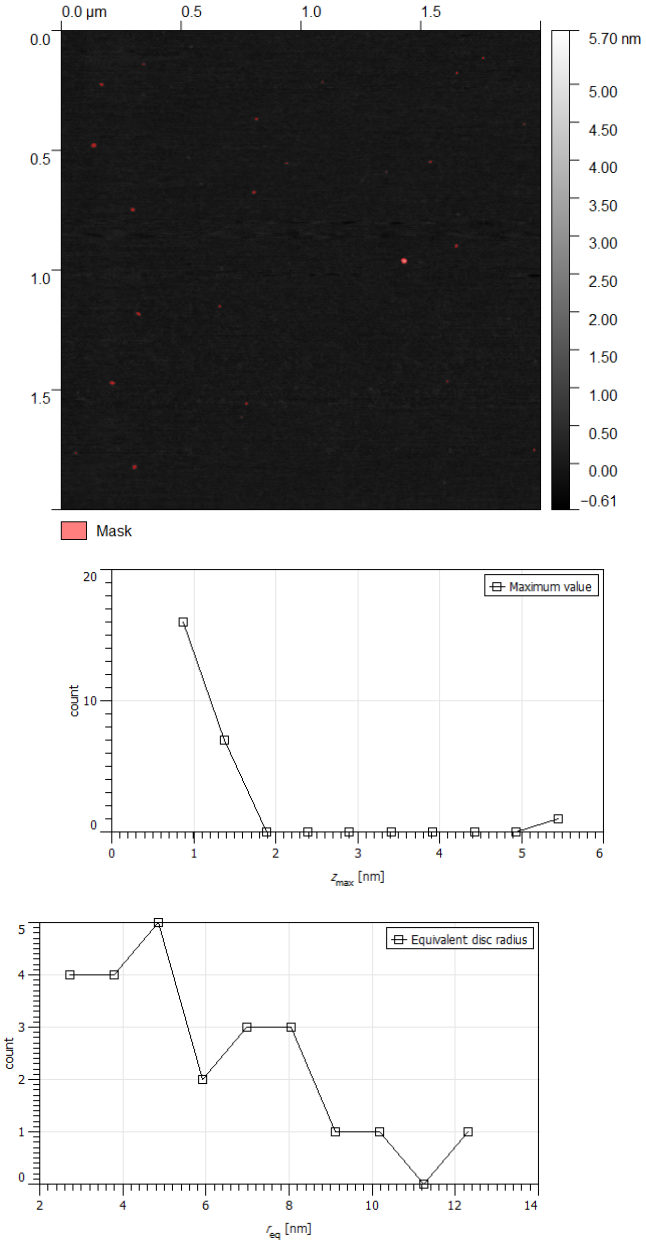

Figure S36. AFM image 5.1 of compound 2 (top), height (middle) and equivalent radius (bottom) distribution of grains (red mask, top picture).

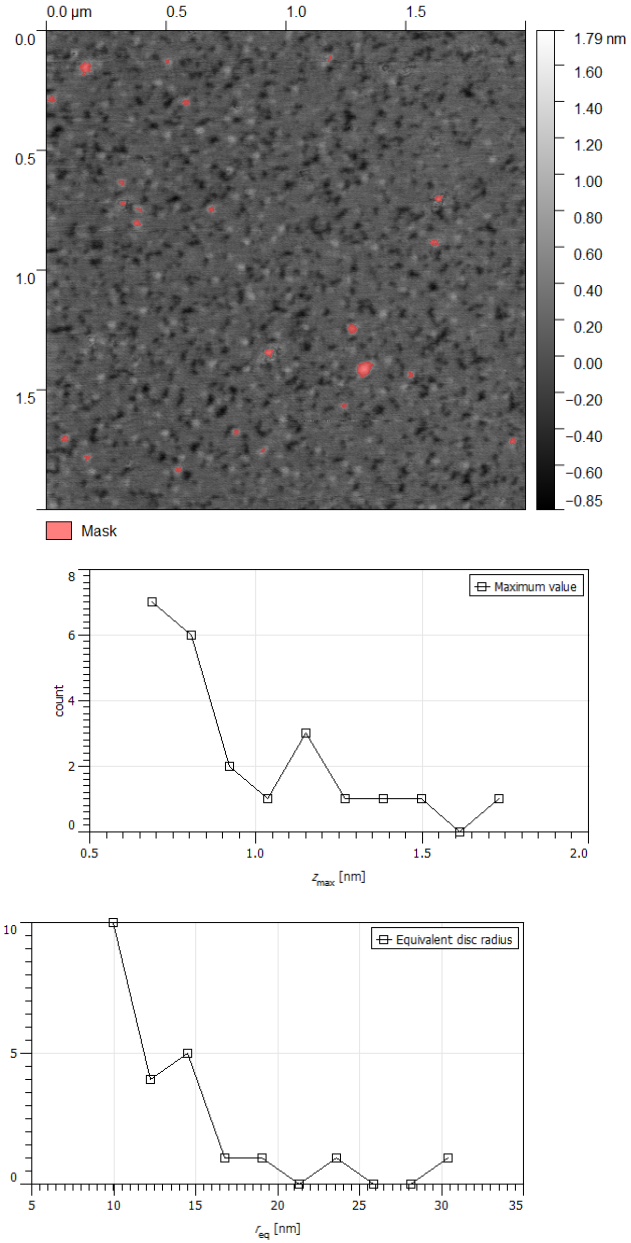

Figure S37. AFM image 5.2 of compound 2 (top), height (middle) and equivalent radius (bottom) distribution of grains (red mask, top picture).

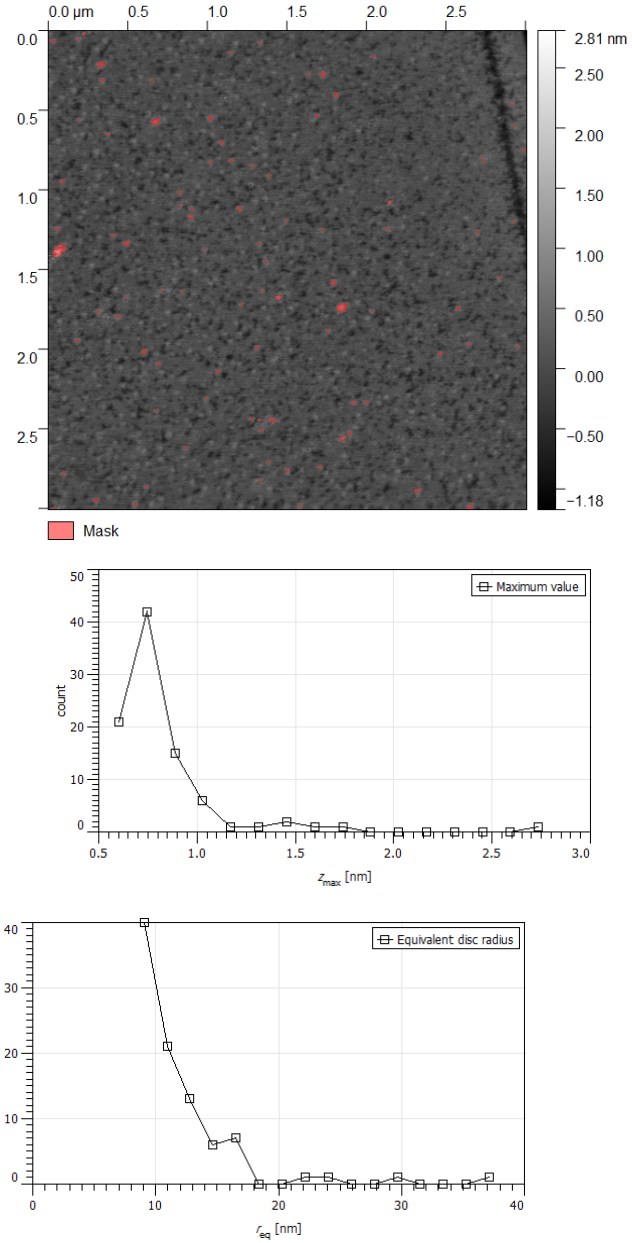

Figure S38. AFM image 5.3 of compound 2 (top), height (middle) and equivalent radius (bottom) distribution of grains (red mask, top picture).

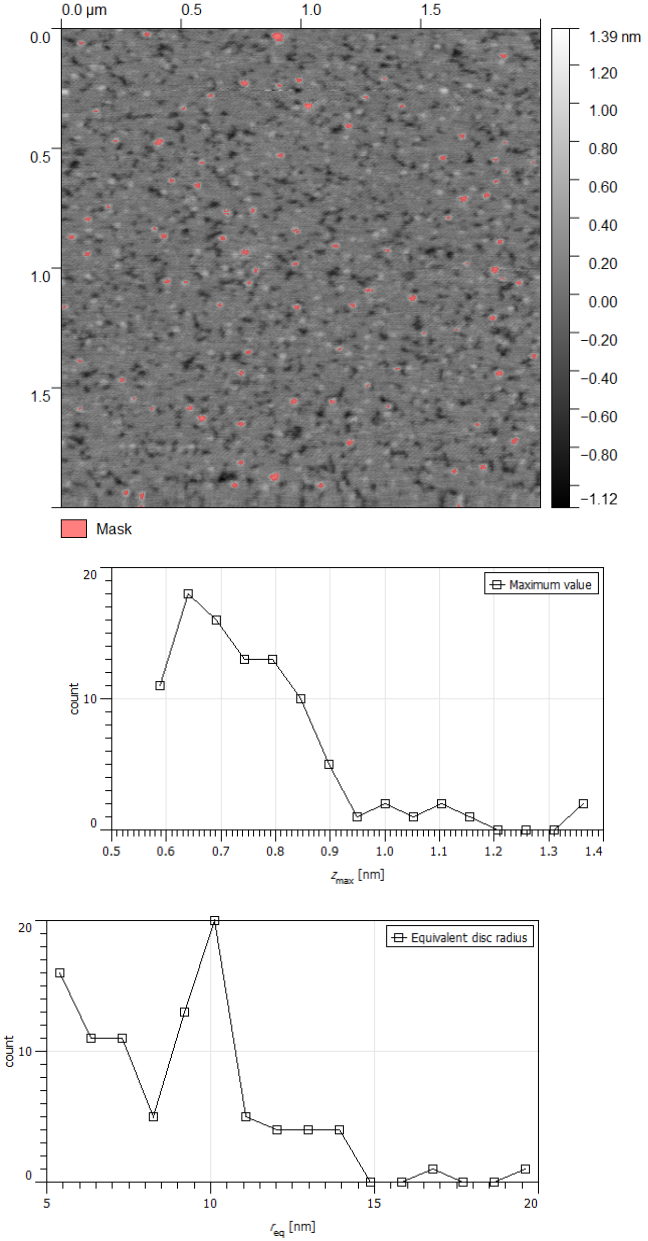

Figure S39. AFM image 6.1 of compound 2 (top), height (middle) and equivalent radius (bottom) distribution of grains (red mask, top picture).

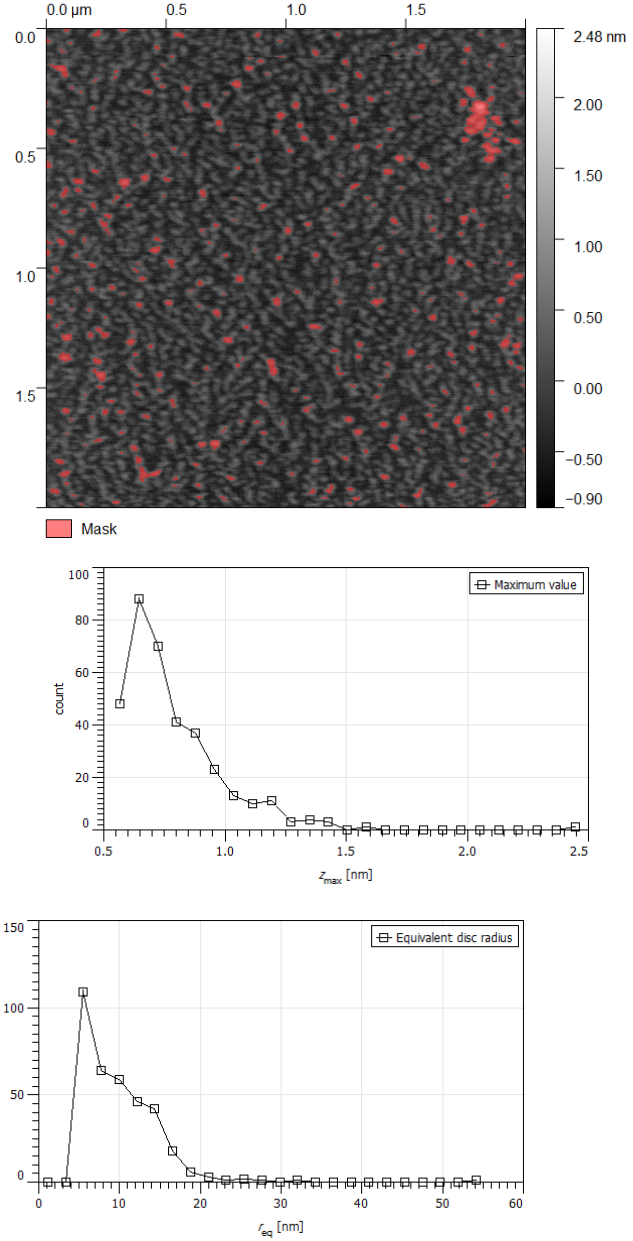

Figure S40. AFM image 6.2 of compound 2 (top), height (middle) and equivalent radius (bottom) distribution of grains (red mask, top picture).

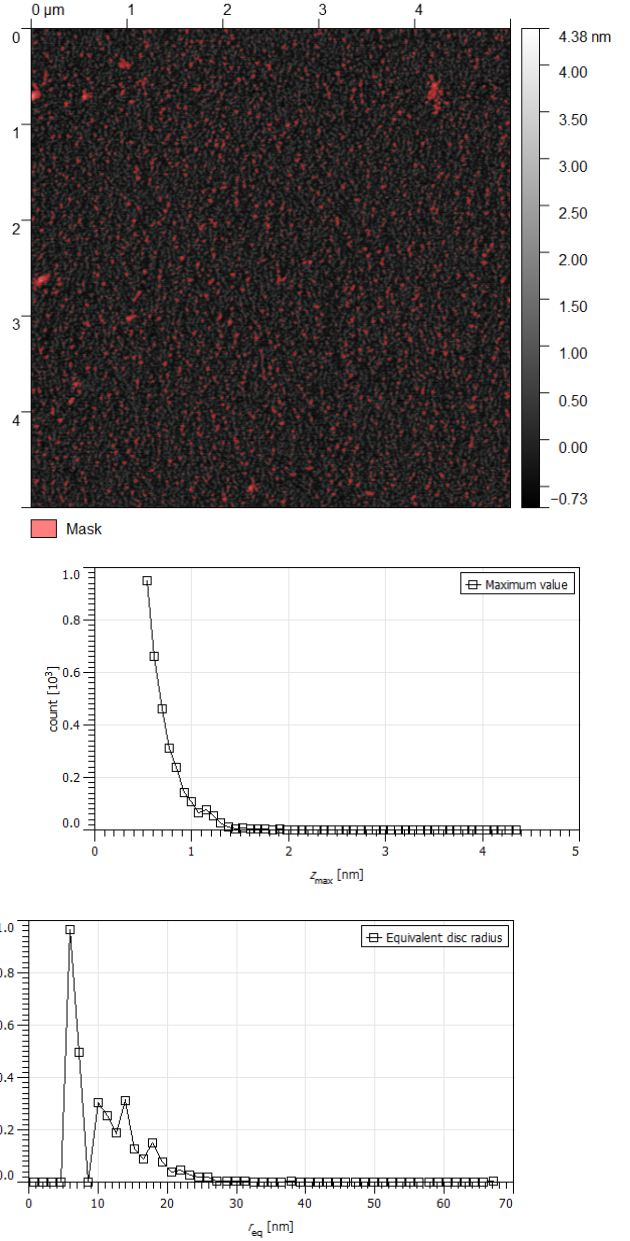

Figure S41. AFM image 6.3 of compound 2 (top), height (middle) and equivalent radius (bottom) distribution of grains (red mask, top picture).

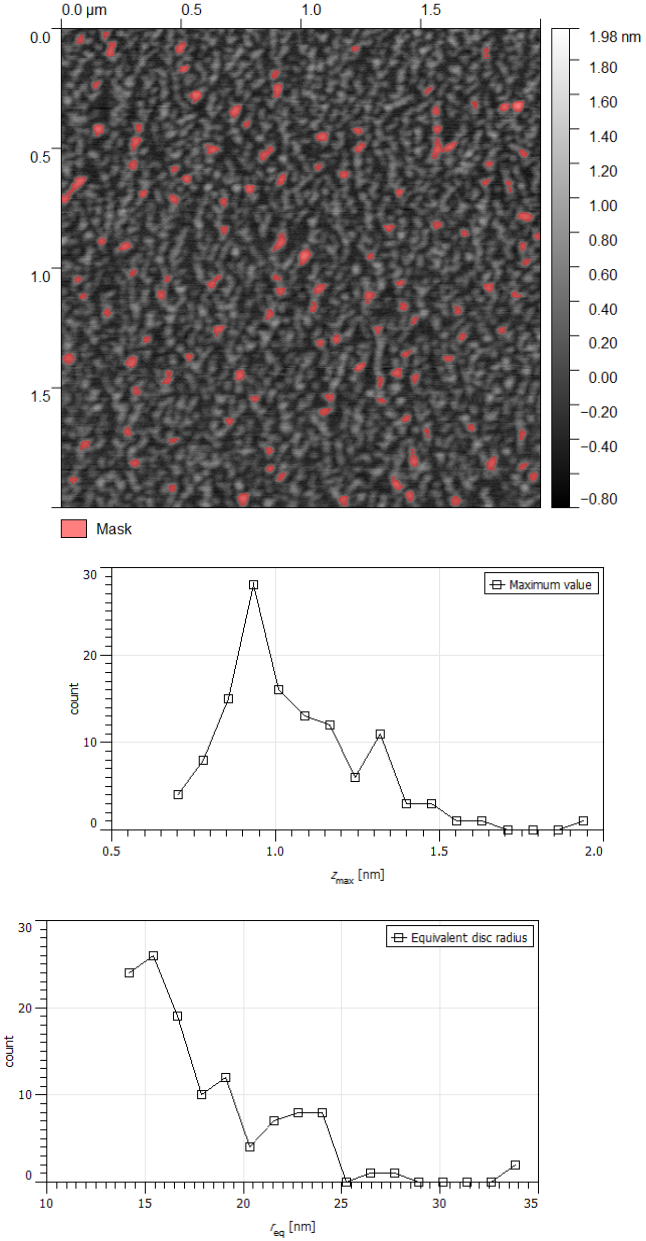

Figure S42. AFM image 6.4 of compound 2 (top), height (middle) and equivalent radius (bottom) distribution of grains (red mask, top picture).

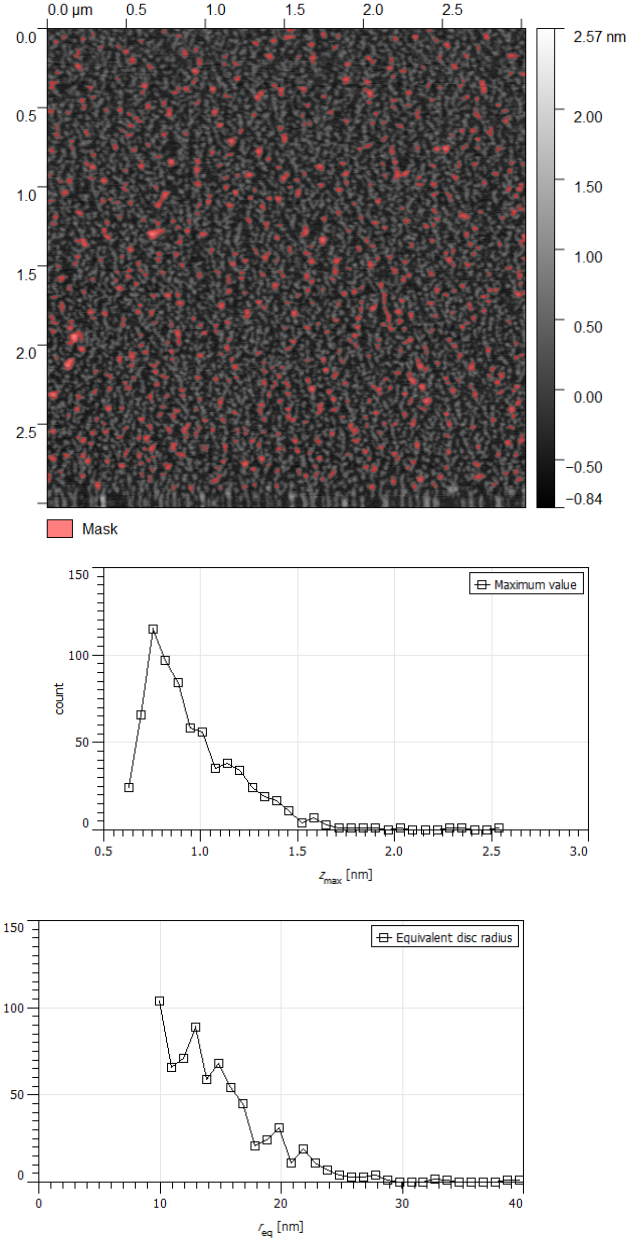

Figure S43. AFM image 7.1 of compound 2 (top), height (middle) and equivalent radius (bottom) distribution of grains (red mask, top picture).

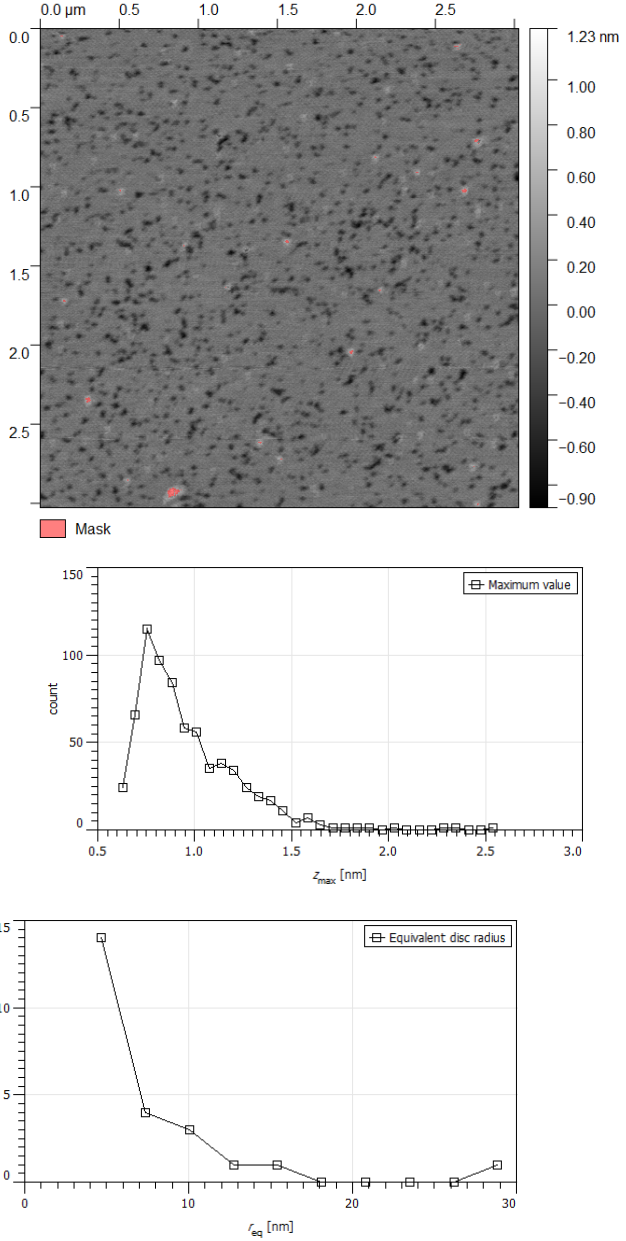

Figure S44. AFM image 8.1 of compound 2 (top), height (middle) and equivalent radius (bottom) distribution of grains (red mask, top picture).

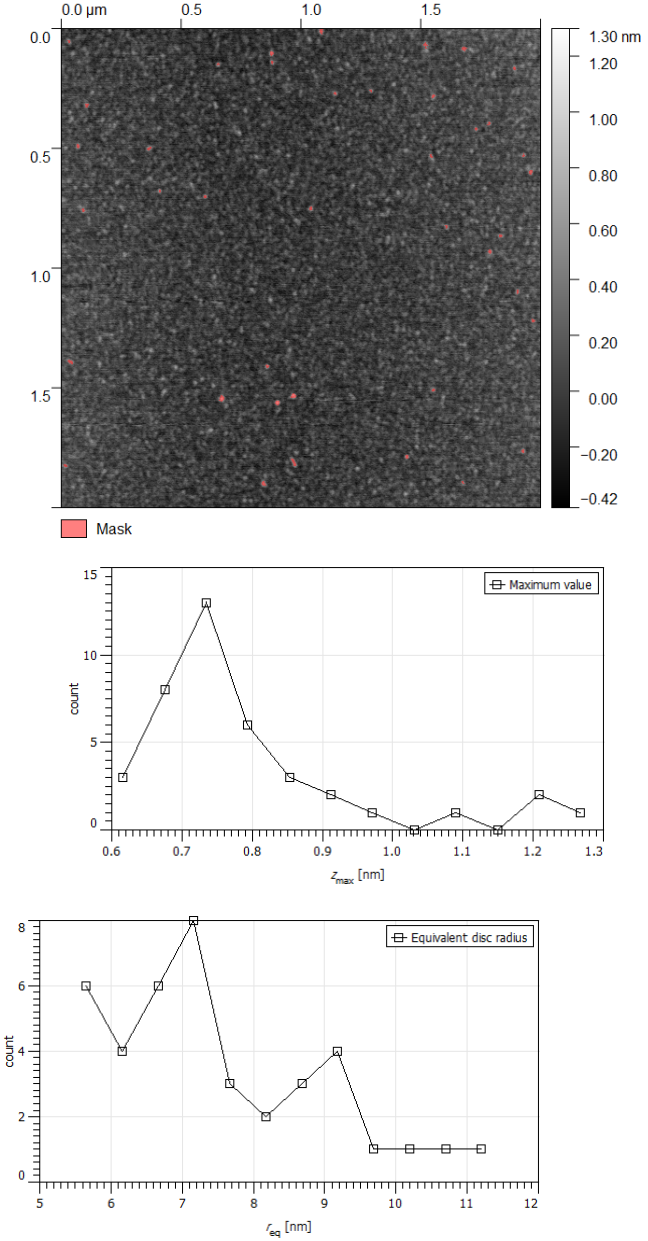

Figure S45. AFM image 9.1 of compound 2 (top), height (middle) and equivalent radius (bottom) distribution of grains (red mask, top picture).

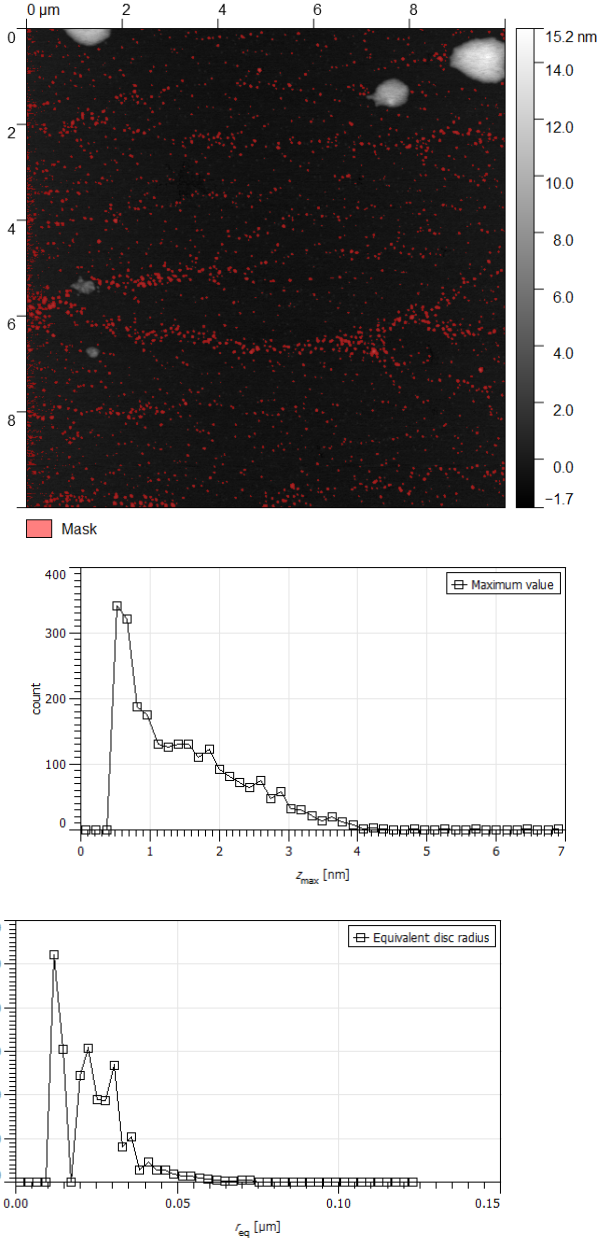

Figure S46. AFM image 9.2 of compound 2 (top), height (middle) and equivalent radius (bottom) distribution of grains (red mask, top picture).

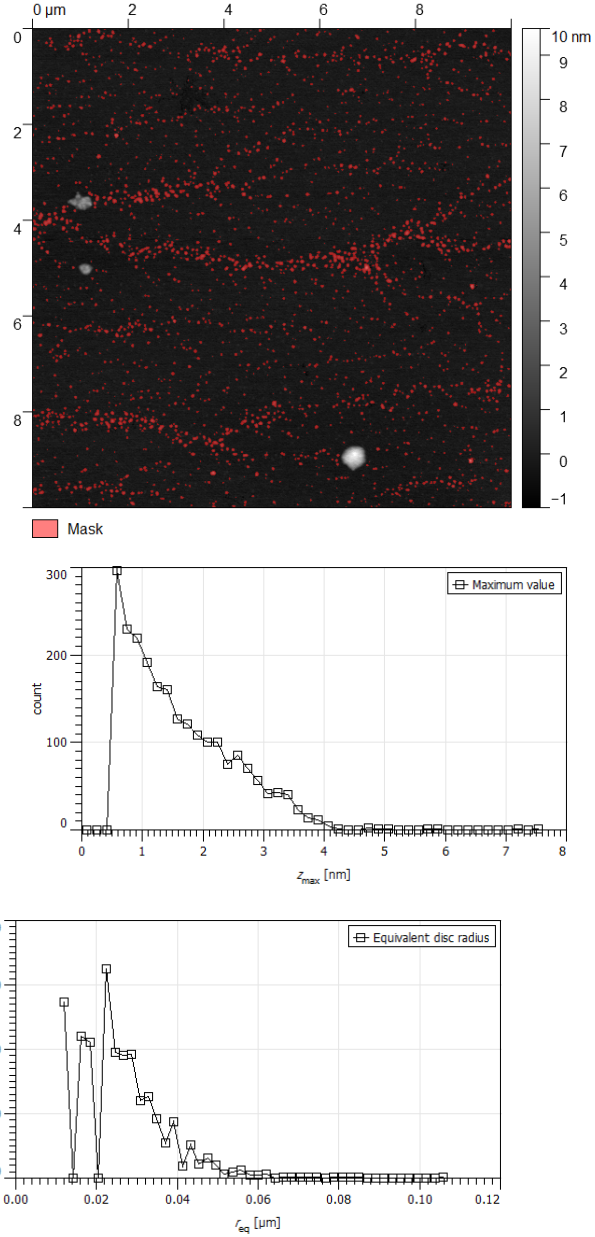

Figure S47. AFM image 9.3 of compound 2 (top), height (middle) and equivalent radius (bottom) distribution of grains (red mask, top picture).

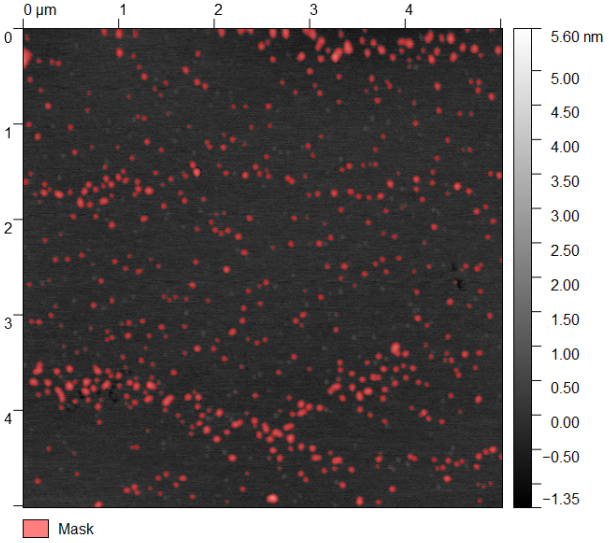

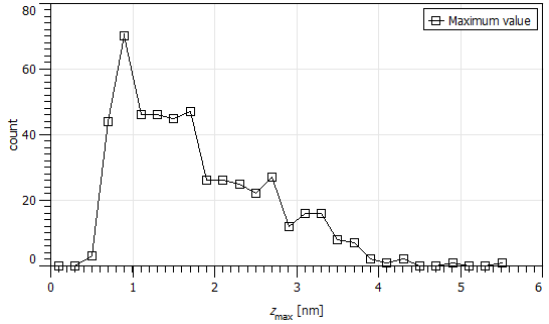

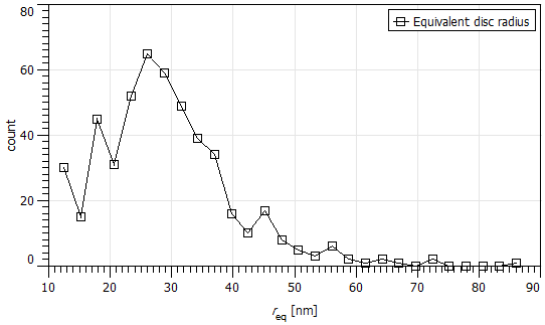

Figure S48. AFM image 9.4 of compound 2 (top), height (middle) and equivalent radius (bottom) distribution of grains (red mask, top picture).

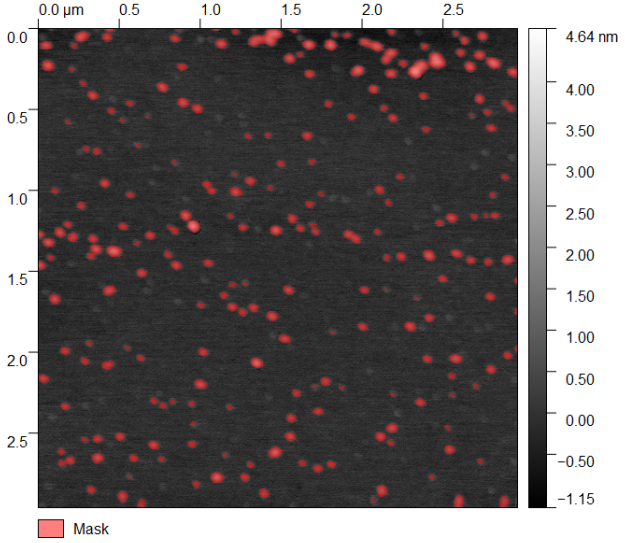

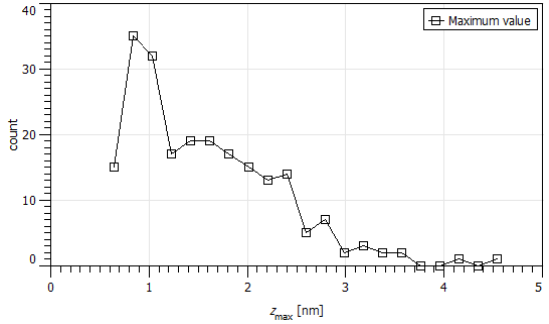

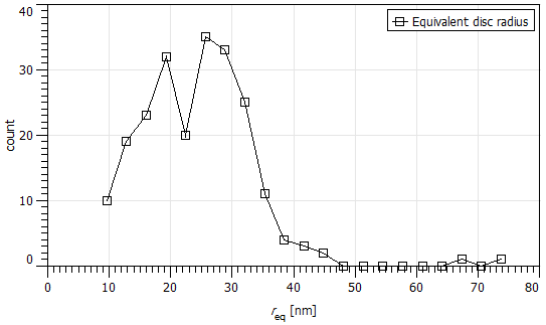

Figure S49. AFM image 9.5 of compound 2 (top), height (middle) and equivalent radius (bottom) distribution of grains (red mask, top picture).

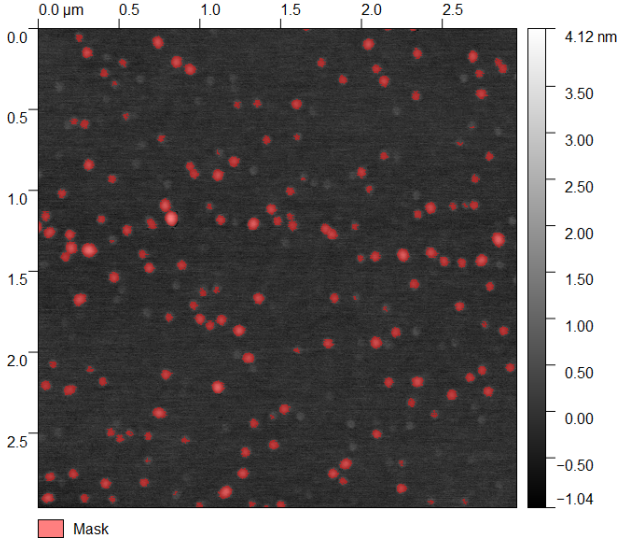

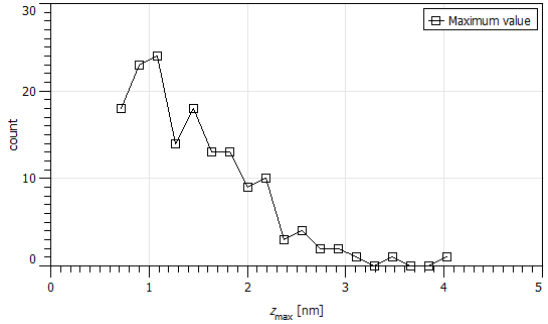

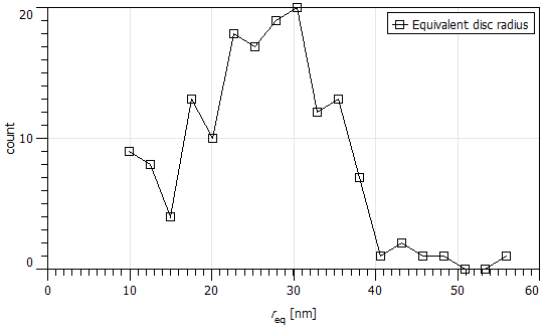

Figure S50. AFM image 9.6 of compound 2 (top), height (middle) and equivalent radius (bottom) distribution of grains (red mask, top picture).

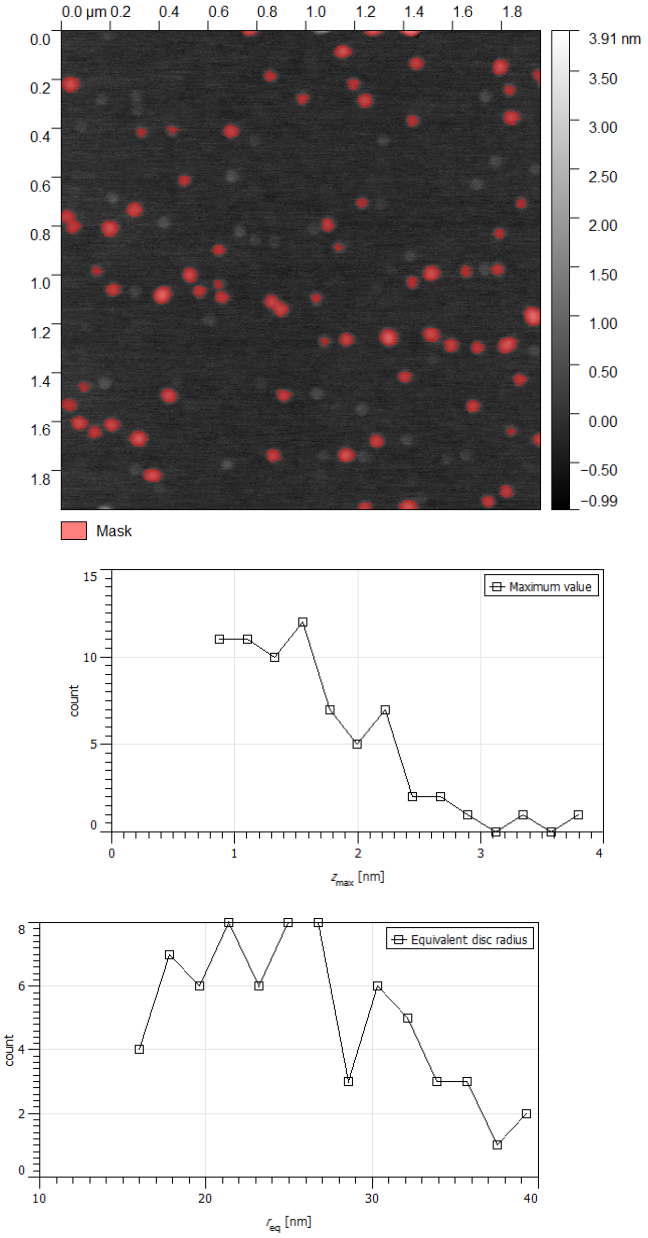

Figure S51. AFM image 9.7 of compound 2 (top), height (middle) and equivalent radius (bottom) distribution of grains (red mask, top picture).

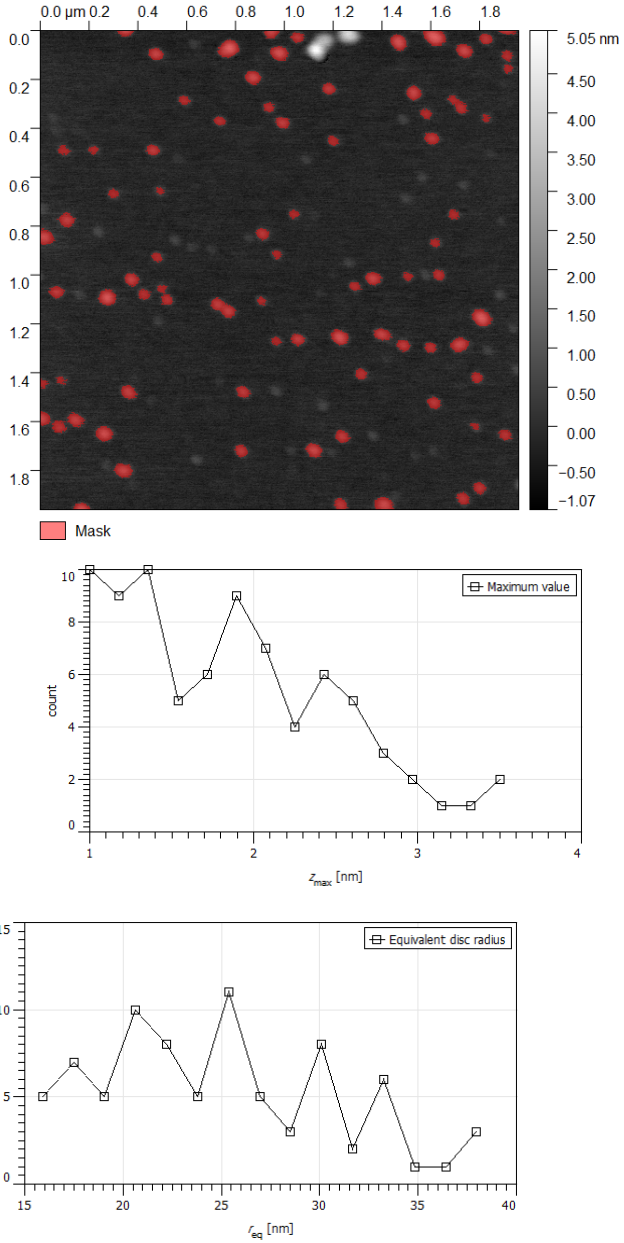

Figure S52. AFM image 9.8 of compound 2 (top), height (middle) and equivalent radius (bottom) distribution of grains (red mask, top picture).

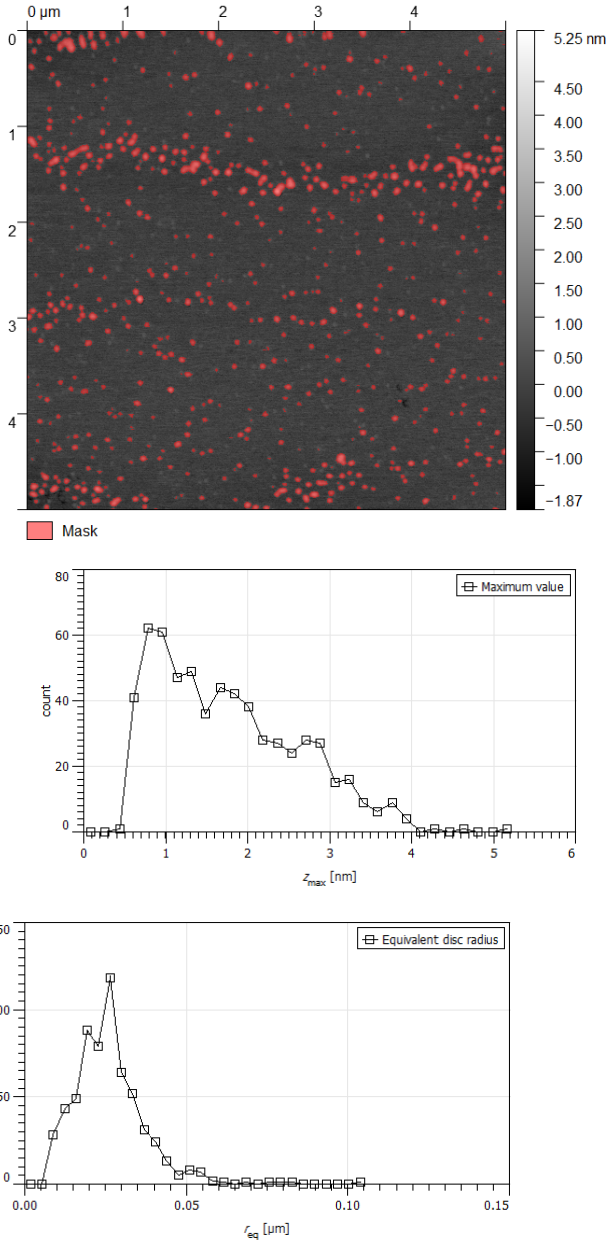

Figure S53. AFM image 9.9 of compound 2 (top), height (middle) and equivalent radius (bottom) distribution of grains (red mask, top picture).

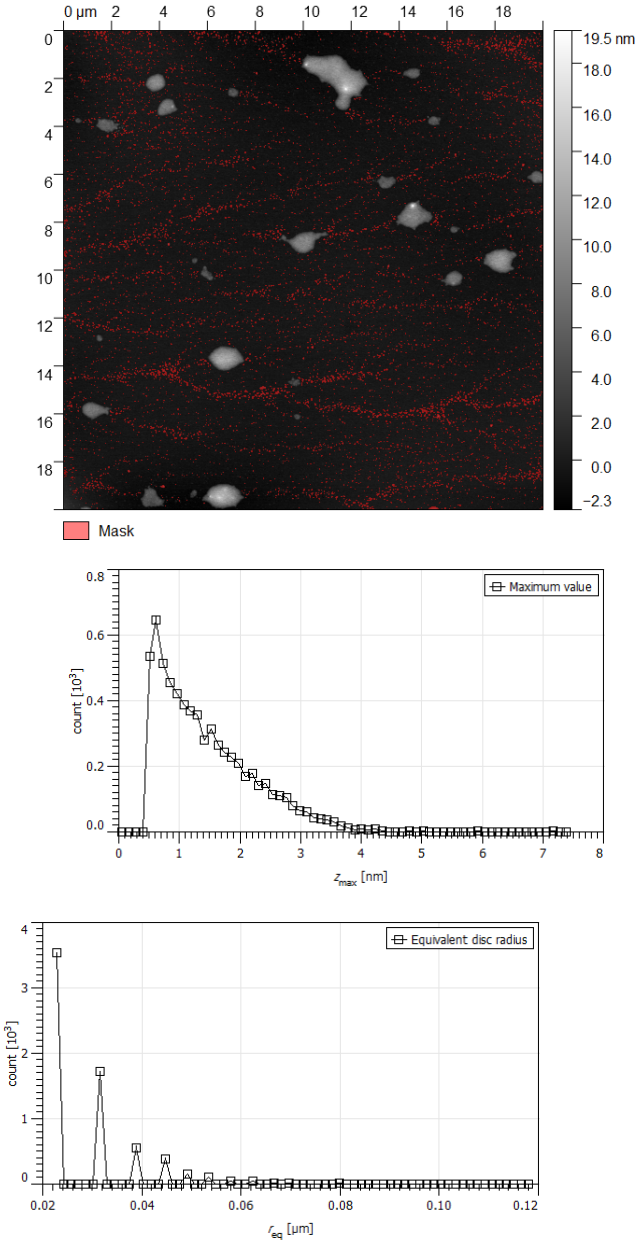

Figure S54. AFM image10.1 of compound 2 (top), height (middle) and equivalent radius (bottom) distribution of grains (red mask, top picture).

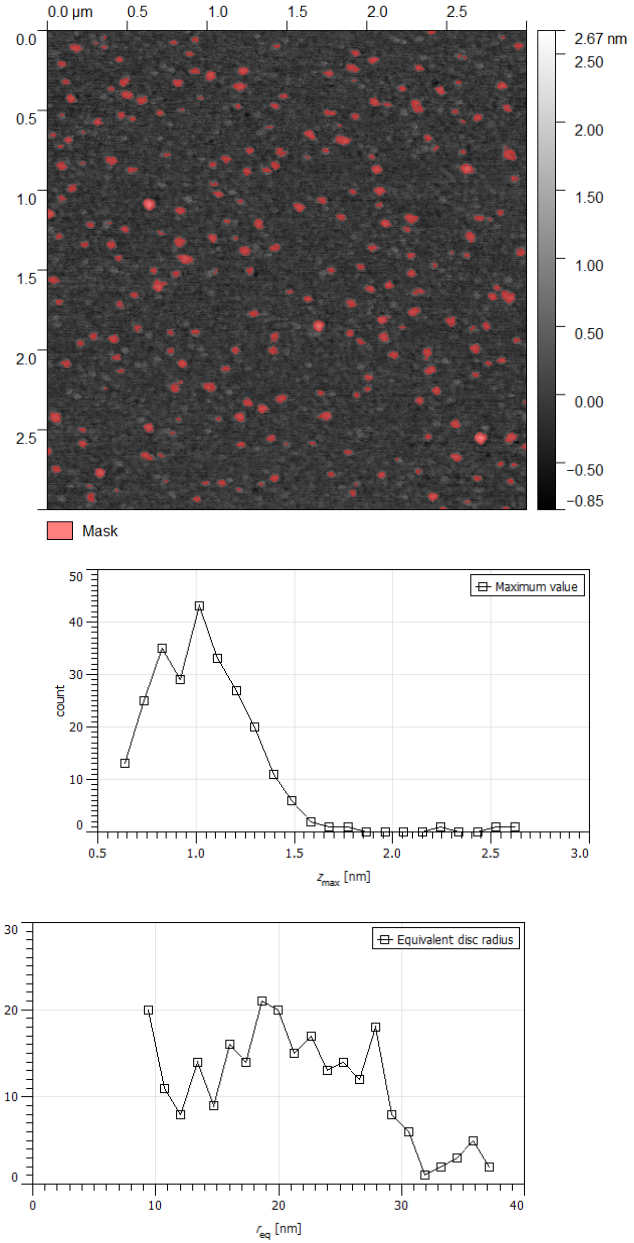

Figure S55. AFM image10.2 of compound 2 (top), height (middle) and equivalent radius (bottom) distribution of grains (red mask, top picture).

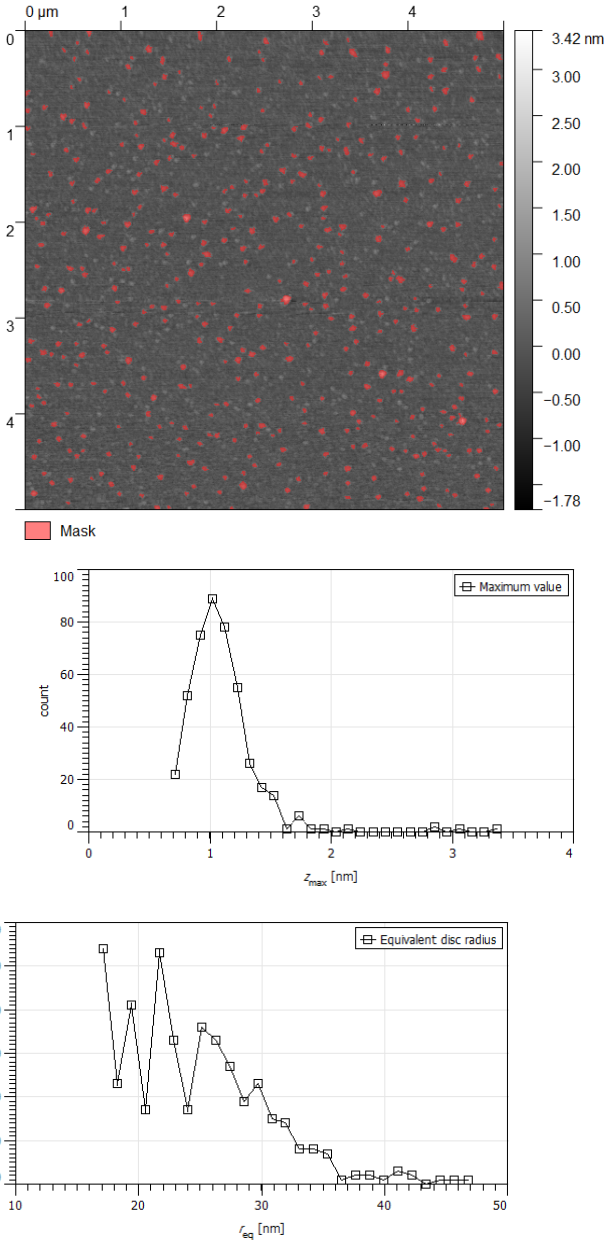

Figure S56. AFM image10.3 of compound 2 (top), height (middle) and equivalent radius (bottom) distribution of grains (red mask, top picture).

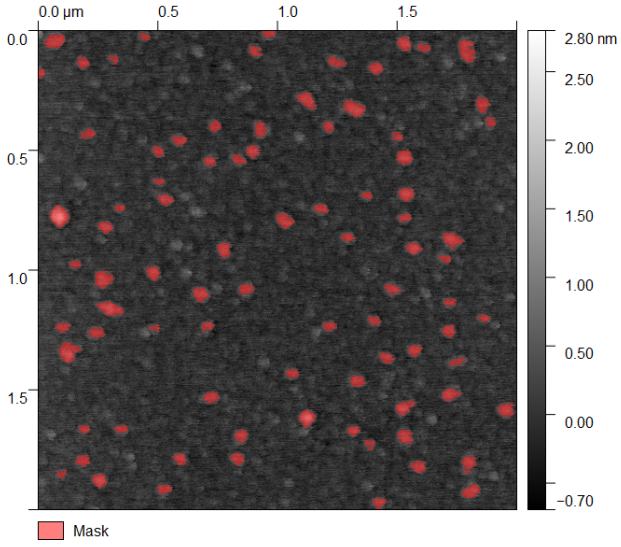

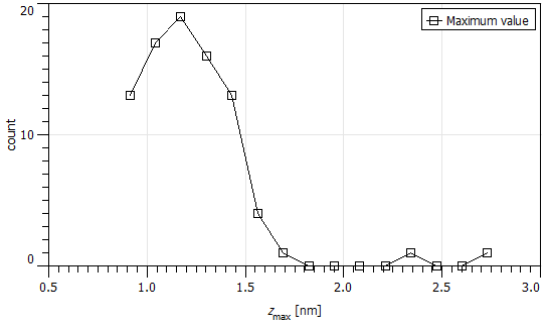

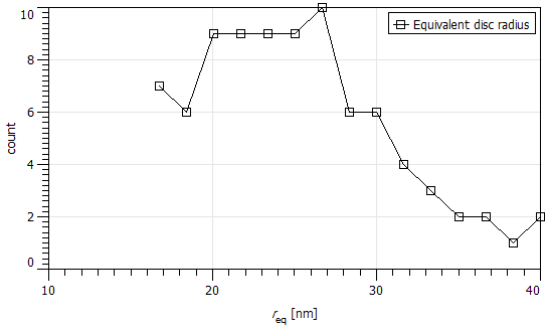

Figure S57. HRMS (ESI) of the commercial CH_3O-PEG-OH M_w 550.

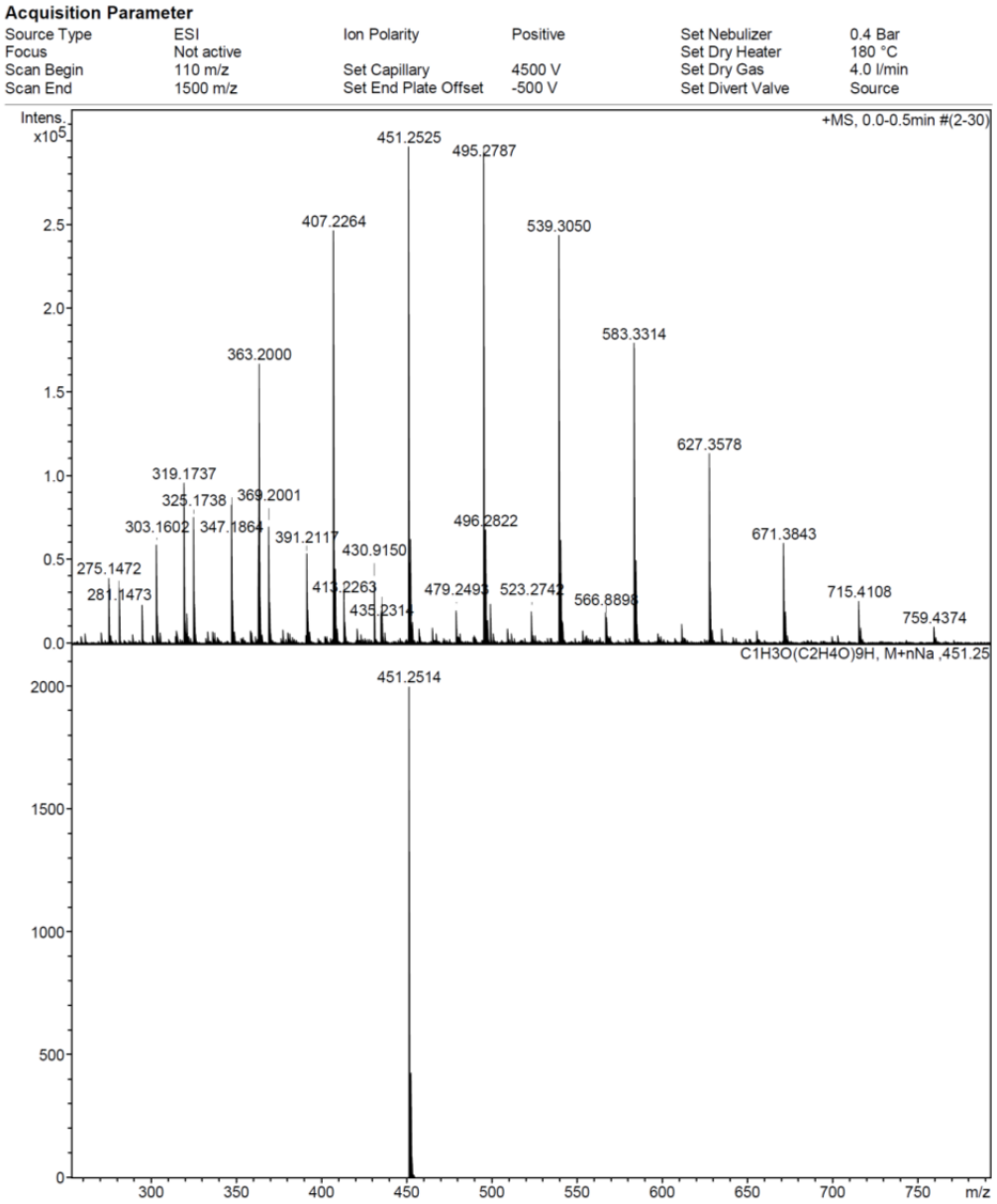

Table S2. Molecular mass distribution of CH_3O-$(CH_2CH_2O)_n$-OH M_w 550.

n	M	$[M+Na]^+$		ΔM/M, ppm	Intensity, %	Molar fraction
		Calcd	Found			
5	252.1573	275.1465	275.1472	2.5	13	0.02
6	296.1835	319.1727	319.1737	3.1	33	0.06
7	340.2097	363.1989	363.2	3.0	57	0.09
8	384.2359	407.2251	407.2264	3.2	83	0.14
9	428.2621	451.2513	451.2525	2.7	100	0.17
10	472.2883	495.2775	495.2787	2.4	100	0.17
11	516.3145	539.3037	539.305	2.4	82	0.14
12	560.3407	583.3299	583.3314	2.6	60	0.10
13	604.3669	627.3561	627.3578	2.7	38	0.06
14	648.3931	671.3823	671.3843	3.0	21	0.03
15	692.4193	715.4085	715.4108	3.2	9	0.01
16	736.4455	759.4347	759.4374	3.6	4	0.01

Figure S58. HRMS (ESI) of CH_3O-PEG-OTs (Compound 15).

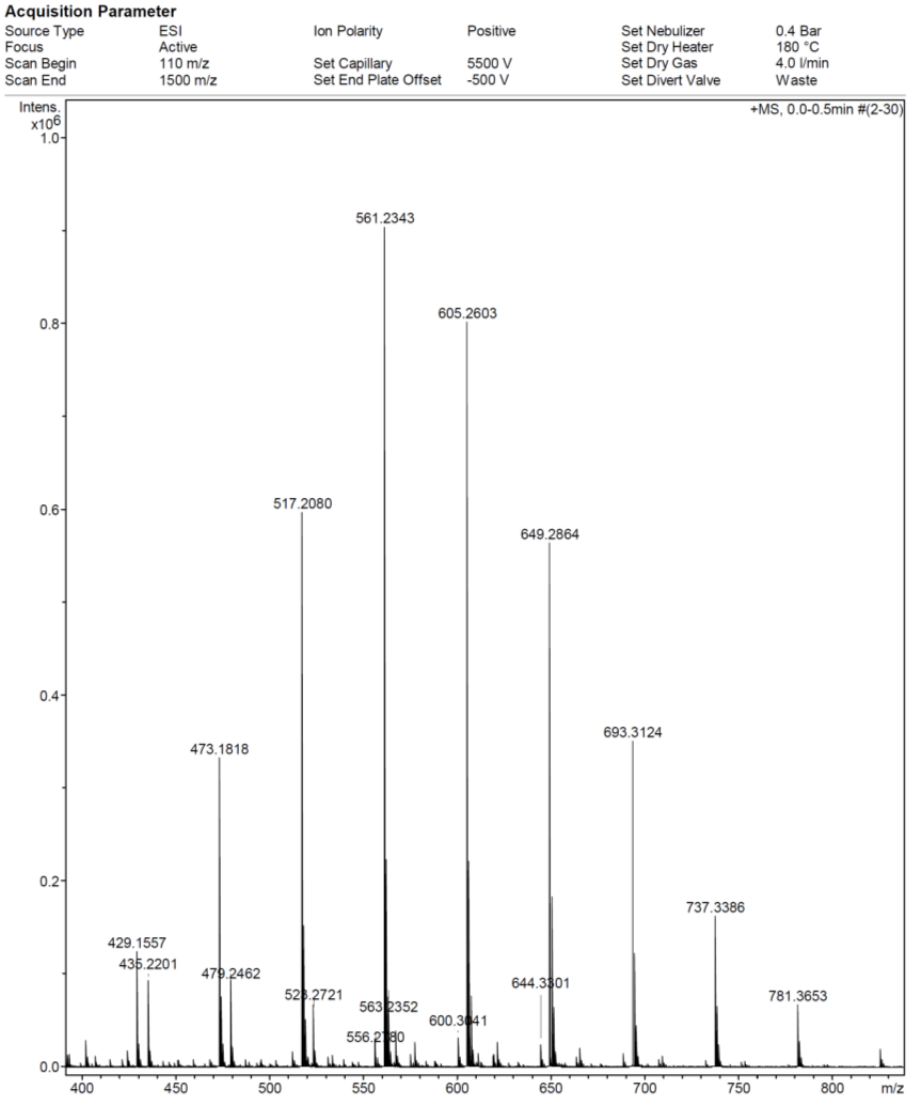

Table S3. Molecular mass distribution of CH_3O-$(CH_2CH_2O)_n$-Ts (15).

n	M	$[M+Na]^+$		ΔM/M, ppm	Intensity, %	Molar fraction
		Calcd	Found			
5	406.1662	429.1554	429.1557	0.7	13	0.03
6	450.1924	473.1816	473.1818	0.4	37	0.09
7	494.2186	517.2078	517.208	0.4	66	0.15
8	538.2448	561.234	561.2343	0.5	100	0.23
9	582.271	605.2602	605.2603	0.2	89	0.20
10	626.2972	649.2864	649.2864	0.0	62	0.14
11	670.3234	693.3126	693.3124	-0.3	38	0.09
12	714.3496	737.3388	737.3386	-0.3	18	0.04
13	758.3758	781.365	781.3653	0.4	8	0.02
14	802.4020	825.3912	825.3928	1.9	2	0.00

Figure S59. HRMS (ESI) of CH_3O-PEG-N_3 (Compound 14).

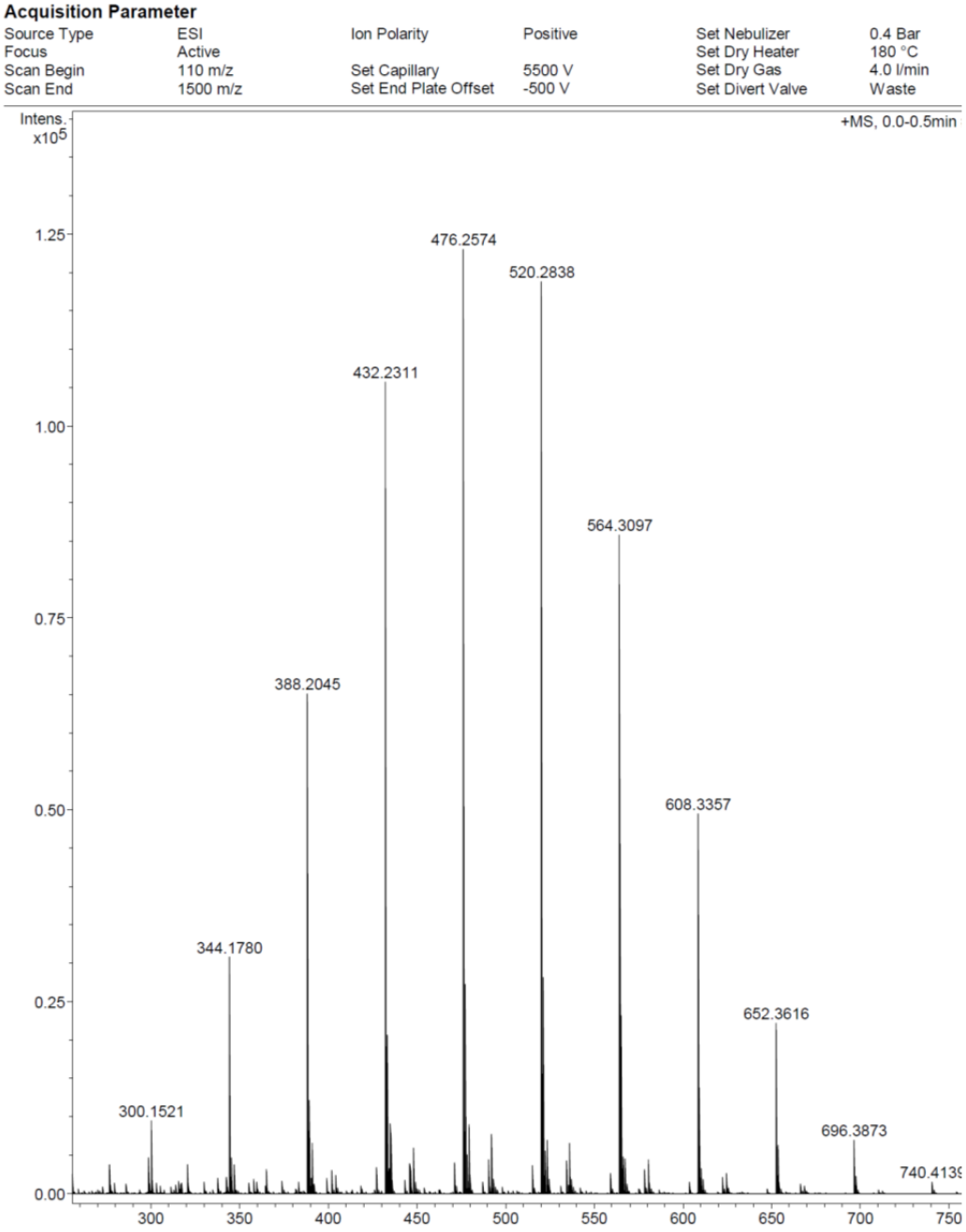

Table S3. Molecular mass distribution of CH_3O-$(CH_2CH_2O)_n$-N_3 (14).

n	M	$[M+Na]^+$		ΔM/M, ppm	Intensity, %	Molar fraction
		Calcd	Found			
5	277.1638	300.153	300.1521	-3.0	8	0.02
6	321.19	344.1792	344.178	-3.5	25	0.05
7	365.2162	388.2054	388.2045	-2.3	53	0.11
8	409.2424	432.2316	432.2311	-1.2	87	0.17
9	453.2686	476.2578	476.2574	-0.8	100	0.20
10	497.2948	520.284	520.2838	-0.4	96	0.19
11	541.321	564.3102	564.3097	-0.9	70	0.14
12	585.3472	608.3364	608.3357	-1.2	40	0.08
13	629.3734	652.3626	652.3616	-1.5	18	0.04
14	673.3996	696.3888	696.3873	-2.2	6	0.01
15	717.4258	740.415	740.4139	-1.5	1	0.00

Table S4. Molecular mass distribution of CH_3O-$(CH_2CH_2O)_n$-aziridine (compound 16) before chromatographic separation (Fig. 1b).

n	M	$[M+Na]^+$		ΔM/M, ppm	Intensity, %	Molar fraction
		Calcd	Found			
5	564.2796	587.2688	587.2693	0.9	6	0.01
6	608.3058	631.295	631.2957	1.1	18	0.04
7	652.332	675.3212	675.3219	1.0	39	0.08
8	696.3582	719.3474	719.3483	1.3	67	0.14
9	740.3844	763.3736	763.3746	1.3	94	0.19
10	784.4106	807.3998	807.4017	2.4	100	0.20
11	828.4368	851.426	851.429	3.5	82	0.17
12	872.463	895.4522	895.457	5.4	51	0.10
13	916.4892	939.4784	939.4855	7.6	24	0.05
14	960.5154	983.5046	983.5146	10.2	8	0.02
15	1004.5416	1027.5308	1027.5434	12.3	2	0.00

HRMS (ESI) spectrum of compound **16** is given in the main text (Fig. 1b).

Table S4. Molecular mass distribution of CH_3O-$(CH_2CH_2O)_n$-aziridine (compound 16) after chromatographic separation (Fig. S60).

n	M	$[M+Na]^+$		ΔM/M, ppm	Intensity, %	Molar fraction
		Calcd	Found			
7	652.332	675.3212	675.3223	1.6	16	0.05
8	696.3582	719.3474	719.3487	1.8	57	0.18
9	740.3844	763.3736	763.3753	2.2	100	0.32
10	784.4106	807.3998	807.4022	3.0	82	0.26
11	828.4368	851.426	851.4294	4.0	41	0.13
12	872.463	895.4522	895.4574	5.8	14	0.05
13	916.4892	939.4784	939.4853	7.3	4	0.01

Figure S60. HRMS (ESI) of CH_3O-PEG-N_3 (Compound 14).

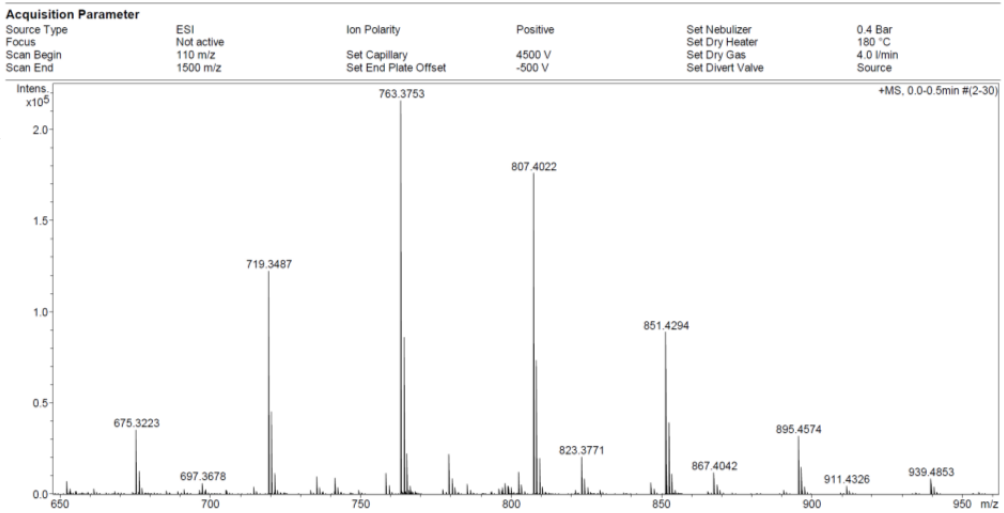

Table S5. Molecular mass distribution of CH_3O-$(CH_2CH_2O)_n$-fulleropyrrolidine (compound 2).

n	M	$[M+Na]^+$		ΔM/M, ppm	Intensity, %	Molar fraction
		Calcd	Found			
5	1284.28	1285.29	1285.7	$3 \cdot 10^2$	9	0.02
6	1328.31	1329.31	1329.35	26	25	0.05
7	1372.33	1373.34	1373.38	28	76	0.16
8	1416.36	1417.37	1417.41	30	100	0.22
9	1460.38	1461.39	1461.44	31	97	0.21
10	1504.41	1505.42	1505.47	33	84	0.18
11	1548.44	1549.44	1549.50	37	47	0.10
12	1592.46	1593.47	1593.51	23	18	0.04
13	1636.49	1637.50	1637.5446	29	7	0.02

HRMS (ESI) spectrum of compound 2 is given in the main text.

Figure S61. HRMS (ESI) of compound 3.

Acquisition Parameter

Source Type	ESI	Ion Polarity	Positive	Set Nebulizer	0.4 Bar
Focus	Active	Set Capillary	4500 V	Set Dry Heater	180 °C
Scan Begin	300 m/z	Set End Plate Offset	-500 V	Set Dry Gas	4.0 l/min
Scan End	3000 m/z	Set Collision Cell RF	1000.0 Vpp	Set Divert Valve	Source

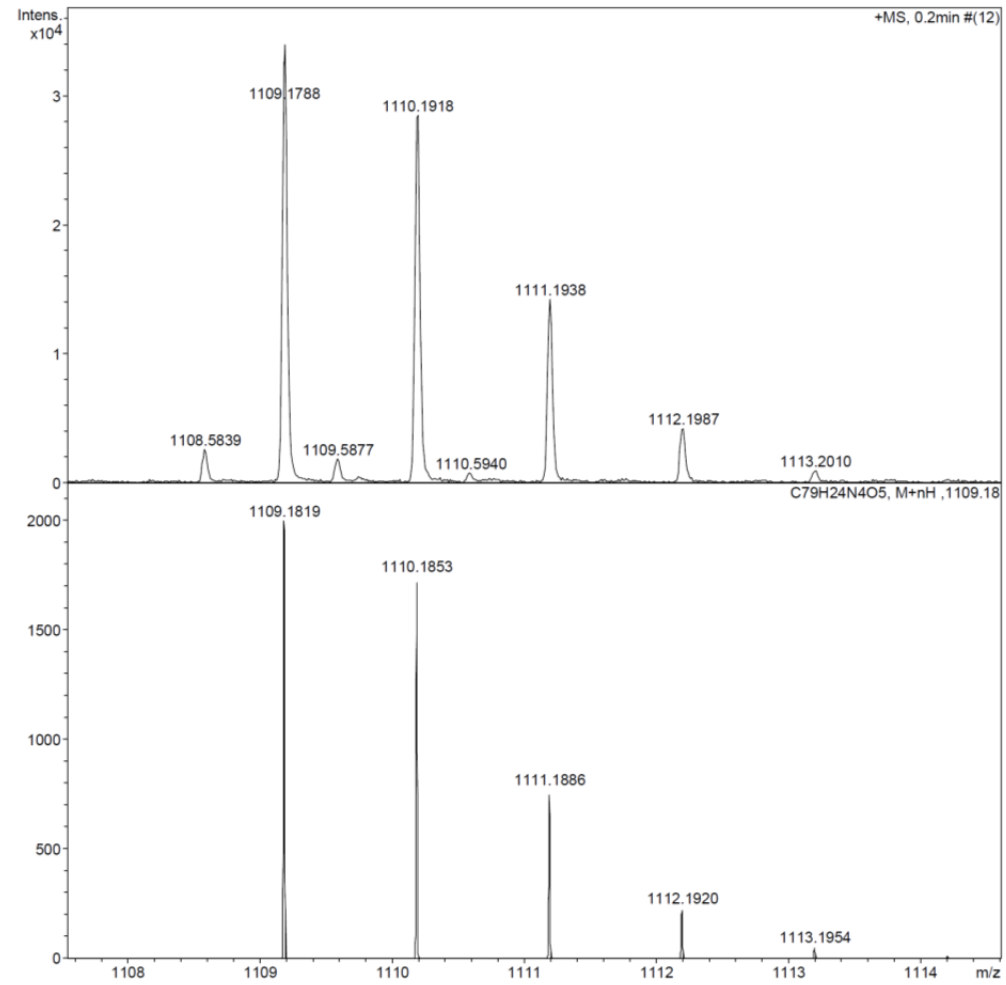

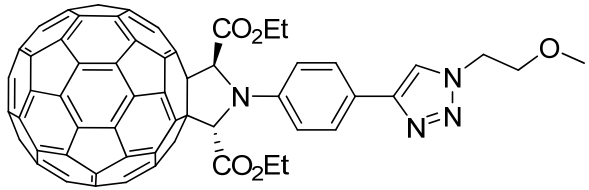

Figure S62. HRMS (ESI) of compound 5.

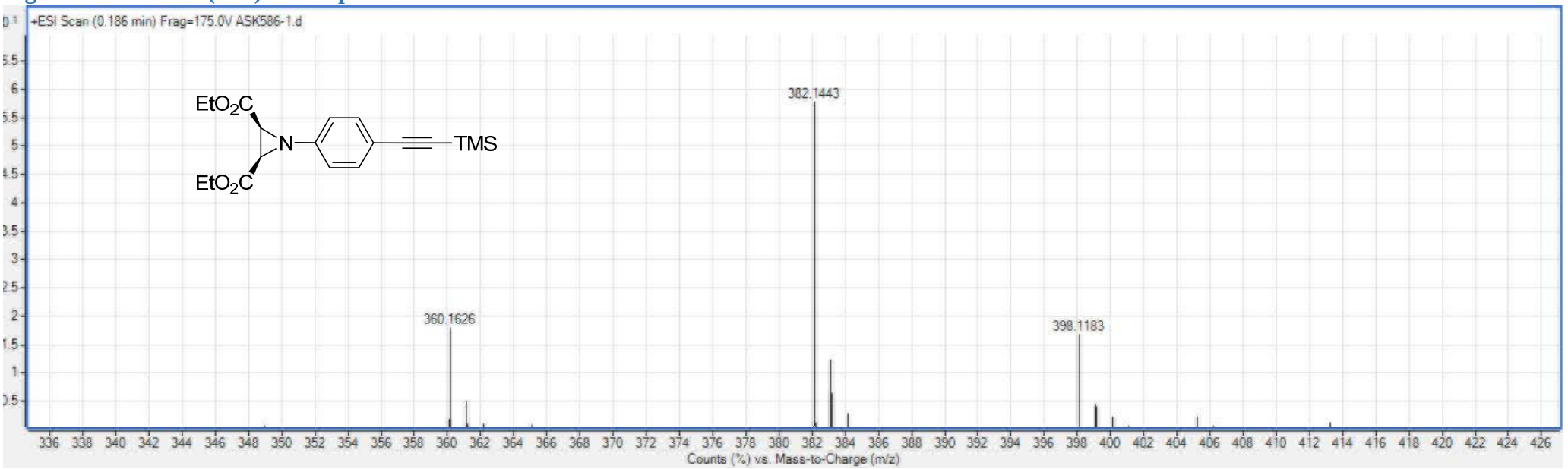

Figure S63. HRMS (ESI) of compound 9.

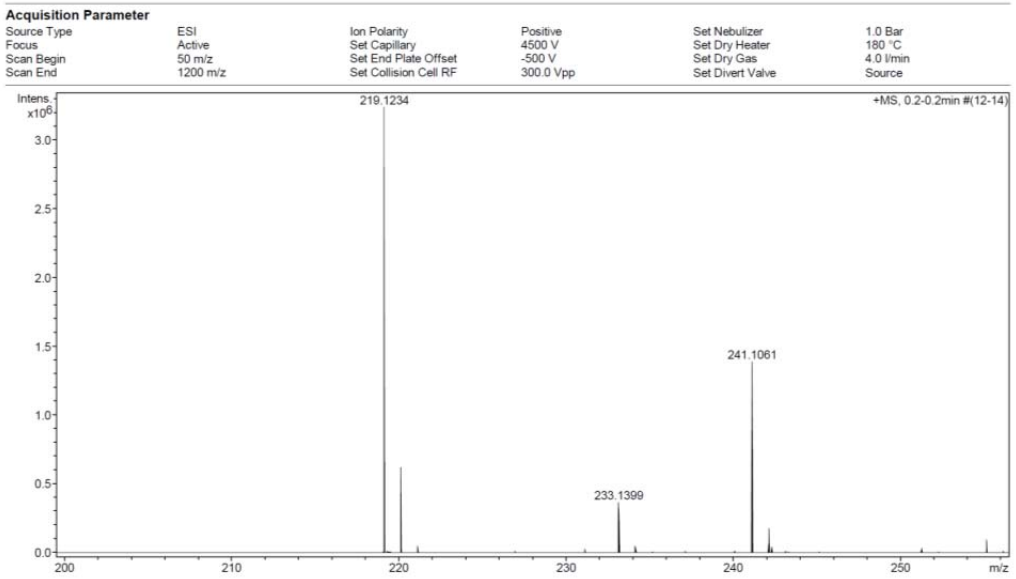

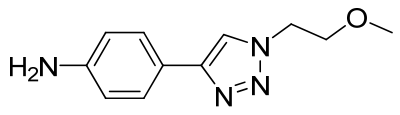

Figure S64. HRMS (ESI) of compound 8.

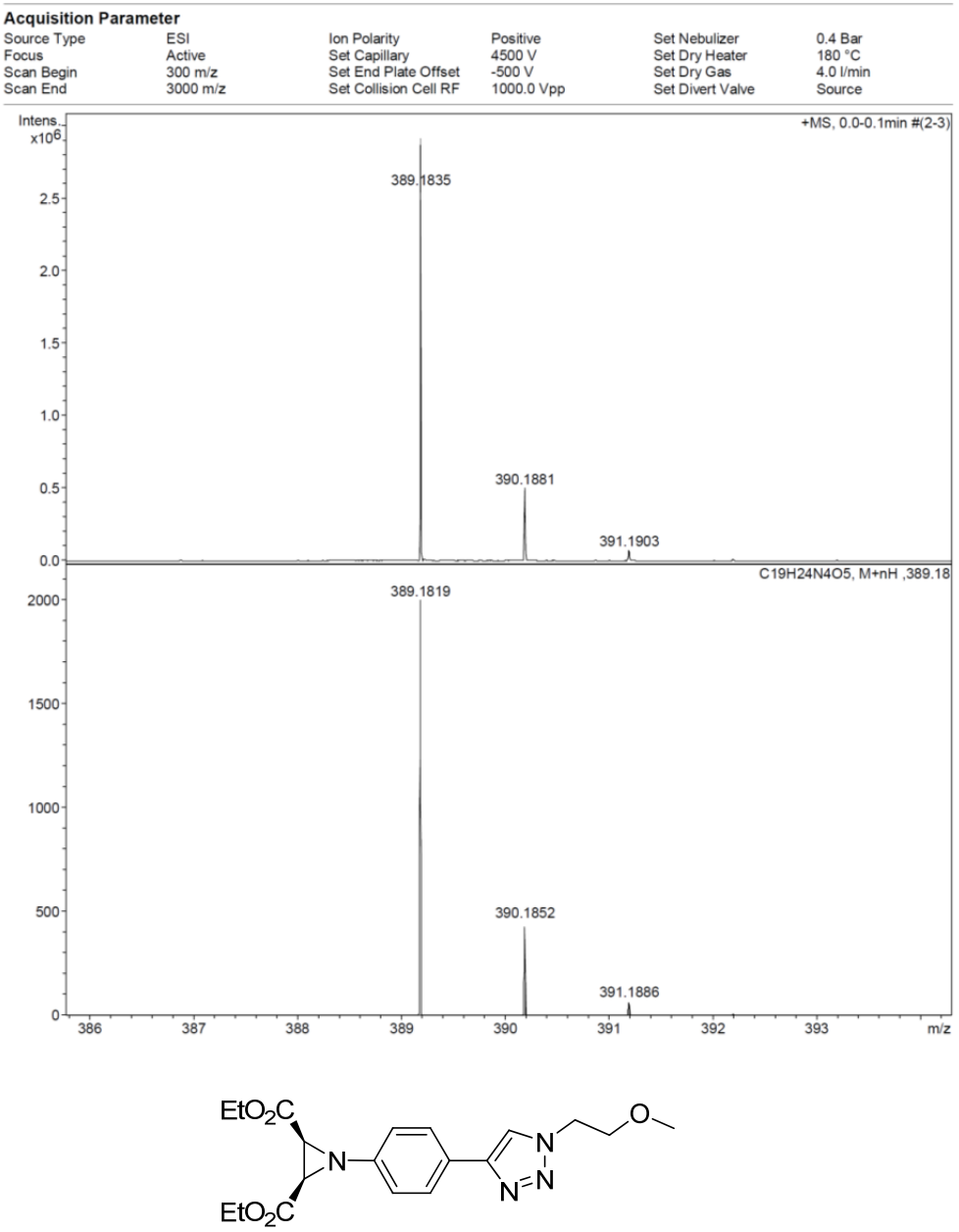

Figure S65. HRMS (ESI) of compound 11.

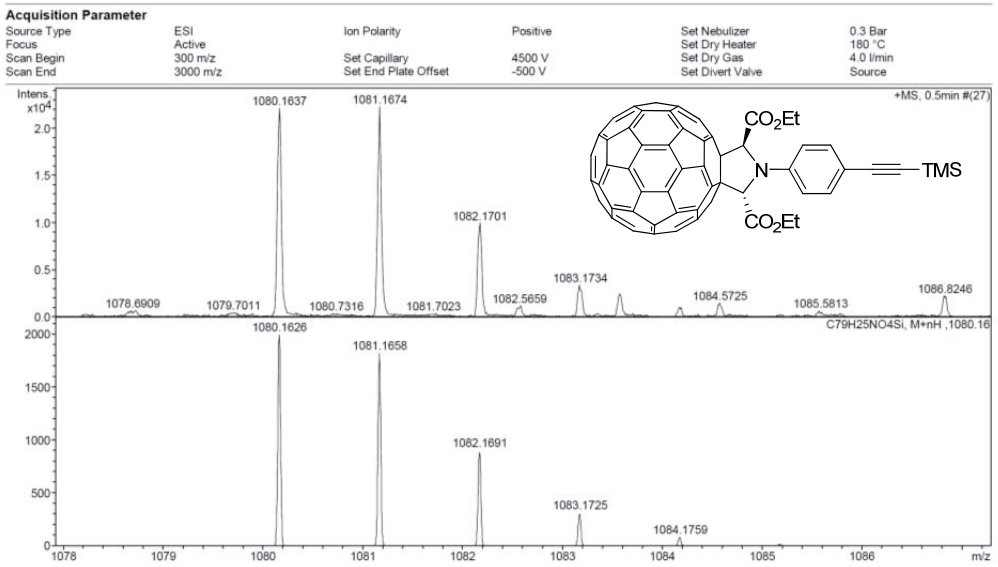

Figure S66. HRMS (ESI) of compound 12.

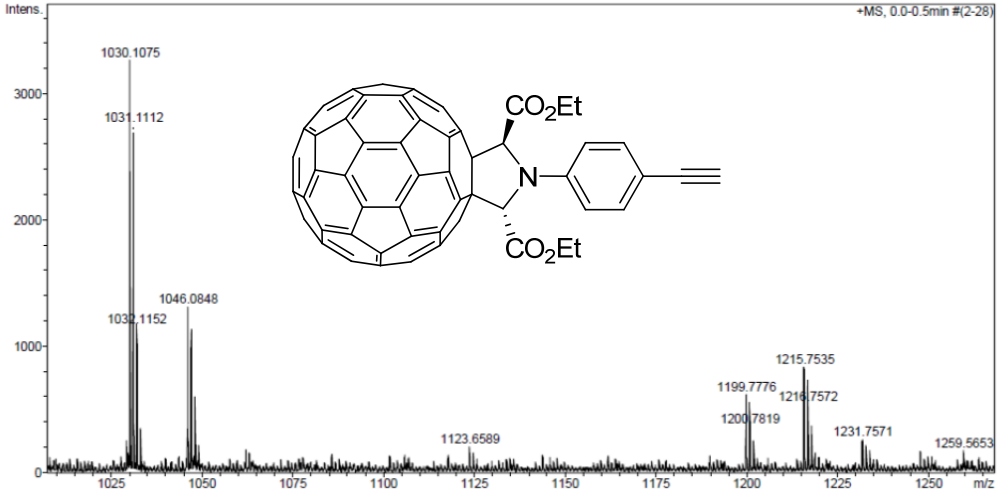

Figure S67. IR spectrum (KBr) of compound 2.

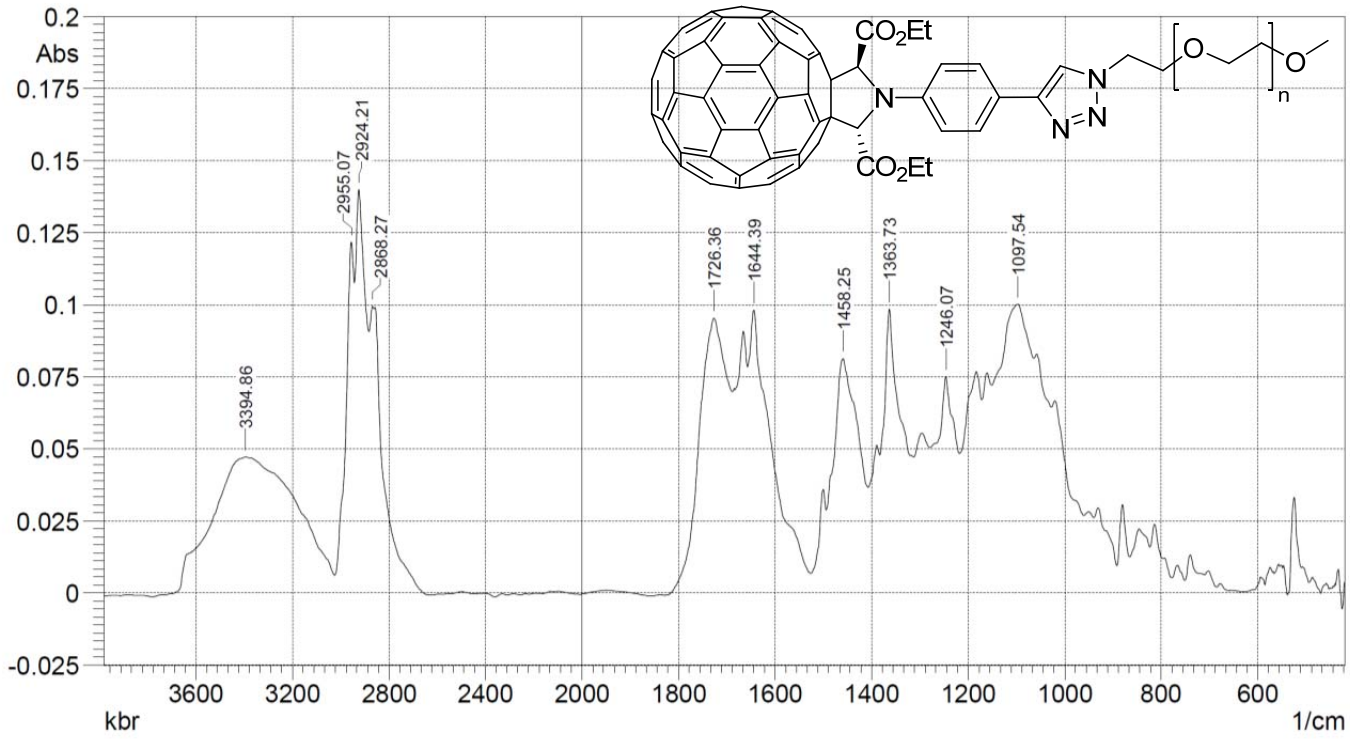

Figure S68. IR spectrum (KBr) of compound 3.

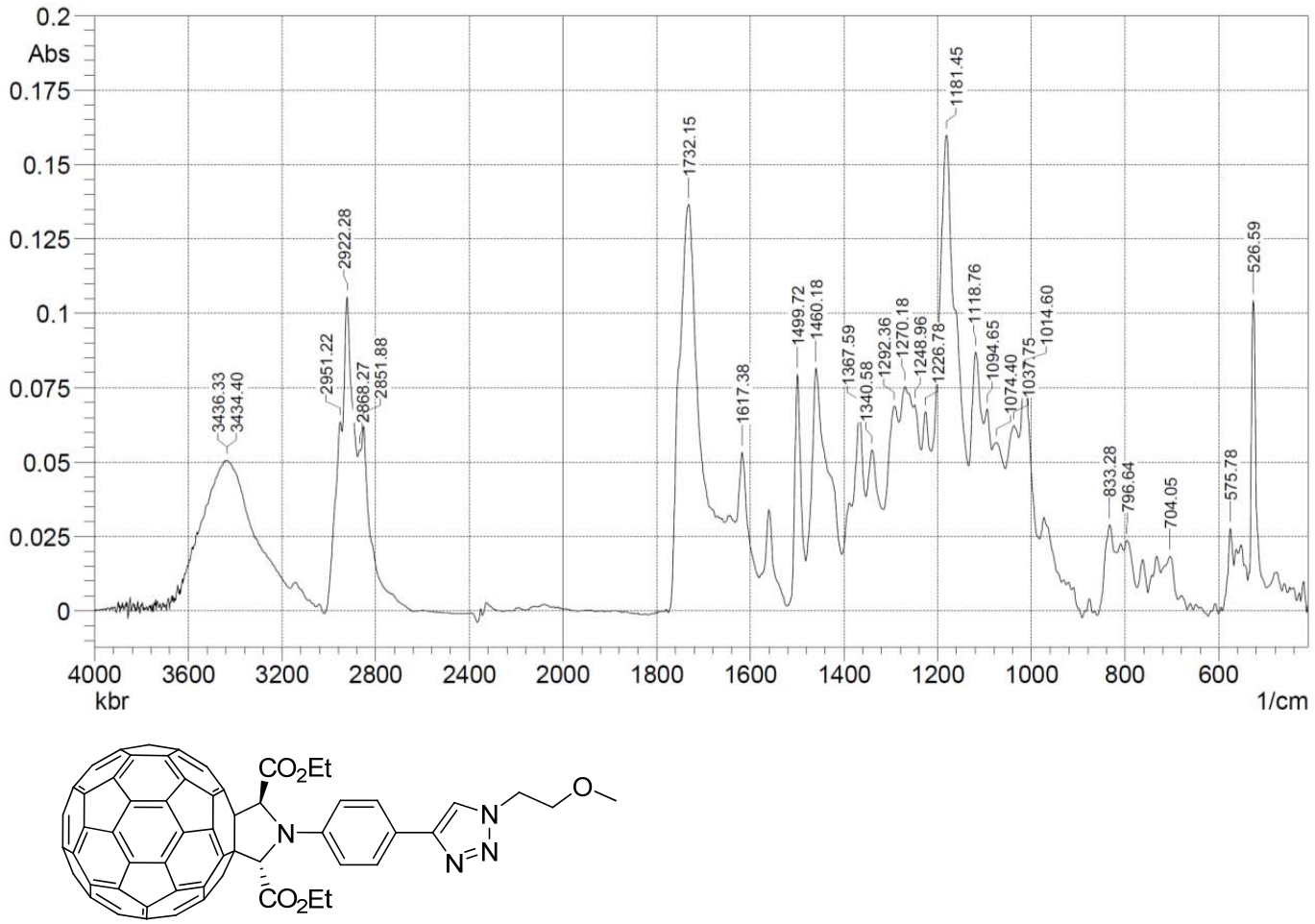

Figure S69. IR spectrum (KBr) of compound 5.

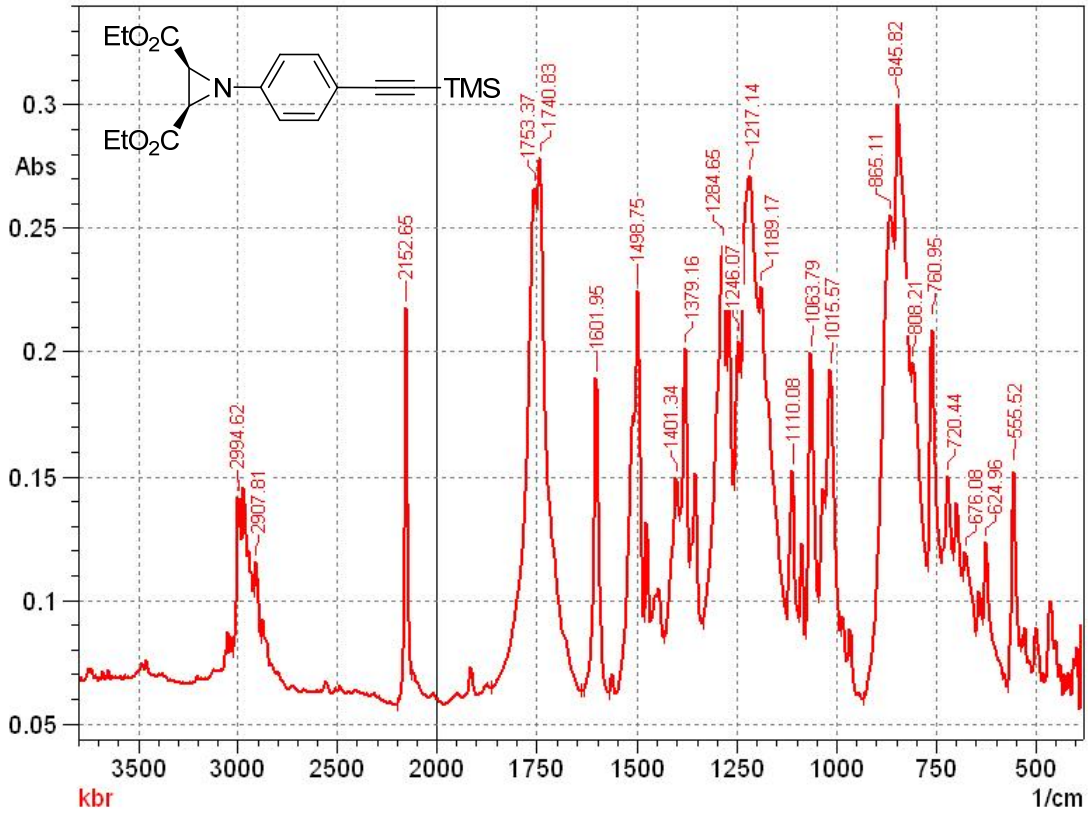

Figure S70. IR spectrum (KBr) of compound 8.

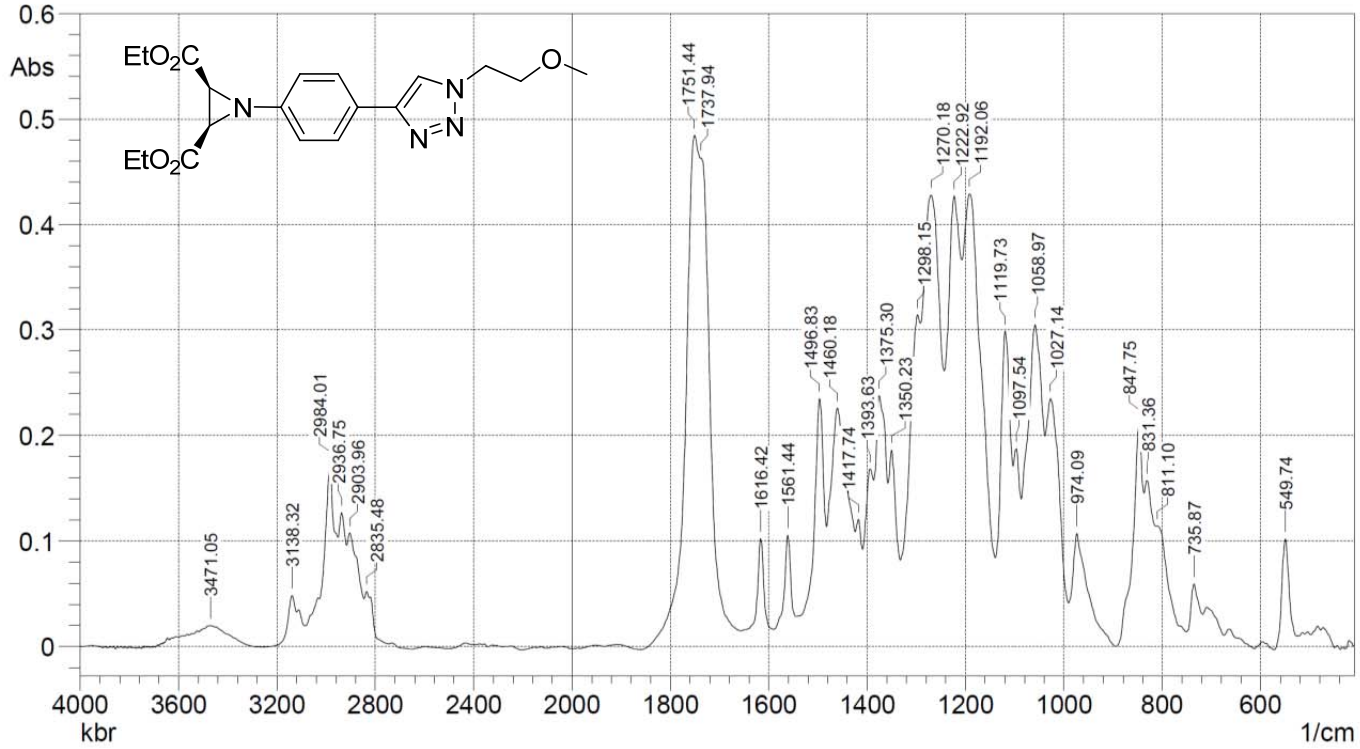

Figure S71. IR spectrum (KBr) of compound 9.

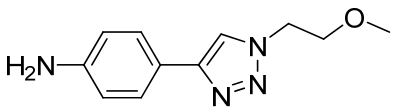

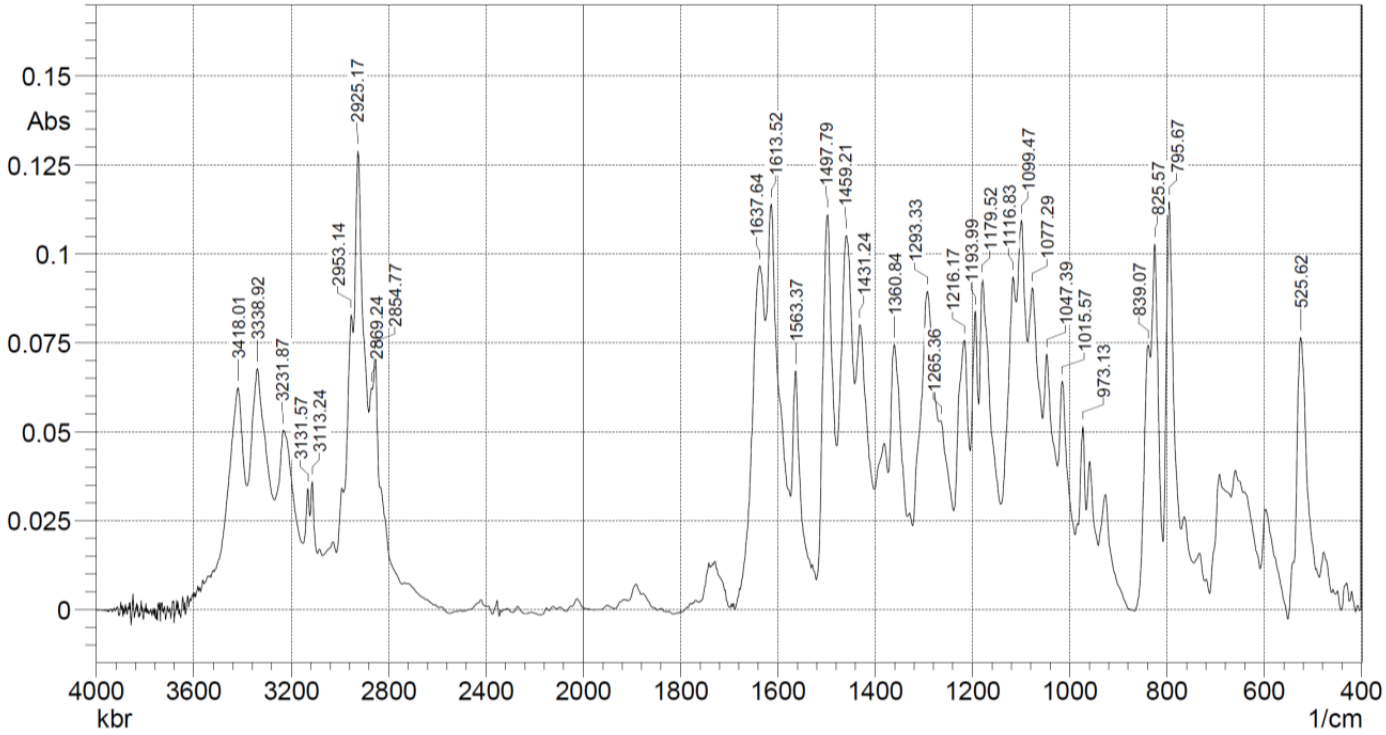

Figure S72. IR spectrum (KBr) of compound 11.

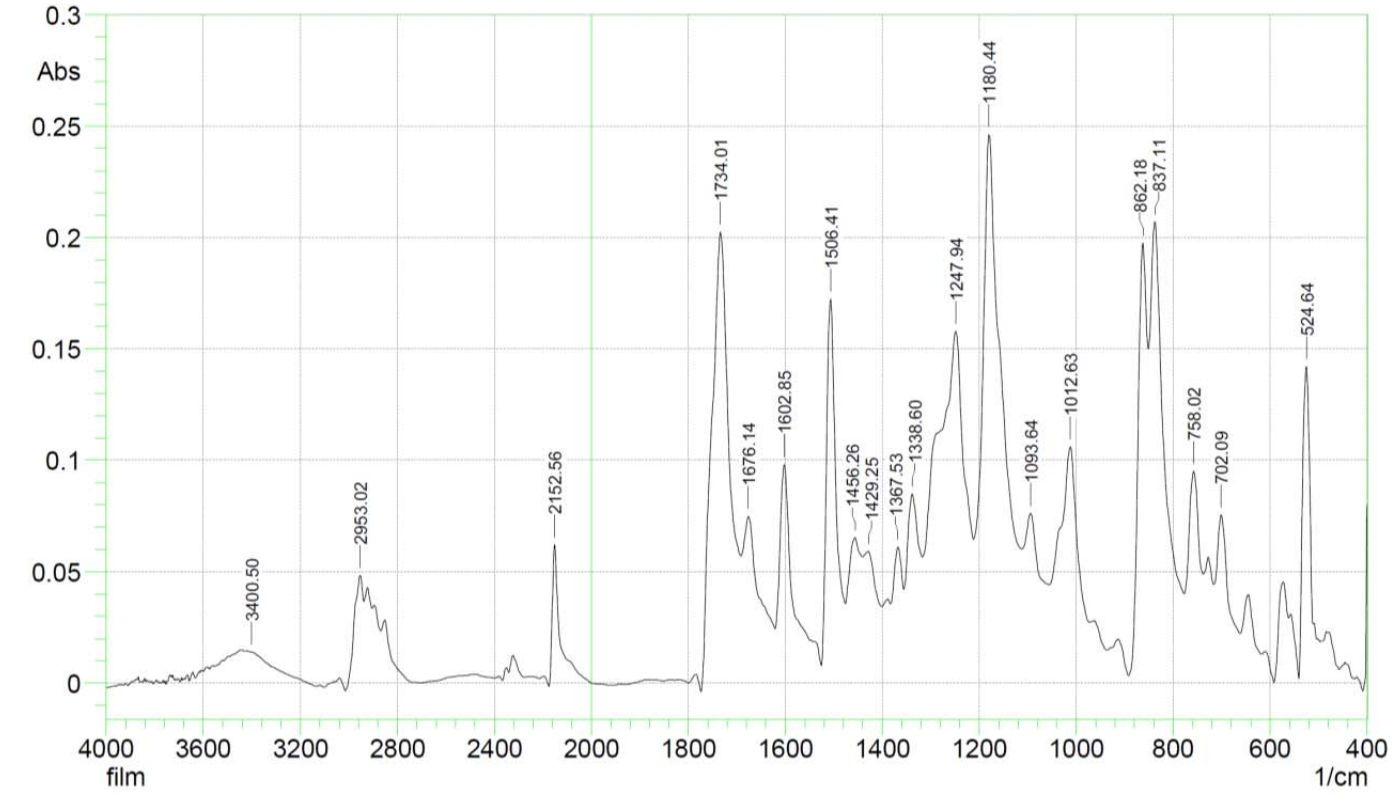

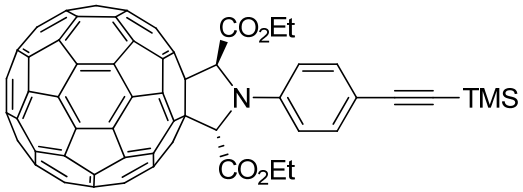

Figure S73. IR spectrum (KBr) of compound 12.

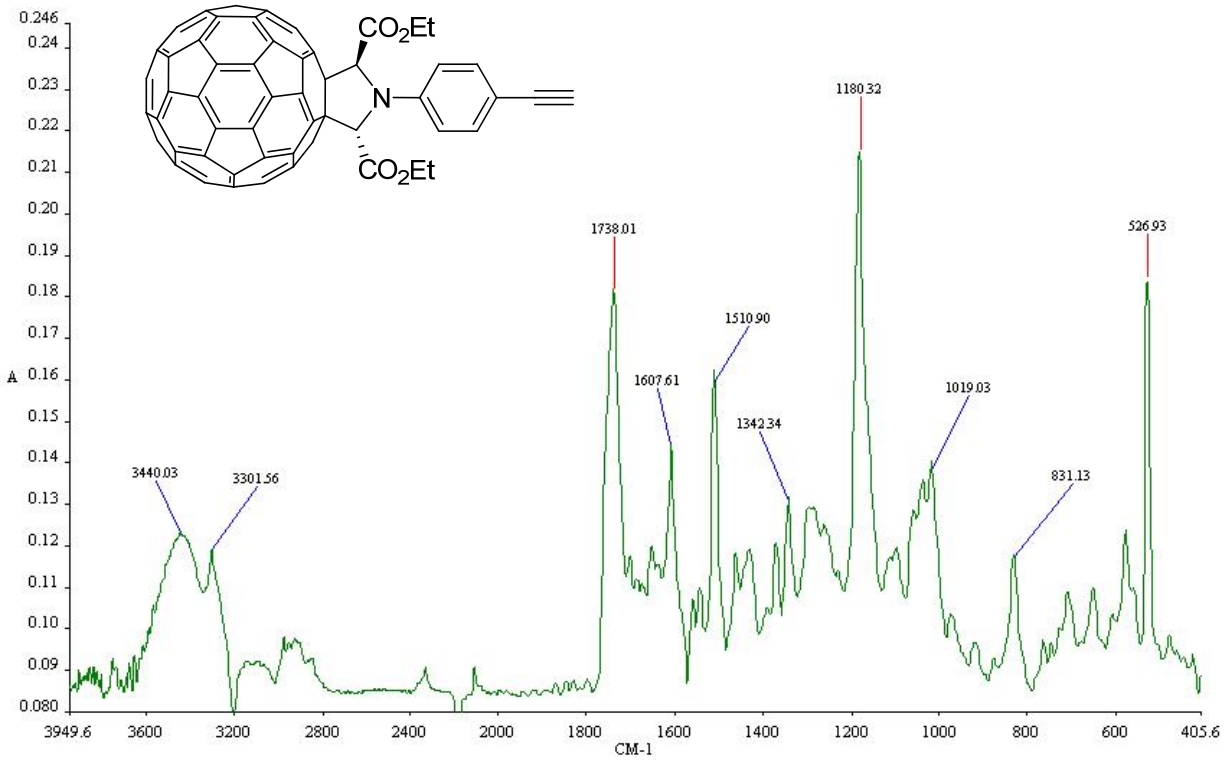

Figure S74. IR spectrum (KBr) of compound 16.

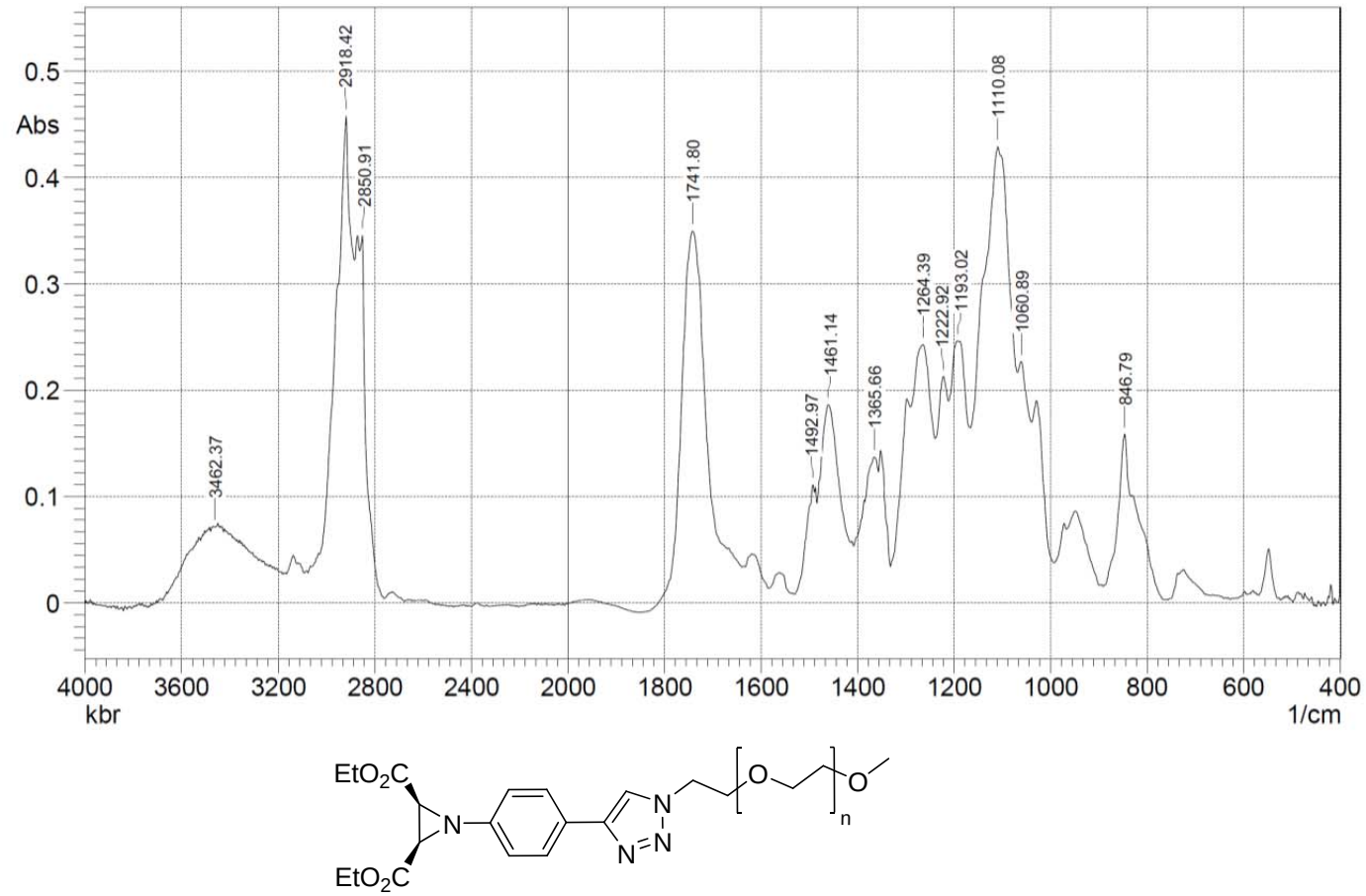

Figure S75. Schlegel diagrams for C_2-symmetric pyrrolofullerene (left) and C_s-symmetric pyrrolofullerene.

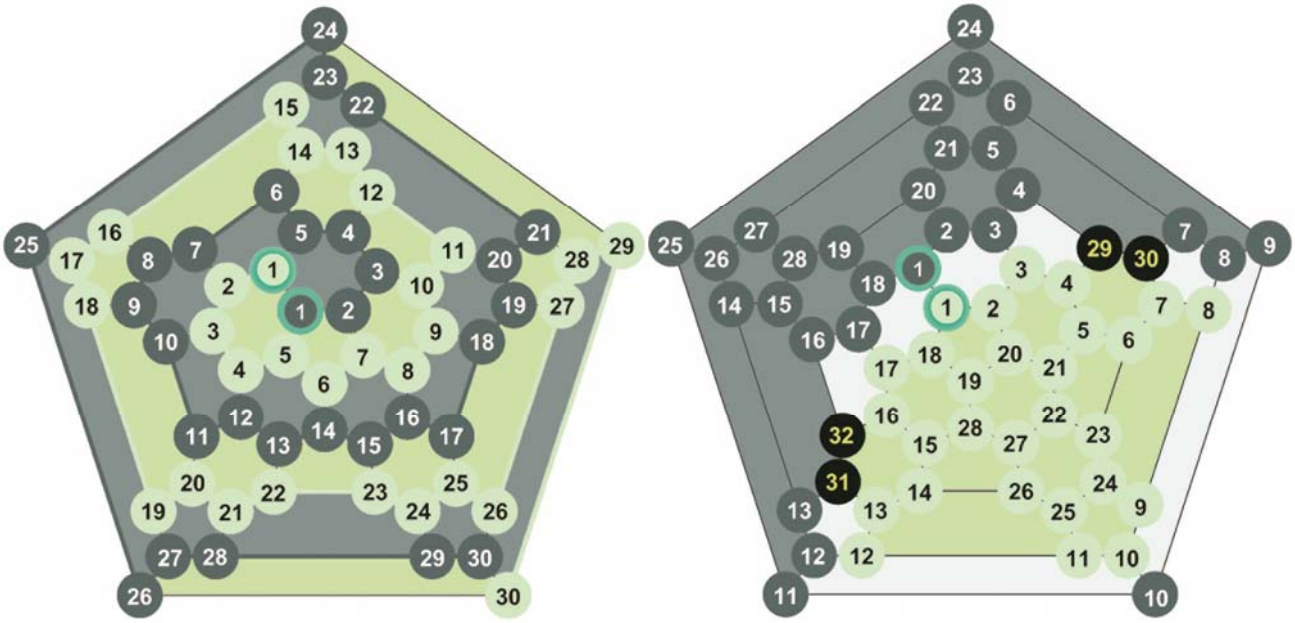

The pyrrolidine ring is fused at carbons 1 (highlighted with green circles). When two equivalent substituents at both carbons 1 have the same configuration (R, R or S, S), which is the case for compounds **2** and **3**, pyrrolofullerene has a C_2-rotation axis and belongs to C_2 symmetry group. In this case, two chains of 30 equivalent carbons pairs (denoted with the same numbers at the left picture) run in the helical manner from one pole of C_{60} (bond 1–1) to the other one (bond 30–30). If the substituents at carbons 1 are enantiotopic pair, the reflection plane appears instead of rotational axis and the molecule belongs to C_s symmetry group. In this case, the fullerene sphere consists of 28 pairs of enantiotopic carbons (denoted with the same numbers at the right picture) and 4 unique carbons at the reflection plane (denoted as black circles with yellow numbers).